# Magnetic Resonance Imaging characteristics of CADASIL

# Magnetic Resonance Imaging characteristics of CADASIL

Proefschrift

ter verkrijging van
de graad van Doctor aan de Universiteit Leiden,
op gezag van de Rector Magnificus Dr. D.D. Breimer,
hoogleraar in de faculteit der Wiskunde en Natuurwetenschappen
en die der Geneeskunde,
volgens besluit van het College voor Promoties
te verdedigen op donderdag 9 maart 2006
klokke 14.15 uur
door

Rivka van den Boom
geboren te Curaçao
in 1973

**Promotiecommissie**


Promotores:
Prof. Dr. M.A. van Buchem
Prof. Dr. M.D. Ferrari

Co-promotor:
Dr. J. Haan (Rijnland ziekenhuis, Leiderdorp)

Referent:
Dr. M. Dichgans (Ludwig Maximilian Universiteit, München)

Overige leden:
Prof. Dr. M.H. Breuning
Prof. Dr. R.G. Westendorp
Prof. Dr. F. Barkhof (Vrije Universiteit, Amsterdam)

Aan mijn ouders

# Contents

# Introduction

## *Introduction*

Up to 1991 several families suffering from an autosomal stroke condition of unknown aetiology were reported under various names such as "hereditary multi-infarct dementia", "chronic familial vascular encephalopathy", and "familial disorder with subcortical ischemic strokes, dementia, and leukoencephalopathy"[1-5]. Because of the confusion raised by all these different names, the acronym of CADASIL (Cerebral Autosomal Dominant Arteriopathy with Subcortical Infarcts and Leukoencephalopathy) was proposed by a French research group in the early 1990s following discovery of the underlying mutation that many of the earlier described families had in common[6-9].

CADASIL is an autosomal dominant disease characterized by migraine, recurrent stroke, and progressive cognitive impairment. This disease is caused by mutations in the *NOTCH3* gene, located on chromosome 19.

In this introductory chapter a summary of the major clinical, genetic, pathological, and radiological aspects of CADASIL will be given and the aims of this thesis will be described.

### *Clinical aspects of CADASIL*

The initial clinical symptoms of CADASIL vary both between and within affected families. Symptoms of this disorder appear from the mid-twenties to around 45 years of age and affected individuals typically die before the age of 65[10].

The most common clinical presentation of CADASIL is the presence of recurrent subcortical ischemic events, which occur in 80% of all patients with a mean age of onset varying from 41 to 49 years. In the early phase of the disease, symptoms are often mild and transient, resembling transient ischemic attacks[8,10,11].

The second most common feature in CADASIL patients is the development of cognitive deficits. Dementia is found in 60% of patients by the age of 45, and in 90% before death[10]. It is characterised by memory impairment and is usually associated with pseudobulbar palsy, gait disturbances, sphincter incontinence and pyramidal signs[8]. It seems that cognitive decline of CADASIL patients can progress in two different ways: a stepwise deterioration due to successive strokes, or the gradual development of a pseudobulbar syndrome[12].

Thirty-five percent of CADASIL patients have attacks of migraine with aura. Migraine with aura  is the earliest clinical manifestation, occurring at a mean age of 26[8,10,11,13]. The prevalence of this type of migraine in the general population is about 6%[14]. However, this symptom should suggest a diagnosis of CADASIL only when associated with white matter hyperintensities (WMHs)

on cerebral magnetic resonance (MR) imaging. Remarkably, CADASIL patients often develop migraine attacks shortly before or after their first stroke, suggesting the occurrence of similar pathophysiological events in CADASIL and migraine[12].

Mood and psychiatric disturbances, including severe depression, sometimes with alternating manic episodes, have been observed in 30% of patients with CADASIL[8,10,11]. Like migraine, mood disorders should suggest a diagnosis of CADASIL only when associated with diffuse WMHs on cerebral MR imaging.

Epileptic insults are present in up to 10% of the CADASIL patients and probably are secondary to cortical damage[8,10,11].

A small number of CADASIL patients may experience an encephalopathic illness characterised by a period of impaired consciousness and neurological abnormalities usually recovering after about two weeks[15-17].

### Genetic aspects of CADASIL

In 1993 CADASIL was linked to chromosome 19[9,18]. In 1996, mutations in *NOTCH3* gene were found[19]. Until now 54 different mutations have been reported[20]. The highly conserved Notch signalling pathway was originally identified and studied in the fruit fly *Drosophila melanogaster*. The name "Notch" derives from the characteristic notched wing found in flies carrying only 1 functioning copy of the gene. Homozygous *NOTCH3* mutations in fruit fly are lethal, and affected embryos have severe abnormalities, including an excess of neural cells[21]. The Notch signalling appears to function as a general development tool, essential for proper embryonic development in species ranging from insects to mammals. The exact mechanism whereby defects in the NOTCH3 protein cause the vasculopathy of CADASIL remains to be determined. In CADASIL, all mutations in *NOTCH3* are the loss, or gain of a cysteine residue.

Mutation analysis for diagnostic purposes is possible[22]. As intervention to prevent or delay onset age or even change the clinical course of CADASIL is not routinely possible, presymptomatic DNA testing in CADASIL families should be done with caution. DNA testing should be accompanied by genetic counselling, informing the patient and his/her family about the course of the disease and the risk of transmitting the abnormal gene to their offspring's[23,24]. Obviously, attention should be paid to psychological reactions such as denial and minimisation in gene carriers and survivor guilt in non-mutation carriers.

### Histopathological aspects of CADASIL

Post mortem studies of affected patients show multiple small infarcts and leukoencephalopathy throughout the subcortical white matter as well as in the basal ganglia and thalamus[2,3,7,25].

The characteristic histological finding is a vasculopathy of small and middle-sized arterioles. Smooth muscle cells of the media are replaced with deposits of basophilic granular electron-dense material known as granular osmiophilic material (GOM) resulting in destruction of vascular smooth muscle cells and fibrous thickening of the arterial wall[7,26].

It is believed that these GOM depositions in the blood vessel wall result in both reduced blood flow and an inability of the blood vessels to regulate blood flow (cerebrovascular reactivity), causing WMHs and lacunar infarcts. Cerebrovascular reactivity reflects the compensatory dilatory capacity of cerebral arterioles to a stimulus such as carbon dioxide or acetazolamide. In elderly individuals impaired cerebrovascular reactivity is associated with WMHs and lacunar infarcts[27-29]. In patients with CADASIL, alterations in cerebral blood flow and cerebrovascular reactivity have also been demonstrated, with a significant reduction in baseline cerebral blood flow and cerebrovascular reactivity in areas of WMHs[30-33]. From these observations, however, cannot be derived whether structural brain changes are secondary to impaired flow, or whether impaired flow is a consequence of brain damage.

Although in CADASIL abnormalities in blood vessels can be found throughout the body, they appear to be most severe in the brain. The vasculopathy in the brain gives rise to the characteristic clinical signs and symptoms in CADASIL patients. The reason for the brain being the site of predilection is still unknown[34].

The diagnosis of CADASIL can be confirmed by electron microscopic (EM) analysis of the arterioles in a skin biopsy[35,36]. Although the identification of characteristic vascular abnormalities (GOM in the media) is highly specific for CADASIL, these abnormalities are not always found. The false negative rate of skin biopsy analysis finding is unknown[37,38].

### Radiological aspects of CADASIL

Two types of lesions have been described in patients with CADASIL. The first type are WMHs, symmetrically distributed and located in the periventricular and deep white matter[39]. There is a relative sparing of the arcuate fibers and cortex[40]. The WMHs are predominantly localized in the frontal lobe, followed by the temporal and parietal lobes. The occipital lobe is markedly less severely affected[41,42]. It has been demonstrated that the external capsules and (anterior) temporal lobes are also sites of predilection for WMHs[43]. Brain stem white matter abnormalities, located mainly in the pons and mesencephalon, are also frequently observed, while involvement of the cerebellum appears

to be very uncommon[39,44]. In symptomatic patients MR imaging of the brain is always abnormal, however WMHs have also been detected in asymptomatic *NOTCH3* mutation carriers[45].

The second type of lesions are lacunar infarcts in the centrum semiovale, thalamus, basal ganglia and pons[40]. The prevalence of both WMHs and lacunar infarcts increase with age.

There are several ways to detect in vivo microscopic damage that remains undetected using conventional radiological techniques. Studies using diffusion tensor imaging, magnetization transfer imaging and MR spectroscopy in CADASIL have shown that microstructural changes are present in both normal and abnormal white matter, probably reflecting neuronal loss and demyelination[46-48]. Also, they found that the degree of the underlying ultrastructural alterations is related to the clinical severity.

### Differential diagnosis

The differential diagnosis of CADASIL depends upon the age of the patient. The diagnosis of CADASIL is often made at a young age and the recurrence of multifocal neurological deficits with relative young age-of-onset, and WMHs on MR imaging that are initially patchy makes it difficult to distinguish CADASIL from multiple sclerosis (MS)[49,50]. Another differential diagnostic consideration of CADASIL, based on the radiological picture, is mitochondrial encephalopathy with lactic acidosis (MELAS). However, this disease is readily distinguished from CADASIL on the basis of a familial pattern suggestive of maternal inheritance, clinical features, or supplementary tests. Binswanger's disease, a rare form of dementia characterized by loss of memory and cognition, mood changes, and abnormal blood pressure, should be considered in older patients because of the confluent WMHs and lacunar infarcts. However, a history of severe long lasting hypertension is often lacking in CADASIL patients, there is no familial occurrence in Binswanger's disease and the age of onset in Binswanger's disease is usually later.

### Purpose and outline of the thesis

The discovery of the mutations in the *NOTCH3* gene in 1996 was an important landmark in CADASIL research since it provides a reliable confirmation of the clinical diagnosis. At the Leiden University Medical Centre (LUMC) a study was started on the clinical, radiological, pathological, neuropsychological, and genetic aspects of CADASIL patients in the Netherlands. Members of 15 unrelated Dutch CADASIL families were asked to participate in this study. Index patients identified through *NOTCH3* mutation analysis were referred from various medical institutions to the LUMC, which serves as a national CADASIL

referral centre. The total number of participants was 63 of which 41 turned out to be mutation carrier and 22 were not. The advantage of this study set-up was that the asymptomatic family members were unaware of their genetic status and a representative control group for the mutated family members was built into the study. The studies that are described in this thesis are based on material that was generated in the Dutch CADASIL study.

The purpose of this thesis is to refine the morphological phenotype of cerebral abnormalities in CADASIL using MR imaging. A diagnosis of CADASIL cannot be made without MR imaging. Recognizing the MR imaging features of CADASIL can help to increase the chance of detecting CADASIL by genetic screening and distinguish this largely underdiagnosed disorder from similar conditions associated with WMHs such as aging, Binswanger's disease, MELAS, and MS. In this thesis we also evaluated the influence of potential risk factors and the effect of the vessel wall pathology on the structural MR lesions.

This thesis addresses the following study objectives:

1) Are cerebral vessels in CADASIL patients more prone to bleed as expressed by the presence of microbleeds?

2) Is there a relation between the amount of microbleeds and disease severity?

3) What is the prevalence and distribution of a type of lacunar lesions that, to our knowledge, has not been described before in the neuroimaging literature in neither CADASIL patients nor in patients with other disorders?

4) What is the typical appearance of MR imaging abnormalities in CADASIL and does this differ and progress per age category?

5) What are the clinical, neuropsychological and radiological features of CADASIL patients under the age of 35 years?

6) Is it possible to distinguishing CADASIL patients from MS patients on the bases of the radiological hallmarks of CADASIL?

7) What is the influence of apolipoprotein E genotype on the development of radiological abnormalities in CADASIL patients?

8) Is a decrease in cerebral blood flow or cerebrovascular reactivity primarily responsible for the development of WMHs and lacunar infarcts?

Chapter 1

# Cerebral microbleeds in CADASIL

# Cerebral microbleeds in CADASIL

S.A.J. Lesnik Oberstein
R. van den Boom
M.A. van Buchem
H.C. van Houwelingen
E. Bakker
E. Vollebregt
M.D. Ferrari
M.H. Breuning
J. Haan

## Abstract

Cerebral autosomal dominant arteriopathy with subcortical infarcts and leukoencephalopathy (CADASIL) is a hereditary arteriopathy leading to recurrent cerebral infarcts and dementia. Intracerebral haemorrhage (ICH) has been described sporadically in patients with CADASIL, suggesting that the affected arteries in CADASIL are not bleed-prone. However, the presence of cerebral microbleeds, which often remain undetected on conventional magnetic resonance (MR) imaging, has not been determined in CADASIL. Purpose was to determine whether cerebral vessels in patients with CADASIL are prone to microbleeding.

T2*-weighted gradient echo MR imaging, which is highly sensitive for visualizing microbleeds, was performed in patients with CADASIL and their family members (n=63). Known risk factors for ICH were determined for all individuals. On an exploratory basis, the presence of cerebral microbleeds was correlated with demographic variables, vascular risk factors, disease progression, ischemic MR lesions, and genotype.

Cerebral microbleeds were present in 31% of symptomatic CADASIL mutation carriers, predominantly in the thalamus. Vascular risk factors such as hypertension did not account for the microbleeds in these patients. Factors associated with microbleeds were age (P=0.008), Rankin disability score (P=0.017), antiplatelet use (P=0.025), number of lacunae on MR images (P=0.009), and the Arg153Cys *NOTCH3* mutation (P=0.017). After correction for age, only the Arg153Cys mutation remained significantly associated with the presence of microbleeds.

Patients with CADASIL have an age-related increased risk of intracerebral microbleeds. This implies that they may have an increased risk for ICH, which should be taken into account in CADASIL diagnosis and patient management.

## *Introduction*

Cerebral autosomal dominant arteriopathy with subcortical infarcts and leukoencephalopathy (CADASIL) is a hereditary small-vessel disease caused by mutations in the *NOTCH3* gene on chromosome 19[19]. Clinically, the disease is characterized by recurrent cerebral infarcts and dementia, and patients may also experience migraine or affective disorders. Magnetic resonance (MR) imaging reveals extensive cerebral white matter lesions and subcortical infarcts. On pathologic examination, there are marked changes in the small cerebral arteries with thickening of the media, loss of vascular smooth muscle cells, and accumulation of extracellular nonamyloid, noncholesterol, electron-dense granular material[51].

Primary intracerebral haemorrhage (pICH) has rarely been described in CADASIL, in contrast to other small-vessel diseases associated with white matter changes and infarcts, including hypertensive lipofibrohyalinosis and cerebral amyloid angiopathy (CAA)[52-54]. This discrepancy could indicate that CADASIL vessels, though thickened, are not fragile and thus do not lead to pICH or that CADASIL patients with pICH remain unrecognized. In the last 5 years, a strong association has been found between ischemic small-vessel disease and the presence of cerebral microbleeds detected on T2*-weighted gradient echo MR images[54-57]. This is a highly sensitive technique to detect haemosiderin deposits and thus remnants of intracerebral microbleeds, which are clearly visualized as small areas of signal loss[56]. Microbleeds in a randomly selected elderly population occur in 6.4% of individuals and are related to other indicators of small-vessel disease, whereas up to 26% of patients with a history of ischemic stroke have microbleeds[55,58]. Determining the presence of microbleeds in patients with CADASIL could answer the question of whether intracerebral extravasation of blood occurs in CADASIL arteriopathy. If so, this may implicate an increased risk of pICH in patients with CADASIL.

We sought to determine whether cerebral microbleeds occur in individuals with a confirmed *NOTCH3* mutation and, if so, whether the presence of microbleeds is associated with other patient characteristics such as severity of concomitant MR lesions, vascular risk factors, and genotype.

## *Materials and methods*

### *Subjects*

Members of 15 families with CADASIL were asked to participate in a clinical and genetic study on CADASIL. For all families, the respective *NOTCH3* mutation had previously been determined in at least one clinically affected member. Symptomatic as well as asymptomatic family members were included in the

study. Participants were considered symptomatic if a clinical diagnosis of CADASIL had been made by a physician before the study, based on a history of unexplained neurologic deficits or cognitive decline and white matter abnormalities with or without lacunar lesions on MR imaging. Participants were considered asymptomatic if they had never consulted a physician with symptoms compatible with CADASIL. Migraine was not included in this definition. Control subjects consisted of asymptomatic family members without a *NOTCH3* mutation. Disability at the time of the study was measured semiquantitatively with the Rankin scale. Sixty-three individuals participated in the study between August 1999 and July 2000. Only individuals cognitively capable of giving informed consent, and who did so, were included. The study was approved by the Medical Ethics Committee of the Leiden University Medical Centre.

### *MR imaging*

MR examinations were performed on a 1.5 T MR system (Philips Medical Systems, Best, the Netherlands). T1-weighted spin echo (SE; slice thickness 6 mm with a 0.6 mm interslice gap [6.0/0.6 mm], repetition time [TR] 600 ms, echo time [TE] 20 ms, matrix of 256 x 205), T2-weighted turbo SE (TSE; 3.0/0.0 mm, TR/TE 3000/120 ms, 256 x 205), proton density-weighted (3.0/0.0 mm, 3000/27 ms, 256 x 205), and fluid-attenuated inversion recovery (FLAIR; 3.0/0.0 mm, TR/TE 8000/100 ms, 256 x 192) images were obtained in the axial plane. To specifically detect cerebral microbleeds, T2*-weighted gradient echo planar imaging was performed (6.0/0.6 mm, TR/TE 2598/48 ms, 256 x 192), echo-planar imaging factor, 25).

Microbleeds were defined as focal areas of signal loss on T2-weighted TSE images that increased in size on the T2*-weighted gradient echo planar images ("blooming effect"). In this way, microbleeds were differentiated from areas of signal loss based on vascular flow void. Areas of symmetric hypointensity in the basal ganglia likely to represent calcification or nonhaemorrhagic iron deposits were disregarded. Finally, to differentiate microbleeds from other intra-axial lesions with a haemorrhagic component, only areas of signal loss that were not locally associated with other abnormalities were counted as microbleeds. The location, number, and size of microbleeds were recorded. White matter lesion load was graded according to the signal hyperintensity rating scale of Scheltens et al on T2-weighted TSE, proton density-weighted, and FLAIR images[59]. Lacunar lesions were defined as focal areas of hyperintense lesions on T2-weighted TSE images, with corresponding hypointense lesions on T1-weighted SE images. The signal intensity of these lesions corresponded with

that of the cerebrospinal fluid . The number, location, and size of lacunar lesions were recorded. All MR images were reviewed by the same neuroradiologist, blinded to genetic and clinical data.

### Mutation analysis

*NOTCH3* mutation carriership was determined in all 63 individuals by direct sequencing analysis, according to previously described techniques[22]. Previously unreported *NOTCH3* mutations were considered disease causative when 1) there was a change in the number of cysteine residues, typical for CADASIL mutations; 2) the mutations did not occur in 100 control chromosomes; and 3) the mutation clustered in affected family members.

To assess whether families with the same mutation had a common ancestor, haplotype analysis was performed with four polymorphic microsatellite markers (D19S929, D19S841, D19S1153, D19S917) located close to the *NOTCH3* gene.

### Risk factors

Vascular comorbidity including hypertension, smoking, diabetes mellitus, history of myocardial infarction, and hypercholesterolemia was recorded in all subjects, with definitions similar to those in comparable studies, as follows[55,58,60].

1. Hypertension: at least two blood pressure measurements of ≥150/95 mm Hg in the medical records of the preceding 5 years or two such measurements on the day of examination or current antihypertensive drug therapy;

2. Smoker: a person currently smoking at least one cigarette, cigar, or pipe per day for at least 1 year or who has done so in the past;

3. Diabetes mellitus: current use of oral antidiabetics or insulin;

4. Hypercholesterolemia: a cholesterol measurement of ≥7 mmol/L in the medical records of the preceding 5 years or current use of cholesterol-lowering drugs; and

5. Myocardial infarction: a history of myocardial infarction in the medical records.

All individuals filled in a structured questionnaire concerning vascular risk factors. In addition, an extensive oral medical history, including medication use, was taken on the day of examination. All affected patients were accompanied by a clinically unaffected family member or spouse who, when necessary, supplied additional medical history. Questionnaires and history were validated with information from medical records supplied by the participants' general practitioners and medical specialists.

*Statistical analysis*

Statistical analysis was performed with SPSS-10 (SPSS, Inc., Chicago, IL). An exploratory analysis was performed to detect any association between the presence of cerebral microbleeds and demographic variables, vascular risk factors, concomitant MR abnormalities, and genotype. The association between microbleeds and the patient variables was studied in the setting of logistic regression. First, all univariate P values were computed, followed by the computation of P values after correction for age. A significance threshold of P<0.05 was maintained.

*Results*

Table 1 gives an overview of the studied variables in carriers of *NOTCH3* mutations with and without microbleeds.

*Table 1 Characteristics of NOTCH3 mutation carriers with and without microbleeds*

| Characteristic | Microbleeds, n=10 | No microbleeds, n=30 | P (p*) |
|---|---|---|---|
| Age, y (range) | 53.4 (43-58) | 43.4 (21-59) | ≤0.008 |
| Male, n (%) | 5 (50) | 14 (47) | ≤0.85 |
| Hypertension , n (%) | 0 | 3 (10) | ≤0.3 |
| Smoking, n (%) | 6 (60) | 19 (63) | ≤0.85 |
| Hypercholesterolemia, n (%) | 3 (30) | 12 (40) | ≤0.6 |
| Diabetes mellitus, n (%) | 0 | 3 (10) | ≤0.3 |
| Myocardial infarction, n (%) | 1 (10) | 5 (17) | ≤0.7 |
| Antiplatelet use, n(%) | 10 (100) | 19 (63) | ≤0.3 (0.025) |
| Antiplatelet use, mean y (range) | 6.5 (1-10) | 2.7 (0-12) | ≤0.2 (0.003) |
| Mean antiplatelet dose, mg/d (range) | 93.2 (38-240) | 53.1 (0-300) | ≤0.8 (0.07) |
| Dipyridamol, n (%) | 4 (40) | 4 (13) | ≤0.5 (0.07) |
| Mean white matter lesion load (range) | 53.8 (37-65) | 41,4 (4-64) | ≤0.9 (0.053) |
| Mean no. of lacunes (range) | 34.1 (5-66) | 16.9 (0-52) | ≤0.3 (0.009) |
| Mean Rankin score (range) | 2.8 (0-5) | 1.5 (0-4) | ≤0.6 (0.017) |

*p\* = P value before correction for age*

*Mutation analysis and subjects*

The 15 participating families had 11 different *NOTCH3* mutations. Some families therefore shared the same genotype. Three mutations were not previously described in the literature (table 2). Per family, the number of participants varied from only the index patient to 10 members. The total number of participants was 63, but one participant had an incomplete MR study because of claustrophobia and was therefore excluded from the analysis. The mean ± SD age of the remaining 62 participants was 43.8 ± 11.5 years (range 21 to 67 years).

Forty participants had a mutation in the *NOTCH3* gene, and 22 did not. Thirty-two mutation carriers were symptomatic, with a wide range of severity from one TIA to multiple strokes and cognitive decline. Eight mutation carriers were asymptomatic. The mean age of the 40 mutation carriers was 45.9 ± 10.5 years (range 21 to 59 years) and of the 22 non mutation carriers 40.0 ± 12.7 years (range 22 to 67 years).

*Microbleeds*

Ten of the 40 participants (25%) with a *NOTCH3* mutation had microbleeds. These 10 individuals were all clinically symptomatic. Thus, almost a third (31%) of the 32 symptomatic *NOTCH3* mutation carriers had microbleeds. None of the eight asymptomatic mutation carriers and none of the 22 individuals without a *NOTCH3* mutation had microbleeds.

Eighty-seven focal areas of signal loss were detected on T2*-weighted gradient echo images. Most of these were smaller than 5 mm in diameter (92%); the largest was 10 mm. These foci all resembled microbleeds in their homogeneous shape and distribution. Microbleeds were located predominantly in the thalamus (table 3; figure 1). Of the cerebral lobes, the occipital lobe had the most microbleeds (nine) compared with five microbleeds in the temporal lobe, two in the parietal lobe, and one in the frontal lobe. Mutation carriers with microbleeds were significantly older than mutation carriers without microbleeds, and microbleeds were present equally in men and women (table 1). All microbleeds occurred in patients with five different mutations. Six of the mutations, therefore, were not associated with microbleeds. Of the 10 patients with microbleeds, six had an Arg153Cys mutation. These six patients originated from two families: four individuals from one family and two from the other. Haplotype analysis showed that these families were unrelated. The Arg153Cys mutation is associated with microbleeds before (P=0.017) as well as after (P=0.037) correction for age.

*Table 2 NOTCH3 mutations in study population*

| Genotype, exon | Subjects with microbleeds n=10 | Total mutated n=40 |
|---|---|---|
| Arg153Cys, 4 | 6 | 12 |
| Arg141Cys, 4 | 1 | 9 |
| Cys446Phe, *8 | 1 | 1 |
| Arg207cys, 4 | 1 | 2 |
| Arg544Cys, 11 | 1 | 1 |
| Cys1015Arg, 19 | 0 | 3 |
| Arg133Cys, 4 | 0 | 2 |
| Arg182Cys, 4 | 0 | 4 |
| Arg1076Cys,*20 | 0 | 3 |
| Cys144Phe, 4 | 0 | 1 |
| Cys162Trp, *4 | 0 | 2 |

*\* previously unreported NOTCH3 mutation*

*Table 3 Cerebral microbleed distribution in CADASIL*

| Cerebral structure | No. of subjects with microbleeds in structure | Total no. of microbleeds, sum (range) |
|---|---|---|
| Subcortical white matter | 5 | 23 (0-15) |
| Thalamus | 8 | 53 (0-18) |
| Basal ganglia | 2 | 2 (0-1) |
| Cerebellum | 2 | 5 (0-4) |
| Brainstem | 3 | 4 (0-2) |
| Cortex | 0 | 0 |

### Concomitant cerebral MR abnormalities

The MR imaging results described here pertain only to the carriers of *NOTCH3* mutations (n=40). Mutation carriers all had white matter abnormalities on MR imaging. Individuals with microbleeds did not have a significantly higher white matter lesion load than those without microbleeds but did have a significantly higher lacunar lesion count (table 1). Those with microbleeds had more lacunae in the temporal lobe ($P=0.025$), occipital lobe ($P=0.015$), and thalamus ($P<0.001$). After correction for age, the difference in mean total lacunar lesion count disappeared.

*Vascular risk factors*

Vascular risk factors (hypertension, smoking, hypercholesterolemia, diabetes mellitus, and history of myocardial infarction) did not occur significantly more in mutation carriers with microbleeds than in those without microbleeds (table 1). Hypertension and diabetes mellitus were not present in any of the individuals with microbleeds. Those with microbleeds had used antiplatelet drugs more (P=0.025) and longer (P=0.003) than those without microbleeds. These associations, however, disappeared after correction for age. One patient with microbleeds had a history of long-term anticoagulant use (>10 years). A patient without microbleeds had started using anticoagulants just before the study, and one had a history of short-term anticoagulant use.

*Rankin score*

An association was found between Rankin score and microbleeds (P=0.017). After correction for age, however, this was no longer present.
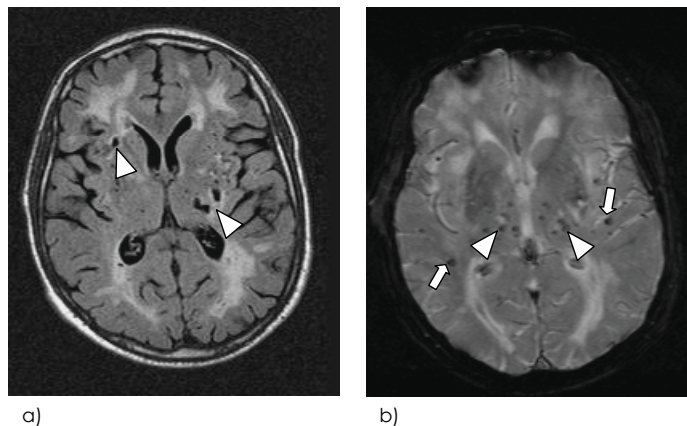


a)    b)

*Figure1 MR images at the level of the basal ganglia in a 55 year old patient with CADASIL. FLAIR image (a) shows periventricular and deep white matter hyperintensities and lacunes in the thalamus and basal ganglia (arrows). T2\*-weighted gradient echo planar image (b) shows numerous circumscript hypodense lesions from previous microbleeds, located in the thalamus (arrowhead) as well as deep and subcortical white matter (white arrow).*

## Discussion

The main finding of the current study is that 31% of symptomatic *NOTCH3* mutation carriers had evidence of cerebral microbleeds on MR imaging. We postulate that the microbleeds are directly related to CADASIL arteriopathy, as known risk factors for cerebral bleeding, such as hypertension, were absent. CAA is a post-mortem diagnosis and therefore could not be excluded as a cause for the microbleeds. However, it is unlikely to have played a role, owing to the relatively young age of our study population and the mainly

thalamic location of the microbleeds, both of which are atypical for CAA[61]. Hereby, the borders of CADASIL disease expression are expanded beyond that of a purely ischemic cerebral disease, to include cerebral bleeding. A relevant clinical implication is that patients with CADASIL may be at increased risk of pICH, which has been shown to be associated with the presence of microbleeds[54,56,57,62].

In this CADASIL population, the Arg153Cys mutation is an independent risk factor for microbleeds. Although confirmation of this finding is warranted because of the small sample size and the exploratory nature of this study, it supports the possibility that various *NOTCH3* mutations may lead to differences in severity or pattern of disease expression, as has been suggested by other authors[63,64].

Microbleeds were found to be age related, and their presence may thus reflect disease progression in CADASIL. This is also suggested by the fact that microbleeds occurred in areas with a large number of lacunae. Possibly, the more damaged the intracerebral vessels become (reflected in increased number of lacunae), the more bleed-prone they tend to get. However, the total number of lacunae and other MR and clinical data reflecting disease progression, such as the Rankin scale and white matter lesion load, were higher in patients with microbleeds, but not within the range of significance after correction for age (table 1).

ICH has so far rarely been reported in patients with CADASIL. Several explanations could account for this. First, when pICH occurs, the underlying CADASIL may be obscured and thus remain undiagnosed, especially because pICH is classically considered not to form part of the CADASIL disease spectrum. A second explanation could be that true pICH in CADASIL is provoked only when additional risk factors are present. Interestingly, of the two CADASIL patients with pICH reported in the literature, one died as a consequence of this at age 30, 6 months after starting anticoagulant therapy[1,7]. In our study, previous anticoagulant use was recorded in only one patient with microbleeds. Therefore, whether anticoagulants play a role in CADASIL ICH, as has also been found in other small-vessel disease, remains to be determined[65]. We did find that patients with microbleeds used antiplatelet drugs more and longer than those without microbleeds. However, the significance of this finding was lost after correction for age, implying that antiplatelet drug therapy probably does not play a role in increased risk for cerebral bleeding in CADASIL. To avoid missing the diagnosis and to further delineate the disease spectrum, CADASIL should be considered in the diagnostic workup of (normotensive) patients presenting with pICH and concomitant white matter abnormalities on MR imaging.

# Subcortical lacunar lesions: an MR imaging finding in patients with CADASIL

# Subcortical lacunar lesions: an MR imaging finding in patients with CADASIL

R. van den Boom
S.A.J. Lesnik Oberstein
S.G. van Duinen
M. Bornebroek
M.D. Ferrari
J. Haan
M.A. van Buchem

## Abstract

Purpose was to assess the prevalence and distribution of subcortical lacunar lesions (SLLs) in patients with cerebral autosomal dominant arteriopathy with subcortical infarcts and leukoencephalopathy (CADASIL), to determine whether SLLs are an abnormal finding by studying their prevalence in healthy subjects, and to assess whether SLLs occur in other conditions associated with small vessel disease and white matter areas of high signal intensity (WMHs).

The presence of SLLs, their location, and their relation to other abnormalities were assessed on magnetic resonance (MR) images (T1-weighted, T2-weighted, and fluid-attenuated inversion-recovery) obtained in 34 CADASIL patients and 20 healthy family members. Three additional control groups of healthy volunteers, elderly patients with vascular risk factors, and patients with another hereditary small vessel disease were also screened for the presence and location of SLLs. Sensitivity and specificity of the presence of SLLs for the diagnosis of CADASIL were assessed.

SLLs were found in 20 (59%) of CADASIL patients. Incidence of SLLs increased with age (20%, <30 years; 50%, 30–50 years; 80%, >50 years). SLLs invariably occurred in the anterior temporal lobes and in areas where diffuse WMHs expanded into arcuate fibers. From the anterior temporal lobe, the lesions could extend dorsally into the temporal lobes and rostrally into the frontal lobes. Lesions were not found in the parietal and occipital lobes. None of the control subjects had SLLs. Specificity and sensitivity of SLLs for CADASIL were 100% and 59%, respectively.

SLLs are an abnormal finding at MR imaging that frequently occur in CADASIL patients.

## Introduction

Cerebral autosomal dominant arteriopathy with subcortical infarcts and leukoencephalopathy (CADASIL) is a hereditary small artery vasculopathy caused by mutations in the *NOTCH3* gene on chromosome 19[19,45,66]. The disease is characterized clinically by transient ischemic attacks, strokes, progressive subcortical dementia, migraine with aura, and mood disturbances[8,10,11]. Pathologic examination of the brain demonstrates characteristic depositions of granular osmiophilic material within the media of the small and medium-sized leptomeningeal and long perforating arteries of the brain. The vasculopathy results in destruction of smooth muscle cells and fibrous thickening of the arterial wall[7]. Magnetic resonance (MR) imaging in patients with CADASIL typically reveals diffuse white matter areas with high signal intensity (WMHs) and lacunar infarcts in the centrum semiovale, thalamus, basal ganglia, and pons[39-41]. In symptomatic patients, MR images of the brain are always abnormal, but signal intensity abnormalities have also been detected in asymptomatic individuals who have the *NOTCH3* mutation[45].

The diagnosis of CADASIL is confirmed by the demonstration of mutations in the *NOTCH3* gene; this confirmation process, however, is laborious because the *NOTCH3* gene is large, comprising 33 exons (i.e., distinct parts of genes which often encode discrete structural and functional units of proteins). Although 65% of known mutations occur in exons 3 and 4, the remaining exons must be screened, as well, in many cases. MR imaging plays an important role in the diagnostic work-up to increase the chance that CADASIL will be detected with genetic screening. It has recently been demonstrated that CADASIL can be differentiated from Binswanger's disease at MR imaging, but differentiation of CADASIL from other diseases that can be associated with white matter abnormalities is unclear[67]. Therefore, the discovery of more specific neuroimaging features of CADASIL might help increase the chance of identifying CADASIL patients.

Recently, we reviewed brain MR imaging studies of members of families with CADASIL as part of a study on the clinical, radiologic, and genetic aspects of CADASIL in the Netherlands. During this study, we observed a pattern of subcortical lacunar lesions (SLLs) in patients with CADASIL that, to the best of our knowledge, has not been previously described. The aim of the present study was threefold: to assess the prevalence and distribution of SLLs in CADASIL patients, to determine whether SLLs are an abnormal finding by studying their prevalence in a control series of healthy subjects from the general population, and to assess whether SLLs occur in other conditions that are associated with small vessel disease and WMHs.

## Materials and methods

Members of 15 unrelated Dutch families with CADASIL were asked to participate in a study on the clinical, radiologic, and genetic aspects of CADASIL. In each family, the index patient had a proven pathogenic *NOTCH3* mutation. Patients were referred from various medical centres to our institution, which serves as a CADASIL referral centre. Patients were referred because they were suspected of having CADASIL on the basis of clinical signs and symptoms, a family history consistent with autosomal dominant inherited disease, or suggestive changes at MR imaging such as WMHs and lacunar infarcts. The presence of SLLs was never the reason for referral. At our institution, the diagnosis of CADASIL was confirmed with direct sequencing analysis of the *NOTCH3* gene according to previously described techniques[22]. Thirty-four patients formed the group in our study.

The following four control groups were used:

1. Members of CADASIL families without the *NOTCH3* mutation.

2. A group of 75 adult subjects (<65 years of age) who were randomly recruited from the general population, did not have abnormalities at standard neurologic examination, and had no history of cardiovascular events.

These two groups served to assess whether SLLs occur in evidently healthy individuals.

To assess whether SLLs occur in patients with other conditions that are associated with small vessel disease and WMHs, we studied two additional control groups:

3. A group of 16 age-matched patients with DNA-proven hereditary cerebral haemorrhage with amyloidosis–Dutch type (HCHWA-D). HCHWA-D is an autosomal dominant small vessel disease of the brain caused by ß-amyloid depositions in cerebral arterioles and leptomeningeal arteries that is associated with extensive supratentorial WMHs[68-70].

4. A group of 75 elderly subjects (>70 years) from the general population with an increased risk of having cerebral WMHs because they had cardiovascular disease or at least one major vascular risk factor (hypertension, cigarette smoking, or diabetes mellitus; for criteria see reference 16). These subjects were randomly selected from a larger study group that had participated in a randomized controlled trial investigating the effect of cholesterol-lowering treatment with pravastatin on cardiovascular disease and stroke. All subjects were imaged at baseline[71].

The patients in all control groups underwent the same MR imaging protocol as the patients with CADASIL. Only cognitively capable subjects were included in this study to ensure informed consent. The medical ethics committee of

our institution approved the protocol of our entire study. Informed consent was obtained from all subjects in each of the four control groups and from all subjects in the CADASIL group.

All MR imaging examinations were performed with a 1.5-T MR system (Philips Medical Systems, Best, the Netherlands) between August 1999 and June 2001. Conventional T1-weighted spin-echo images (section thickness, 6 mm; intersection gap, 0.6 mm; repetition time msec/echo time msec, 600/20; matrix, 256 x 205; field of view, 220 x 165 mm), dual T2-weighted fast spin-echo images (section thickness, 3 mm; no intersection gap; 3000/27, 120; matrix, 256 x 205; field of view, 220 x 220 mm), and fast fluid-attenuated inversion-recovery (FLAIR) images (section thickness, 3 mm; no intersection gap; repetition time msec/echo time msec/inversion time msec, 8000/100/2000; matrix, 256 x 192; field of view, 220 x 176 mm) were obtained. To detect haemosiderin deposits, we performed a T2*-weighted gradient-echo pulse (echo-planar imaging [EPI]) sequence (section thickness, 6 mm; intersection gap, 0.6 mm; 2598/48; matrix, 256 x 192; field of view, 220 x 198 mm; EPI, 25). All sequences were performed in the axial plane parallel to the inferior border of the genu and splenium of the corpus callosum.

SLLs were defined as linearly arranged groups of rounded, circumscribed lesions just below the cortex at the junction of the grey and white matter with a signal intensity that was identical to that of cerebrospinal fluid (CSF) on images obtained with all pulse sequences. On each section of the brain, the following aspects of SLLs were assessed: anatomic location, distribution, bilaterality, size, and relation to other abnormalities such as WMHs and haemosiderin deposits. With the validated visual rating score of Scheltens et al, deep white matter lesions were rated on the basis of film hard copies of FLAIR MR images[59]. A Scheltens score of deep WMHs of 1 or more was considered to indicate presence of WMHs, while a score of 0 implied absence of deep WMHs. When SLLs were visible, the presence of haemosiderin deposits in the vicinity of the SLLs was recorded on the basis of T2*-weighted gradient-echo MR images. In addition, prevalence of SLLs in the groups of CADASIL patients and control subjects was assessed. Finally, in CADASIL patients, prevalence of SLLs was established in male and female patients separately, and the relationship between SLLs and age was established. All MR images were reviewed by the same neuroradiologist (MAvB) who was blinded to clinical and genetic data.

During this study, we reviewed histologic information about any subject participating in the study in whom this information might be available. In one patient who died and in whom we found SLLs before death, we had the opportunity to investigate formalin-fixed tissue of the anterior temporal lobe (tissue was investigated with permission of the family and was kindly

supplied by Frits F.J.M. Sutorius, MD, Stichting Laboratorium Pathologie Oost Nederland, Enschede, the Netherlands). Tissue was embedded in paraffin, and haematoxylin-eosin and Klüver-Barrera stains were used.

Descriptive statistics were calculated for differences in age and sex and for the presence of SLLs in various areas of the brain. The sensitivity and specificity of the presence of SLLs for the diagnosis of CADASIL were calculated by comparing data from CADASIL patients with data from the elderly subjects and from the HCHWA-D patients. Comparisons after grouping subjects by age (i.e., <30 years, 30–50 years, and >50 years) were assessed with the Fisher exact test. Values of $P<0.05$ were considered to represent a statistically significant difference. The statistical analysis was performed with SPSS-10 software (SPSS, Chicago, Ill).

## *Results*

The total number of participants from families with CADASIL was 54. Thirty-four participants had a mutation in the *NOTCH3* gene and 20 did not (for group characteristics, see table 1). In the majority of *NOTCH3* mutation carriers, the mutation was located in exon 4; in the remaining patients, it was located in exon 8, 19, or 20. Twenty-six mutation carriers were symptomatic; eight were asymptomatic. The group of mutation carriers included 17 women and 17 men, with a mean age of 45 years ± 12 (SD) and 46 years ± 11, respectively. In all CADASIL patients, deep WMHs were present. Eight (40%) of the CADASIL family members without mutations, 44 (59%) of the normal adults, 11 (69%) of the HCHWA-D patients, and 64 (85%) of the elderly patients with vascular risk factors had deep WMHs.

*Table 1 Characteristics of study groups*

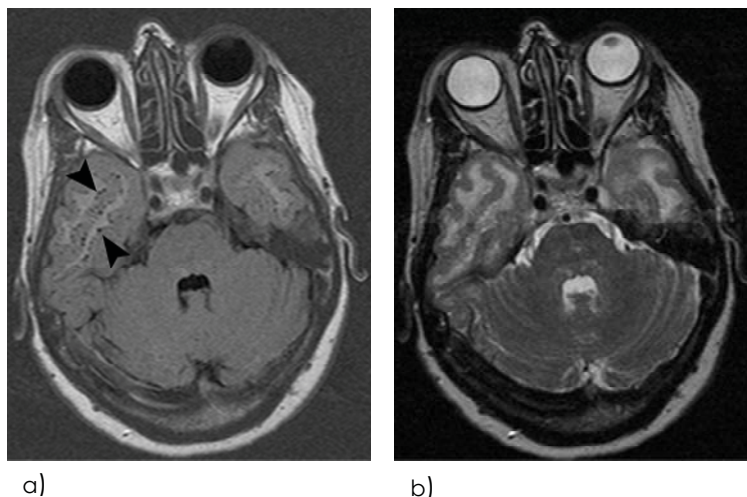| Study group | No. of subjects | Age (y) | | Sex | | No. of SLLs |
|---|---|---|---|---|---|---|
| | | Mean ± SD | Range | Men | women | |
| CADASIL patients | 34 | 46 ± 11 | 21-60 | 17 | 17 | 20 |
| CADASIL family members without mutation | 20 | 40 ± 13 | 22-67 | 8 | 12 | 0 |
| Healthy control subjects | 75 | 48 ± 8 | 34-62 | 24 | 51 | 0 |
| Elderly with vascular risk factors | 75 | 78 ± 3 | 72-85 | 56 | 19 | 0 |
| HCHWA-D patients | 16 | 48 ± 9 | 34-63 | 10 | 6 | 0 |

a)                    b)

*Figure 1 Axial MR images in patient with CADASIL at the level of the pons. Hyperintense confluent white matter lesions in the temporal lobe are visible on (a) a FLAIR image and a (b) T2-weighted image. On the FLAIR image, the SLLs (arrowheads) are clearly visible on the T2-weighted image they hardly be discriminated from the adjacent WMHs.*

Because of the high contrast between SLLs and WMHs on FLAIR MR images, SLLs were detected only on these images. Therefore, the results given next are based on the visibility of SLLs on FLAIR MR images. SLLs were found in 20 of 34 CADASIL patients (59%; mean age, 49 years ± 8) (table 1). The signal intensity of SLLs was equivalent to that of CSF on images obtained with all pulse sequences. The low contrast between these lesions and the abutting confluent areas with low signal intensity on T1-weighted images and high signal intensity on T2-weighted images lessened the visibility of SLLs with these sequences (figure 1). None of the four control groups had SLLs (table 1). Specificity and sensitivity of the presence of SLLs in CADASIL were 100% (95% CI: 98, 100) and 59% (95% CI: 41, 75), respectively (table 2). SLLs were found in one (20%) of five patients less than 30 years of age, in seven (50%) of 14 patients 30–50 years of age, and in 12 (80%) of 15 patients more than 50 years of age. The difference in prevalence of SLLs between these three age groups was significant (P<0.05). SLLs were more prevalent in male CADASIL patients: Eight female (47% of all women) versus 12 male (71% of all men) patients were affected, but the difference was not significant (P>0.05). When SLLs were present, they were numerous, their size varied between 1 and 2 mm, and they occurred in all cases in the temporopolar part of the brain (defined as the part anterior to the temporal horns[67]). In four patients, the lesions expanded from this anterior location posteriorly and affected the entire temporal lobe (figures 2a, 2b). In five patients (25%), SLLs were also located in the operculum of the frontal lobe (figure 2c). In one patient with extensive white matter

lesions, SLLs were visible throughout the whole temporal and frontal lobes (figure 2d). SLLs were never observed in the parietal and occipital lobes or infratentorially. The lesions had a symmetric distribution in 85% of patients; in 15% of patients, SLLs occurred unilaterally. SLLs invariably abutted white matter areas, with confluent areas of high signal intensity on FLAIR MR images. They were never found in juxtaposition to white matter with a normal appearance on images obtained with this sequence. The surface of the SLLs that abutted the cortical ribbon did not show signal intensity abnormalities. No evidence of haemosiderin deposits was found in the vicinity of the lesions.
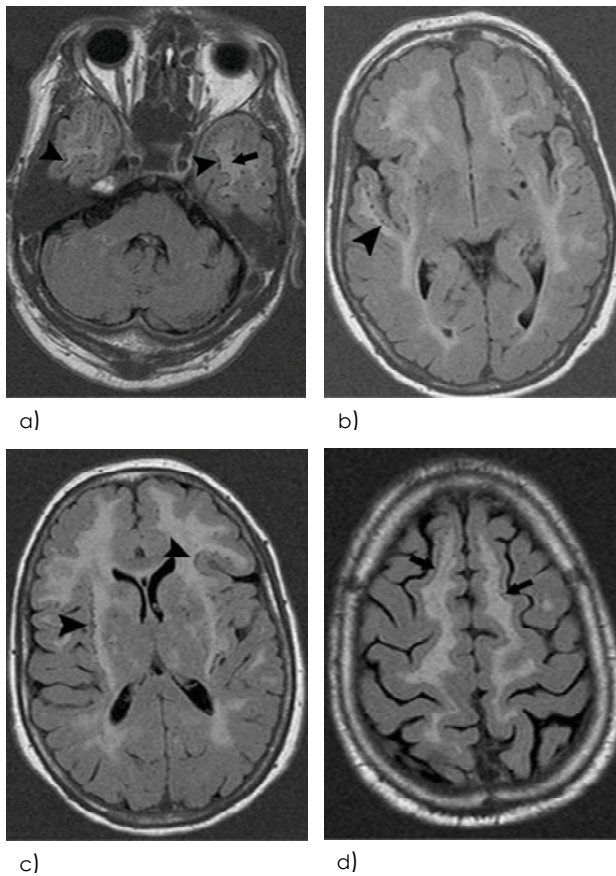


a)  b)  c)  d)

*Figure 2 Axial FLAIR MR images in four CADASIL patients at the level of (a) the pons, (b) the operculum of the temporal lobe, (c) the basal ganglia, and (d) the high convexity. Images show bilateral SLLs affecting a) the anterior part and (b) the operculum of the temporal lobe (arrowheads) at the junction of grey and white matter. The lesions are abutting WMHs (arrow in a). From this location, lesions could expand to (c) the subinsular region and operculum of the frontal lobe (arrowheads). (d) In one patient with extensive white matter lesions, subcortical lacunar lesions were visible throughout the whole frontal lobe (arrows).*

Histologic examination of the tissue sections of the anterior temporal lobe from one patient revealed vascular changes characteristic of CADASIL[7]. Furthermore, when slides were viewed macroscopically, they showed in several areas a typical periodicity of lacunae perpendicular to the border of the grey and white matter. This phenomenon was caused microscopically by a clear zone around perforating vessels (figure 3b). These vessels occasionally showed a thickened wall with granular material but often lacked obvious changes. The clear zone consisted of a distended perivascular space, which often contained some haemosiderin, and spongiosis (oedema) of the adjacent parenchyma (figure 3c). A row of several of these periodically arranged lacunae represent the substrate for the linear lesions observed at MR imaging (figure 3a).

*Table 2 Visibility of SLLs on FLAIR MR Images in the CADASIL group and in two other groups with conditions associated with small vessel disease and WMHs (elderly patients with vascular risk factors and patients with HCHWA-D)*

| SLLs status | CADASIL patients | Elderly and HCHWA-D patients (n = 91) |
|---|---|---|
| Present | 20 | 0 |
| Absent | 14 | 91 |
| Total | 34 | 91 |

*Note: The finding of SLLs on FLAIR MR Images has a sensitivity of 59% and a specificity of 100% for the diagnosis of CADASIL.*

## Discussion

In this article, we describe a type of lacunar lesion that, to our knowledge, has not been previously described in the neuroimaging literature in either patients with CADASIL or patients with other disorders. Microscopic examination reveals that the lacunae are caused by a distention of the perivascular space of perforating arteries at the level of the junction of grey and white matter and by spongiosis in the surrounding parenchyma. The observed widened perivascular space, which is known to contain CSF, provides an explanation for the observation in our study that the signal intensity of SLLs at MR imaging was equivalent to that of CSF. Furthermore, the presence of spongiosis in the surrounding parenchyma may explain the confluent aspect of SLLs that is frequently found at MR imaging. The abnormalities we found microscopically have a strong resemblance to the laminar lacunar lesions between the cortical ribbon and the subcortical white matter that have been described by Ruchoux et al in a post-mortem study of a patient with CADASIL[34]. The

presence of spongiosis and haemosiderin in the surrounding parenchyma suggests local damage to the blood-brain barrier at the junction of grey and white matter in perforating arteries.
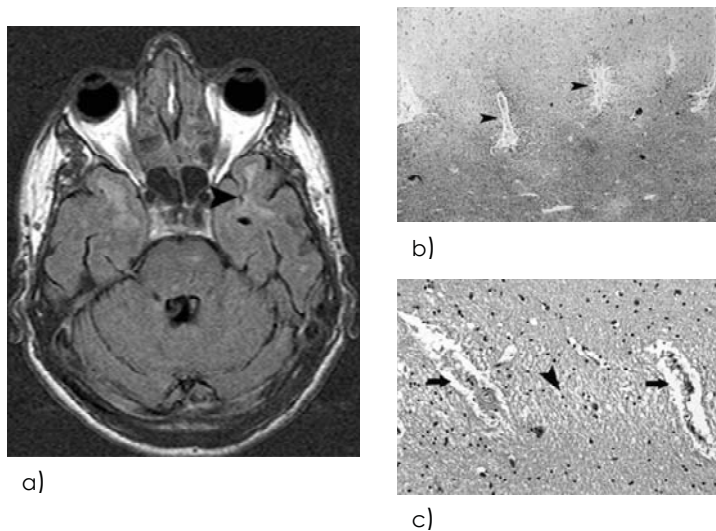


*Figure 3 Axial FLAIR MR image (a) in a patient with CADASIL in whom we obtained formalin-fixed tissue of the anterior temporal lobe after death. Subcortical lacunar lesions are present in the temporal lobe (arrowhead). Photomicrograph (b) shows a row of perforating vessels at the border of grey matter (top of image) and white matter with an obvious clear zone (arrowheads). (Klüver-Barrera stain; original magnification, x20.) Photomicrograph (c) shows detail of two vessels. The lower part of the vessel on the left shows characteristic thickening of the arterial wall; both vessels have a distended perivascular space (arrows) and spongiosis of the adjacent parenchyma (arrowhead). (Haematoxylin-eosin stain; original magnification, x100.*

Despite the histologic similarity of SLLs to dilated perivascular or Virchow-Robin spaces, it is possible to distinguish SLLs from otherwise widened Virchow-Robin spaces on MR images based on their location. At MR imaging, widened Virchow-Robin spaces are often seen in healthy individuals in the deep white matter of the high convexity, at the base of the brain adjacent to the anterior or posterior surface of the lateral portion of the anterior commissure, in the midbrain, and in the subinsular white matter[72]. SLLs cannot be confused with Virchow-Robin spaces in the white matter of the high convexity, at the base of the brain, and in the midbrain because (a) SLLs occur only at the subcortical junction of the grey and white matter and (b) the sites of predilection of SLLs are the anterior, temporal, and frontal lobes, where Virchow-Robin spaces are not usually found in healthy individuals. SLLs with a subinsular location could be confused with Virchow-Robin spaces because of their location. However, unlike Virchow-Robin spaces, SLLs appear only in the presence of WMHs, are always accompanied by SLLs in the anterior temporal lobe, and do not have the featherlike appearance that is characteristic of Virchow-Robin spaces in

this location[73]. In addition to being confused with Virchow-Robin spaces, SLLs can also be confused with normal variations in the temporal lobe. Hippocampal sulcus remnants are apparent at MR imaging as small circumscribed areas with a signal intensity similar to that of CSF in the hippocampus[74]. These structures can be differentiated from SLLs by their location because hippocampal sulcus remnants occur within the hippocampus and are surrounded by hippocampal grey matter, whereas SLLs are seen only at the cortical junction of grey and white matter. Furthermore, contrary to hippocampal sulcus remnants, SLLs will never appear only in this region; they are always accompanied by SLLs in the anterior part of the temporal lobe.

In this study, we observed SLLs in the temporal lobes and to a lesser extent in the frontal lobes. Within the temporal lobes, the anterior (temporopolar) part was a site of predilection for SLLs; this area was invariably affected in patients with SLLs. This distribution pattern of SLLs closely resembles the pattern of WMHs in CADASIL patients that has recently been described. Both Auer et al and O'Sullivan et al demonstrated that temporal pole WMHs are a characteristic finding of CADASIL, which enables the differentiation of CADASIL from Binswanger's disease[43,67]. In addition, Auer et al demonstrated that expansion of WMHs into the arcuate fibers is typical of CADASIL; this finding further helps in differentiating CADASIL from Binswanger's disease[67]. In addition to this similarity in distribution of SLLs and WMHs, in our study, SLLs were always observed to be abutting WMHs that had expanded into the subcortical arcuate fibers. The similarity in distribution of SLLs and WMHs and their invariable side-by-side occurrence suggests that they have the same pathogenesis. Both phenomena probably result from local degeneration of the perforating arteries at the level of the cortical junction of grey and white matter. The observation that SLLs were never found without WMHs expanding into arcuate fibers, whereas such WMHs lesions were found without SLLs, suggests that WMHs precede the occurrence of SLLs and that SLLs are a manifestation of more advanced disease than are WMHs.

Although SLLs were found in the majority of patients with CADASIL in our study, to our knowledge, the presence of SLLs has not been reported in the numerous previously published articles on neuroimaging findings in patients with CADASIL. This discrepancy between our and other imaging studies might be explained by our use of FLAIR MR images with thin sections (3 mm). In most previous MR imaging studies of CADASIL, only T1- and T2-weighted MR images were used for detecting brain lesions[39-41]. On T1- and T2-weighted images, SLLs are hard to detect because both SLLs and WMHs have low signal intensities on T1-weighted images and high signal intensities on T2-weighted images. The similar signal intensities and the existence of SLLs and WMHs in close proximity make it hard to detect the subtle SLLs at the border of the

larger and more obvious confluencing WMHs. However, on FLAIR images, a high contrast is generated between SLLs and WMHs. On FLAIR images, the signal intensity of CSF is selectively suppressed, rendering CSF and CSF-filled structures black, whereas the high signal intensity of most pathologic changes of brain parenchyma is maintained. Because of this high contrast, the CSF-filled SLLs are clearly visible on FLAIR MR images as black lesions between the grey cortex and the WMHs. Because SLLs are small, they are more visible when thin sections are used.

In conclusion, SLLs are a previously unreported imaging finding in patients with CADASIL. In this study, SLLs were found in 59% of patients with CADASIL; this suggests that SLLs are characteristic of the disease. SLLs were not found in healthy control subjects, which suggests that SLLs are not a normal condition like the physiologic Virchow-Robin spaces that are often detected at MR imaging in healthy individuals. SLLs were not found in two other populations with a high prevalence of WMHs induced by small vessel disease. This suggests that SLLs might be specific for CADASIL, and that detection of their presence may help to narrow the differential diagnosis and even establish the diagnosis in patients with WMHs. Further studies of the occurrence of SLLs in other cerebral diseases are needed to assess the specificity of SLLs for CADASIL.

# CADASIL: MR imaging findings at different ages, 3rd-6th decade

FOUR

# CADASIL: MR imaging findings at different ages, 3rd-6th decade

R. van den Boom
S.A.J. Lesnik Oberstein
M.D. Ferrari
J. Haan
M.A. van Buchem

## Abstract

Purpose was to depict various brain lesions that have been described in patients who have cerebral autosomal dominant arteriopathy with subcortical infarcts and leukoencephalopathy (CADASIL) with prospective standardized magnetic resonance (MR) imaging in patients of different age groups.

Forty patients with CADASIL in different age groups (20–30 years, n=5; 31–40 years, n=4; 41–50 years, n=16; 51–60 years, n=15) underwent axial MR imaging with T1-weighted dual fast spin-echo, fluid-attenuated inversion-recovery, and T2*-weighted gradient-echo sequences. Images were analyzed by one neuroradiologist for the presence of areas of hyperintensity, lacunar infarcts, microbleeds, and subcortical lacunar lesions (SLLs) in different anatomic locations. Descriptive statistics were obtained for the presence of MR imaging abnormalities in various brain areas and for distribution according to age.

The mean age of the 40 mutation carriers (21 women, 19 men) was 45 years ± 10 (SD). In patients with CADASIL who were 20–30 years old, characteristic hyperintense lesions in the anterior temporal lobe (100% [five of five]) and SLLs (20% [one of five]) were the only abnormalities seen on MR images. In patients who were 30–40 years old, lacunar infarcts were found in 75% (three of four) of cases. More areas of hyperintensity were noted, and they frequently involved the external capsule, basal ganglia, and brainstem. In patients 41–50 years old, microbleeds were observed in 19% (three of 16). In patients older than 50 years, areas of hyperintensity (100% [15 of 15]), SLLs (73% [11 of 15]), lacunar infarcts (93% [14 of 15]), and microbleeds (47% [seven of 15]) were frequently observed.

The four types of brain lesions that are observed in patients with CADASIL were seen in patients of different age groups.

*Introduction*

Cerebral autosomal dominant arteriopathy with subcortical infarcts and leukoencephalopathy (CADASIL) is an inherited systemic disease of the small artery caused by mutations in the *NOTCH3* gene on chromosome 19[19]. Histopathological studies of the small and medium-sized leptomeningeal arteries and the long perforating arteries of the brain revealed luminal narrowing or even obliteration caused by deposition of electron-dense granular material close to the membrane of the vascular smooth muscle cells, as well as loss of vascular smooth muscle cells[7]. Clinical manifestations of the disease include ischemic stroke, dementia, migraine with aura, and mood disturbances[75]. The first clinical manifestations of the disease often start in patients during the 3rd decade, and death often occurs in patients during the 6th decade[75]. Main magnetic resonance (MR) imaging findings in patients with CADASIL are diffuse areas of hyperintensity of white matter that occur predominantly in the subcortical areas and lacunar infarcts that are present in the semiovale centre, the thalamus, the basal ganglia, and the pons[39-41]. Recent MR imaging study findings demonstrated microbleeds and subcortical lacunar lesions (SLLs) as additional radiologic features of CADASIL[76-78].

The definite diagnosis of CADASIL is established with detection of *NOTCH3* mutations, and detection of these mutations is a laborious process that is performed at a limited number of specialized centres. Presently, *NOTCH3* mutation analysis is considered only in patients who have unexplained neurologic symptoms, such as ischemic episodes, cognitive deficits, and a positive family history of these symptoms, and who have suggestive MR imaging abnormalities. The radiologic findings of patients with advanced stages of the disease are well documented. On the basis of these descriptions, radiologists can adequately help in the identification of patients with an indication for further molecular or pathologic testing for CADASIL[39-43,67]. However, the radiologic appearances during earlier stages of the disease have not been described in detail, and this lack of information may lead to inadequate guidance of patients through the diagnostic work-up.

To our knowledge, findings of the only published study about the development of cerebral changes over time in patients with CADASIL were reported by Chabriat et al[39]. In that study, the development of areas of hyperintensity and of lacunar infarcts was studied in the periventricular and subcortical white matter, the basal ganglia, and the infratentorial areas. However, after publication of that study, other radiologic hallmarks of CADASIL, such as SLLs, microbleeds, and areas of hyperintensity in the anterior temporal lobe and in the external capsule, were detected6[67,76-78]. The temporal evolution of these more recently described radiologic phenomena of CADASIL remains to be

elucidated. Thus, the purpose of our study was to depict various brain lesions that have been described in patients who have CADASIL with prospective performance of standardized MR imaging in patients of different age groups.

## Materials and methods

### Subjects

Members of 15 unrelated Dutch families who had CADASIL were asked to participate in a study about the clinical, radiologic, and genetic aspects of CADASIL in patients from the Netherlands. In each family, at least one member had a confirmed *NOTCH3* mutation. These patients were referred to Leiden University Medical Centre from various medical centres; this institution serves as a national CADASIL referral centre. The total number of participants was 63 and included symptomatic, as well as asymptomatic, family members. Participants were considered symptomatic when they had a history of neurologic deficits or cognitive decline. The diagnosis of CADASIL was confirmed after the MR imaging examination with identification of pathogenic mutations of the *NOTCH3* gene, as previously described[22].

The families included in this study were all of the families seen between August 1999 and July 2000. To ensure informed consent, only cognitively capable subjects were included in this study. The institutional medical ethics committee approved the study protocol. Since one individual of the 63 participants did not consent to undergo MR imaging, the final number of subjects was 62; 40 of these subjects had a mutation in the *NOTCH3* gene and 22 did not.

### MR imaging

All MR imaging examinations were performed with a 1.5-T MR system (Philips Medical systems, Best, the Netherlands). Participants underwent MR imaging with a standardized protocol that included the following: conventional T1-weighted spin-echo (repetition time msec/echo time msec, 600/20; section thickness, 6.0 mm; intersection gap, 0.6 mm; matrix, 256 x 205; field of view, 220 x 165 mm), dual T2-weighted fast spin-echo (3000/27, 120; section thickness, 3.0 mm; intersection gap, 0 mm; matrix, 256 x 205; field of view, 220 x 220 mm), and fast fluid-attenuated inversion-recovery (FLAIR) (repetition time msec/echo time msec/inversion time msec, 8000/100/2000; section thickness, 3.0 mm; intersection gap, 0 mm; matrix, 256 x 192; field of view, 220 x 176 mm) sequences. In addition, a T2*-weighted gradient echo planar (2598/48; section thickness, 6.0 mm; intersection gap, 0.6 mm; matrix, 256 x 192; field of view, 220 x 198 mm; echo-planar imaging factor, 25) sequence was

performed to detect haemosiderin deposits. All images were obtained in the axial plane parallel to the inferior border of the genu and splenium of the corpus callosum.

Areas of hyperintensity were defined as areas of brain parenchyma with increased signal intensity on intermediate, T2-weighted, and FLAIR MR images, and they were rated from hard copies of axial dual T2-weighted fast spin-echo MR images with the semiquantitative visual scoring system described by Scheltens et al[59]. In this scale, the brain is anatomically divided into deep white matter, basal ganglia, and infratentorial regions. For each region, a score of 0–6 is assigned according to the following scale: score 0, absent; score 1, up to five areas of white matter hyperintensity of less than 3 mm in diameter; score 2, six or more areas of white matter hyperintensity of less than 3 mm in diameter; score 3, as many as five areas of white matter hyperintensity of 4–10 mm in diameter; score 4, six or more areas of white matter hyperintensity of 4–10 mm in diameter; score 5, one or more areas of white matter hyperintensity of more than 10 mm in diameter; and score 6, confluent areas of white matter hyperintensity. In addition, scores were assigned to the frontal and occipital periventricular "caps" and periventricular "bands" as follows: score 0, absent; score 1, as much as 5 mm in diameter; and score 2, more than 5 mm in diameter. Because the Scheltens scoring system does not fully reflect the characteristic lesion distribution in patients who have CADASIL, three anatomic locations were added to the Scheltens score: external and internal capsule and the temporal region. The external and internal capsules were assigned separate scores for the presence of areas of subcortical hyperintensity, and the temporal region was assigned a separate score for the presence of areas of periventricular hyperintensity. In our experience, areas of hyperintensity in young patients who have CADASIL often are located in the anterior temporal lobe; for this reason, we assigned separate scores for the presence of areas of hyperintensity in the anterior temporal lobe and the posterior temporal lobe. We defined the border between the anterior temporal lobe and the posterior temporal lobe as the posterior margin of the amygdala[43]. To obtain an overall supratentorial lesion load score, the periventricular score was added to the Scheltens subcortical score. To calculate the prevalence of areas of hyperintensity, a Scheltens score of 1 or higher was considered to be positive for areas of hyperintensity, and a score of 0 implied absence of areas of hyperintensity.

Lacunar infarcts were defined as parenchymal defects that did not extend to the cortical grey matter, with a signal intensity similar to that of cerebrospinal fluid with all pulse sequences, irrespective of size. There are three locations where lacunar infarcts can be difficult to distinguish from normal Virchow-Robin spaces: the basal ganglia, the subinsular region, and the semiovale

centre. To differentiate a lacunar infarct from a Virchow-Robin space, we excluded lesions in the following areas because they were most likely to represent a Virchow-Robin space: (a) basal ganglia: lesions that were isointense to cerebrospinal fluid with all pulse sequences and were located in the lower one-third of the corpus striatum[79,80]; (b) subinsular region: areas with a featherlike configuration that were isointense to cerebrospinal fluid on T1- and T2-weighted MR images but did not have high signal intensity on FLAIR images[73]; (c) semiovale centre: all lesions with a transverse diameter of 2 mm or smaller or with a tubular appearance following the course of perforating arteries[81].

Microbleeds were defined as focal areas of signal intensity loss on T2-weighted fast spin-echo MR images that increased in size on the T2*-weighted gradient-echo images ("blooming effect")[76]. In this way, microbleeds were differentiated from areas of signal loss that were based on vascular flow voids. Areas of symmetric hypointensity of the globus pallidus that were likely to represent calcification or nonhemorrhagic iron deposits were excluded.

SLLs were defined as linearly arranged groups of rounded circumscribed lesions that were just below the cortex at the grey matter–white matter junction and had a signal intensity that was identical to that of cerebrospinal fluid with all pulse sequences[78].

One experienced neuroradiologist (MAvB) who was blinded to the diagnosis of CADASIL assessed the presence of areas of hyperintensity, lacunar infarcts, microbleeds, and SLLs in all 62 participants. For lacunar infarcts and microbleeds, size and number were assessed in the following brain areas: supratentorial region (frontal, temporal, occipital, and parietal lobes and internal and external capsules), infratentorial region (cerebellum, pons, medulla oblongata, and mesencephalon), thalamus, and basal ganglia (globus pallidus, caudate nucleus, and putamen). The presence of SLLs was assessed in each patient who had CADASIL.

### Statistical analysis

Descriptive statistics were obtained in regard to the presence of MR imaging abnormalities in various areas of the brain according to age (percentage of patients affected per anatomic structure per decade). Differences in areas of hyperintensity, lacunar infarcts, and microbleeds between male and female patients who had CADASIL were investigated with the Student t-test for unpaired data. Differences in SLLs were tested by using the $X^2$ test. A difference with $P<0.05$ was considered significant. A statistical software package (SPSS-10; SPSS, Chicago, Ill) was used for data analysis.

## Results

### Subjects

One individual did not consent to undergo MR imaging. Of the 62 family members who had CADASIL, 40 individuals had a mutation in the *NOTCH3* gene and 22 did not. The mean age of the 40 mutation carriers who were included in our study population was 45 years ± 10 (SD) (range, 21–59 years); 21 women (mean age, 45 years ± 11) and 19 men (mean age, 46 years ± 10) were included. The age and sex distribution of the 40 mutation carriers are listed in table 1. Thirty-two of the 40 *NOTCH3* mutation carriers had a mutation in exon 4; the remaining eight patients had mutations in exon 19, 20, 8, or 11. Thirty-two mutation carriers were clinically symptomatic. The symptoms varied in severity, ranging from one transient ischemic attack to multiple strokes and cognitive decline.

*Table 1 Baseline characteristics of NOTCH3 mutation carriers according to age group*

| Characteristic | 20-30 years | 31-40 years | 41-50 years | 51-60 years |
|---|---|---|---|---|
| No. of patients | 5 | 4 | 16 | 15 |
| Sex | | | | |
| M | 2 | 2 | 7 | 7 |
| F | 3 | 2 | 9 | 8 |
| Clinical manifestation | | | | |
| Symptomatic | 0 | 3 | 14 | 15 |
| Asymptomatic | 5 | 1 | 2 | 0 |

### MR imaging

Figure 1 shows the prevalence of areas of hyperintensity, SLLs, lacunar infarcts, and microbleeds among patients of different age groups. Areas of hyperintensity were observed in all mutation carriers. The load of areas of hyperintensity as quantified with the Scheltens score did not differ significantly (P=0.5) between men (mean score, 52) and women (mean score, 48). Thirty-two (80%) of 40 mutation carriers had lacunar infarcts, with a mean of 19 (range, 1–60) lacunar infarcts per patient. This group of mutation carriers with lacunar infarcts had a mean age of 49 years ± 6 (age range, 38–59 years). Men had significantly (P=0.01) more lacunar infarcts (n=22) than did women (n=9). Microbleeds were found in ten (25%) mutation carriers, with a mean age of 53 years ± 5 (age range, 43–58 years). Per patient, a mean of nine microbleeds (range, 1–35) was found. The prevalence of microbleeds did not differ significantly (P=0.3) between men and women. Twenty-two (55%)

mutation carriers with a mean age of 49 years ± 8 (age range, 25–59 years) had SLLs. SLLs were significantly (P=0.02) more prevalent in men (n=14) than they were in women (n=8).
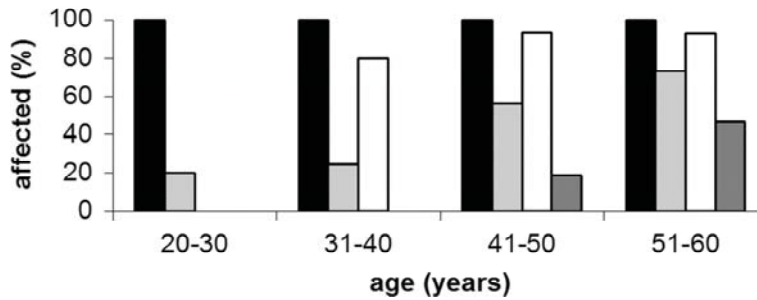


*Figure 1 Graph shows prevalence of areas of hyperintensity (black bars), SLLs (light grey bars), lacunar infarcts (white bars), and microbleeds (dark grey bars) in different age groups. Areas of hyperintensity were present in all mutation carriers. SLLs were found in patients in the 3rd decade and older; lacunar infarcts, in those in the 4th decade and older; and microbleeds, in those in the 5th decade and older.*
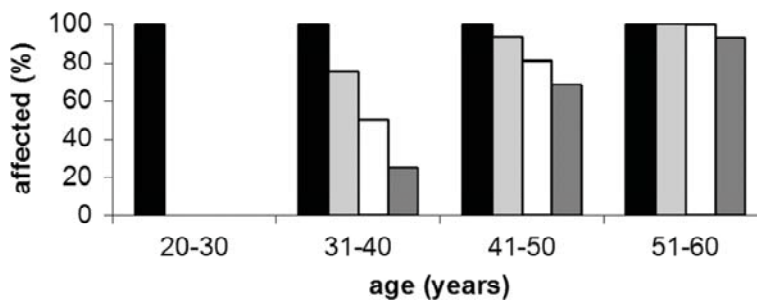


*Figure 2 Graph shows prevalence of areas of hyperintensity per location in relation to age. In patients in the 3rd decade, only supratentorial areas of hyperintensity (black bars) were present. With increasing age, areas of hyperintensity were found in other locations too. In patients in the 6th decade, almost all mutation carriers had areas of hyperintensity in every region. Areas of hyperintensity were observed in the following areas: thalamus (white bars), infratentorial region (light grey bars), and basal ganglia (dark grey bars).*

Figure 2 shows the prevalence of areas of hyperintensity in different age groups classified according to the supratentorial white matter, the infratentorial structures, the basal ganglia, and the thalamus. In patients in the 3rd decade, only areas of hyperintensity in the supratentorial white matter were present (figure 3). Areas of hyperintensity in the infratentorial structures, the basal ganglia, and the thalamus were present in patients in the 4th decade. In the 6th decade, all mutation carriers had areas of hyperintensity in each compartment. To further characterize the distribution of areas of hyperintensity

within the supratentorial white matter at different times, we subcategorized this compartment into several anatomic regions and assessed the presence of areas of hyperintensity in the different age groups (figure 4). In all young mutation carriers, subtle areas of hyperintensity in the anterior temporal lobe were found (figure 3). Although the occipital lobe was less affected in patients younger than 40 years as compared with other lobes, all lobes were equally affected in patients older than 40 years. Areas of hyperintensity in the external capsule were present in patients older than 30 years; areas of hyperintensity in the internal capsule were seen in patients older than 40 years (figures 5, 6). Frontal periventricular areas of hyperintensity and periventricular bands were seen in four mutation carriers; temporal periventricular areas of hyperintensity, in two mutation carriers; and occipital periventricular areas of hyperintensity, in one mutation carrier younger than 30 years. The total periventricular Scheltens score in this group varied between 0 and 4. In patients older than 30 years, all mutation carriers had periventricular areas of hyperintensity in every region. With the exception of one mutation carrier who had a score of 3, all other patients had a total periventricular Scheltens score that varied between 6 and 8, the maximal score for periventricular areas of hyperintensity.
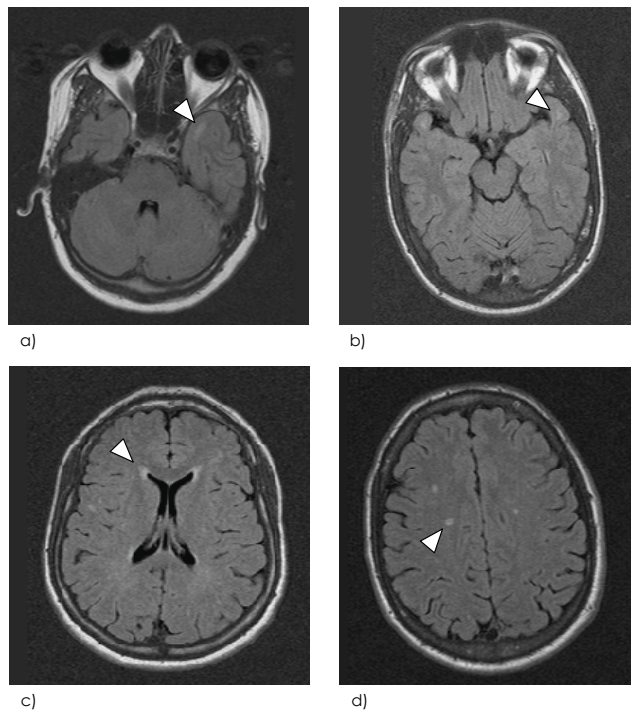


a)

b)

c)

d)

*Figure 3 Axial FLAIR MR images in NOTCH3 mutation carriers who were 20-30 years old (a-d). Image shows areas of hyperintensity (arrowhead in a) in the anterior temporal lobe. Image shows SLLs (arrowhead in b). Image shows small ventricular caps (arrowhead in c). Image shows small areas of hyperintensity in the semiovale centre (arrowhead in d).*
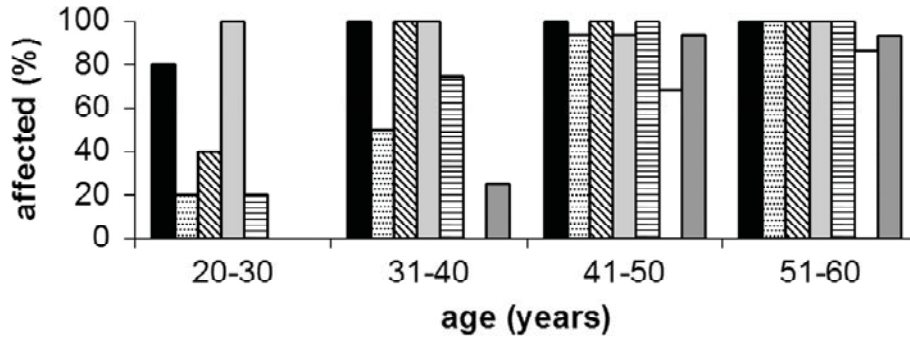
Figure 4 Graph shows supratentorial areas of hyperintensity distributed among the different regions according to age. In the 3rd decade in all mutation carriers, areas of hyperintensity were observed in the anterior temporal lobe. Areas of hyperintensity were found in the external capsule in patients in the 4th decade and older and in the internal capsule in patients in the 5th decade and older. Areas of hyperintensity were observed in the following regions: frontal lobe (black bars), occipital lobe (dotted bars), parietal lobe (diagonally striped bars), temporal anterior lobe (light grey bars), temporal posterior lobe (horizontally striped bars), internal capsule (white bars), and external capsule (dark grey bars).
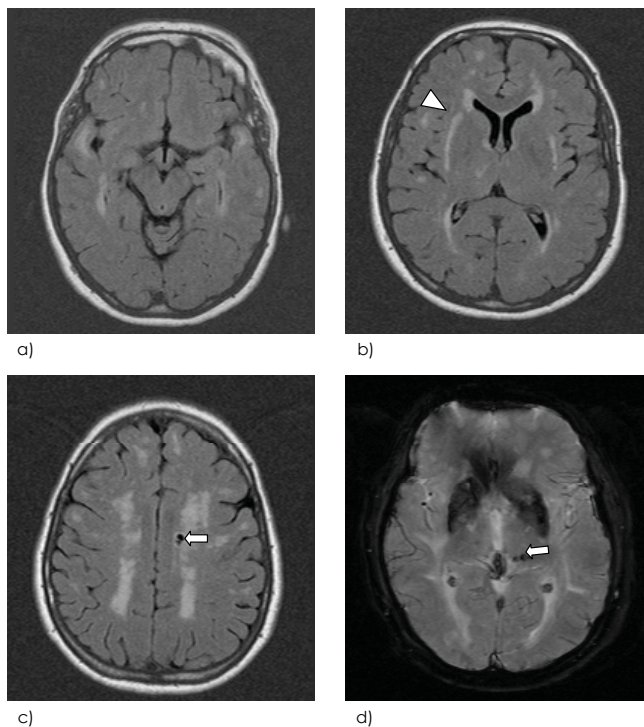


Figure 5 Axial FLAIR MR images (a-c). T2*-weighted gradient-echo MR image (d). Images obtained in NOTCH3 mutation carriers who were 41-50 years old show confluent areas of hyperintensity in all lobes (a-c). Involvement of the external capsule (arrowhead) is an important feature at this age. Lacunar infarcts (arrow in c) and microbleeds (arrow in d) are present.

Of the total 606 lacunar infarcts, 249 were located in the basal ganglia; lacunar infarcts were also found in the frontal lobe (n=125), the parietal lobe (n=129), the temporal lobe (n=44), the pons (n=27), the thalamus (n=22), the cerebellum (n=5), the occipital lobe (n=4), and the mesencephalon (n=1). Only 10 (1.7%) lacunar infarcts were larger than 10 mm in diameter. Figure 7 shows the prevalence of lacunar infarcts per location in the different age groups. The supratentorial lacunar infarcts were seen in patients in the 4th decade, and their prevalence was greater in those during the 5th decade (figures 5, 6, 8). Lacunar infarcts in the basal ganglia were present in patients in the 4th decade. In patients in the 5th decade, their prevalence was 81%, and this percentage was the same in patients during the 6th decade. In the 6th decade, *NOTCH3* mutation carriers had lacunar infarcts in the infratentorial region (53%) and in the thalamus (47%).
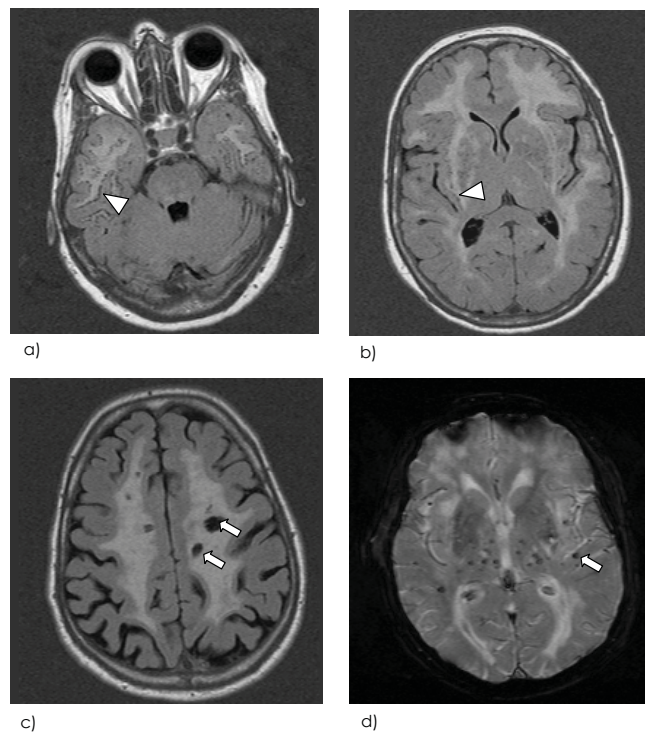


a)

b)

c)

d)

*Figure 6 Axial FLAIR MR images(a-c). T2\*-weighted gradient-echo MR image(d). Images obtained in NOTCH3 mutation carriers who were 51-60 years old show complete penetrance of CADASIL: confluent areas of hyperintensity (a-c), lacunar infarcts (arrows in c), SLLs (arrowheads), and microbleeds (arrow in d).*
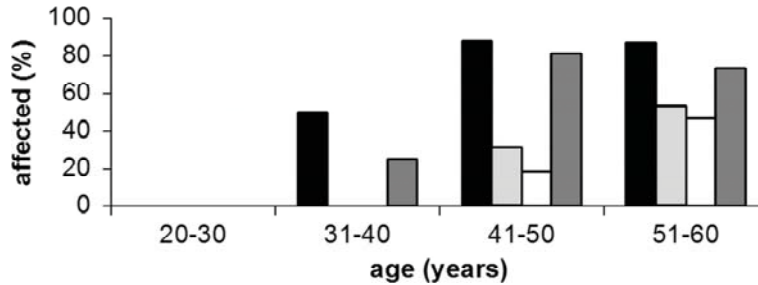
*Figure 7 Graph shows prevalence of lacunar infarcts per location in relation to age. In patients in the 4th decade, lacunar infarcts were present in the supratentorial region (black bars) and in the basal ganglia (dark grey bars). Lacunar lesions in the infratentorial region (light grey bars) and in the thalamus (white bars) were present in patients older than 40 years.*

The distribution of the total 85 microbleeds was as follows: thalamus (n=53), occipital lobe (n=11), temporal lobe (n=5), cerebellum (n=5), brainstem (n=4), parietal lobe (n=4), basal ganglia (n=2), and frontal lobe (n=1). Seventy-eight (92%) microbleeds were smaller than 5 mm in diameter; the largest was 10 mm in diameter (figures 5, 6). The prevalence of microbleeds per location in the different age groups is illustrated in figure 9.

## Discussion

The spectrum of MR imaging abnormalities in patients who have CADASIL has been described in several studies[39-43,77,78]. These abnormalities include areas of hyperintensity, lacunar infarcts, a characteristic pattern of SLLs, and microbleeds. To the best of our knowledge, this study is the first to determine the presence of these lesions, on the basis of radiologic appearances in patients with CADASIL during the 3rd, 4th, 5th, and 6th decades.

As early as the 3rd decade, cerebral abnormalities can be found in patients who have CADASIL. In this study, supratentorial areas of hyperintensity were observed in all patients, and SLLs were observed in one patient. A notable site of predilection of the areas of hyperintensity is the anterior temporal lobe. These areas of hyperintensity are found in all patients of this age group, invariably as a highly characteristic pattern of bilateral hyperintense areas located directly below the cortical ribbon. Although this type of abnormality has been described by others as a characteristic finding in patients who have CADASIL, the early involvement of the anterior temporal lobe has not been reported before, to our knowledge[67]. A pattern of multiple, although often few, small patches with high signal intensity was observed in other locations. Periventricular white matter areas of hyperintensity are frequently seen as smooth caps around the frontal horns and seldom are seen around

the posterior and temporal horn of the lateral ventricles. In young patients, SLLs were another characteristic observation, and SLLs always were observed in conjunction with the observation of areas of hyperintensity in the anterior temporal lobe. SLLs are a recently described abnormality that is considered to be specific for CADASIL[92]. The radiologic phenomenon of SLLs is based on the presence of dilated perivascular spaces of perforating arteries at the level of the grey matter–white matter junction and spongiosis in the surrounding parenchyma. Detection of areas of hyperintensity with or without SLLs in the anterior temporal lobes in young patients is highly characteristic of findings in young patients with CADASIL, and detection of these areas of hyperintensity suggests the diagnosis.

In the 4th decade, in addition to areas of hyperintensity and SLLs, lacunar infarcts were seen in patients who have CADASIL. These lacunar infarcts are found in 75% of patients of this age group, and they occur in the supratentorial white matter and in the basal ganglia. In the supratentorial white matter, areas of hyperintensity in the external capsule are a new finding in this age group, and this finding can be observed in 25% of patients. The prevalence of subcortical areas of hyperintensity increases in all lobes, and larger periventricular areas of hyperintensity are present. Subcortical and periventricular areas of hyperintensity may become confluent. The areas of hyperintensity in the anterior temporal lobe increase in size and expand posteriorly in the temporal lobe. Apart from the supratentorial white matter, areas of hyperintensity are now also observed in the basal ganglia, the thalamus, and the brainstem. Although the number of patients in whom SLLs are observed does not increase, the number of SLLs per patient is higher than it is in the preceding age group, and the distribution of SLLs follows the expanding white matter areas of hyperintensity of the anterior temporal lobes.

In patients in the 5th decade, microbleeds may be observed in addition to areas of hyperintensity, SLLs, and lacunar infarcts. Microbleeds are found in 19% of patients in this age group, and they can be observed in the thalamus, the brainstem, and the supratentorial white matter. The number of patients in whom areas of hyperintensity are observed further increases, although there are still patients in whom areas of hyperintensity are not observed in the infratentorial white matter, in the basal ganglia, or in the thalamus. The number and size of areas of hyperintensity further increase, giving rise to large confluent areas of high signal in subcortical and periventricular white matter. Areas of hyperintensity can also involve the internal capsule. The prevalence of lacunar infarcts (94%) and SLLs (56%) increases. Now lacunar infarcts also are present in the brainstem and the thalamus.
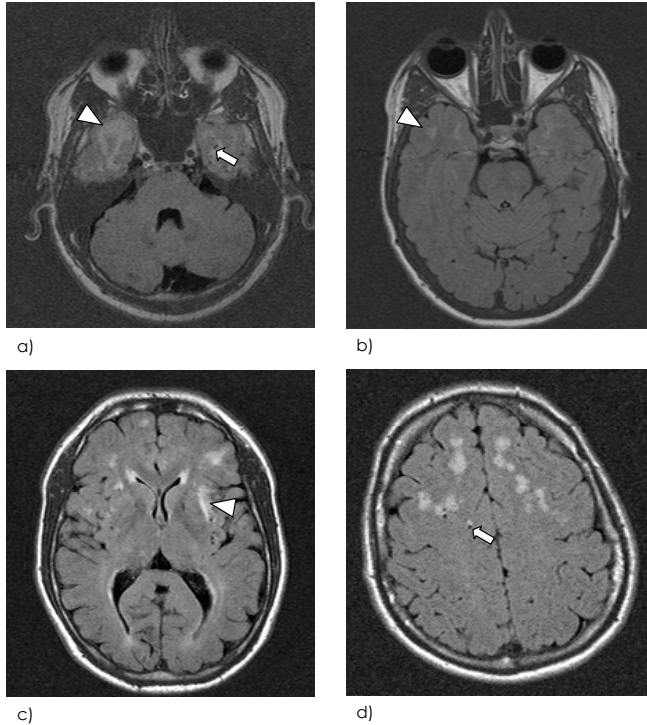
*Figure 8 Axial FLAIR MR images obtained in NOTCH3 mutation carriers who were 31-40 years old. At this age, areas of hyperintensity (arrowhead in a and b) and SLLs (arrow in a) expand from the anterior temporal lobe posteriorly and affect the whole temporal lobe. Areas of hyperintensity in the semiovale centre become larger. Areas of hyperintensity in the external capsule (arrowhead in c) and lacunar infarcts (arrow in d) are present.*

In patients in the 6th decade, no new types of lesions are seen, and areas of hyperintensity, SLLs, lacunar infarcts, and microbleeds are observed in most patients. Areas of hyperintensity are always found in all lobes, in the brainstem, in the basal ganglia, and in the thalamus. In almost all cases, areas of hyperintensity are also found in the internal and external capsule. During this stage, most of the supratentorial white matter may show a symmetric pattern of large homogeneous areas of increased signal intensity involving the subcortical and periventricular white matter. Lacunar infarcts are found in more than 90% of cases. SLLs are found in 73% of cases; microbleeds, in 47%. SLLs may now be observed in the temporal lobe, in the subinsular white matter, and in the operculum of the frontal lobe.

In patients older than 30 years, CADASIL shares several radiologic characteristics with other diseases accompanied by small vessel disease, which implies that differentiating CADASIL from these disorders based on findings of radiologic examinations may be difficult. Nonspecific areas of hyperintensity in the periventricular, the frontal, the parietal, and the occipital regions are seen

in a number of other small vessel diseases[82]. Brainstem abnormalities located predominantly at the rostrocaudal centre of the pons are frequently observed in patients who have CADASIL, but they can also be found in patients who have atherosclerosis[83]. The occurrence of lacunar infarcts and microbleeds is also considered to be characteristic of cerebral small vessel disease in general and is not characteristic of only CADASIL[55,84]. Still, the distribution of the areas of hyperintensity and the presence of SLLs seem to specifically suggest the diagnosis of CADASIL. By using image post processing software that is based on statistical parametric mapping, Auer et al compared patterns of areas of hyperintensity in a group of patients who had CADASIL and a group of patients who had Binswanger's disease[67]. In that study, it was suggested that the presence of white matter areas of hyperintensity in the anterior temporal lobe was characteristic of patients who had CADASIL. The image processing technique used in that study only permitted detection of differences between groups and did not help in determination of the diagnosis in patients. In our study, the characteristic areas of hyperintensity in the anterior temporal lobe were present in 39 of 40 patients who had CADASIL, and this result demonstrates that the prevalence of this finding in patients who have CADASIL is high, which makes it a useful radiologic hallmark of the disease. The presence of areas of hyperintensity in the external capsule also has been described to be characteristic of CADASIL[43]. Because of its high prevalence (94%) among patients with CADASIL after the age of 40, this is another sign that is helpful in the suggestion of the diagnosis later during the course of the disease. Finally, the prevalence of SLLs increases considerably in patients older than 40 years, and therefore, this lesion is helpful for detection of the disease in patients with increasing age.
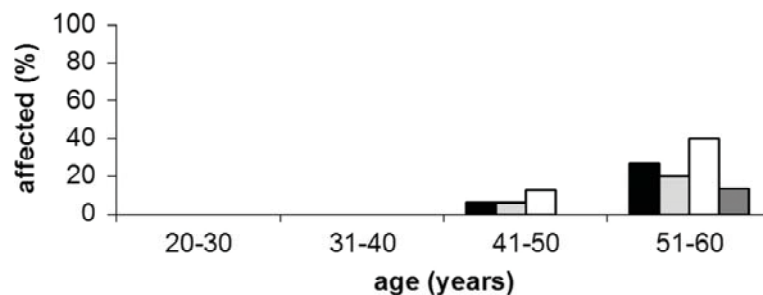


*Figure 9 Graph shows prevalence of microbleeds per location in relation to age. Microbleeds were present in patients older than 40 years, predominantly in the thalamus (white bars). Graph also shows data for those observed in the following areas: supratentorial region (black bars), infratentorial region (light grey bars), and basal ganglia (dark grey bars).*

In our study, men were more frequently affected by lacunar infarcts and SLLs than were women. For this observation, there is no simple explanation. A difference in age at death between men and women who have CADASIL has been found[19]. Death occurs at a significantly younger age in men, and although this difference may reflect the generally observed difference in life expectancy, it may also be caused by differences in the disease dynamics in men and women.

In summary, in patients who have CADASIL, imaging abnormalities are found in the brain earlier than expected clinically. In young patients who have CADASIL, cerebral abnormalities are highly characteristic, although limited. The areas of hyperintensity in the anterior temporal lobe and the SLLs that are observed in these young patients continue to help in the recognition of the underlying condition later in life.

# Incipient CADASIL

# Incipient CADASIL

S.A.J. Lesnik Oberstein
R. van den Boom
H.A.M. Middelkoop
M.D. Ferrari
Y.M. Knaap
H.C. van Houwelingen
M.H. Breuning
M.A. van Buchem
J. Haan

## Abstract

Cerebral autosomal dominant arteriopathy with subcortical infarcts and leukoencephalopathy (CADASIL) is caused by mutations in the *NOTCH3* gene. Knowledge of disease expression in young adult *NOTCH3* mutation carriers (MCs) is limited. The aim of the study was to characterize clinical, neuropsychological, and radiological status in *NOTCH3* MCs younger than 35 years.

Individuals younger than 35 years who were at a 50% risk of a *NOTCH3* mutation, from our CADASIL database. Thirteen individuals, from 8 families, met the criteria. *NOTCH3* mutation carriership was determined in these individuals after completion of clinical, genetic, neuropsychological, and radiological investigations in order to be able to compare mutation carriers (MCs) to non mutation carriers (NMCs) in a double-blinded setting. Magnetic resonance images were scored according to a standardized white matter hyperintensities rating scale.

Six individuals, from five families, were MCs. Clinical symptoms consisted of migraine (with aura), stroke, and stroke like episodes. We did not find evidence for psychiatric disturbances, functional disability, or cognitive dysfunction, compared with non-MCs. Radiologically, a characteristic magnetic resonance imaging lesion pattern emerged for all MCs. This comprised white matter hyperintensities in the anterior temporal lobes, the frontal lobes, and the periventricular frontal caps.

In conclusion migraine (with aura) and stroke can present in *NOTCH3* MCs younger than 35 years; however, more importantly, physical function and cognition are intact. Possible subtle cognitive dysfunction needs to be assessed in a larger study. White matter hyperintensities on magnetic resonance imaging are characteristic, and are consistently visualized from the age of 21 years and onward. Awareness of the clinical and radiological features of CADASIL in those younger than 35 years should increase early diagnosis and allow for customized counselling of young adults from families with CADASIL.

## Introduction

Cerebral autosomal dominant arteriopathy with subcortical infarcts and leukoencephalopathy (CADASIL) is a hereditary microangiopathy caused by mutations in the *NOTCH3* gene[19]. Distinctive ultrastructural granular osmiophilic material in the vascular media and degeneration of vascular smooth muscle cells compose the pathological hallmark[51,85]. The clinical diagnosis of CADASIL is considered in patients with otherwise unexplained central nervous system symptoms, extensive white matter changes with or without subcortical infarctions on magnetic resonance (MR) imaging, and a family history of neurological disorders[10]. The disease presentation and natural history are diverse, but, typically, the diagnosis is made in the fifth decade of life when mutation carriers (MCs) present with recurrent stroke like episodes and/or cognitive decline. Up to 40% of persons diagnosed as having the disease have a history of migraine with aura, with onset in their mid-20s. Psychiatric disturbances can play a role in about a third of affected individuals[10].

CADASIL is considered a late-onset hereditary disease, with a mean age at onset of 45 years[8]. Abnormalities on MR imaging are present before the onset of clinical symptoms, and it is generally accepted that by the age of 35 years, all *NOTCH3* MCs have white matter hyperintensities (WMHs) to some extent[6,8,86]. Although several studies have included clinical or radiological, reports of asymptomatic MCs, these studies did not focus specifically on young adults[8,10,39,42,87]. This prompted us to prospectively study the clinical, neuropsychological, and radiological profiles of individuals younger than 35 years who were at a 50% risk of a *NOTCH3* mutation. We expect that more insight into the clinical and radiological aspects of CADASIL in young adults will improve early diagnosis in this age group and allow for more tailored counselling of asymptomatic young adults at risk for CADASIL.

## Materials and methods

### Subjects

Individuals participating in the study gave informed consent, and the medical ethics committee of the Leiden University Medical Centre approved the study. All those younger than 35 years who were at a 50% risk of being a carrier, irrespective of signs and symptoms, were selected from a database of 15 families with CADASIL who had a known *NOTCH3* mutation; these families were participating in an ongoing study of CADASIL in the Netherlands. Individuals younger than 18 years were not included for ethical reasons. The database included 63 symptomatic and asymptomatic individuals, of whom 13 met the inclusion criteria for the present study. These 13 individuals were

members of 8 unrelated families, with varying mutations in the *NOTCH3* gene. Clinical, neuropsychological, and radiological examinations were completed before mutation analysis. Consequently, examiners (SAJLO, YMK, HAMM, and MAvB) and participants were blinded to carrier status. Mutation analysis was performed according to previously described techniques[22]. Before the study commenced, it was agreed with participants that the results of mutation analysis and an MR examination would not be disclosed. Counselling was performed by an independent genetic counsellor for those individuals who requested presymptomatic testing.

### Clinical data

We obtained a full medical history from all participants and obtained their medical records from their physicians and general practitioners. In a semistructured interview, specific questions were asked pertaining to possible undocumented past episodes of focal neurological deficits, migraine (with aura), and psychiatric history. Criteria for migraine were maintained according to the international Headache Classification Committee[88]. All participants completed a structured questionnaire concerning the presence of cardiovascular disease–related risk factors and drug use. The questionnaire included questions about nicotine and alcohol abuse, body weight and height, and history of hypercholesterolemia, hypertension, and diabetes mellitus. These conditions were defined as previously described[76]. Disability at the time of the study was measured semiquantitatively with the Rankin scale score, which ranges from 0 (no symptoms at all) to 5 (severe disability requiring constant nursing). Depression and anxiety were measured with the Hospital Anxiety and Depression Scale (HADS)[89,90]. The HADS is a 4-point, 14-item, self-assessment instrument developed for detecting levels of depression and anxiety in the setting of a hospital outpatient clinic. The global outcome measure was used, with a cut-off score of 13, because this is more appropriate than the anxiety and depression subscores in samples with minor psychiatric disorders[91].

### MR imaging

A uniform MR imaging protocol was performed on a 1.5-T MR imaging system (Philips Medical Systems, Best, the Netherlands) on the same day as the neuropsychological testing. The same neuroradiologist (MAvB), blinded to clinical and genetic data, reviewed all MR scans. Labelling MR scans with a number, instead of patient name and age, further ensured blinded scoring. The MR imaging protocol and grading of WMHs and lacunar infarctions were performed as previously described[76]. In brief, T1-weighted spin-echo, dual T2-weighted turbo spin-echo, and fluid-attenuated inversion recovery images were obtained in the axial plane. White matter hyperintensity lesion load was

graded according to the validated signal hyperintensities' rating scale of Scheltens et al[59]. In this scale, the brain is anatomically divided into deep white matter, basal ganglia, and infratentorial regions. For each region, a score of 0 to 6 is assigned according to the following scale: 0, absent; 1, up to 5 WMHs with less than a 3-mm diameter; 2, 6 or more WMHs with less than a 3-mm diameter; 3, up to 5 WMHs with a 4- to 10-mm diameter; 4, 6 or more WMHs with a 4- to 10-mm diameter; 5, 1 or more WMHs with a greater than 10-mm diameter; and 6, confluent hyperintensity. In addition, frontal and occipital periventricular "caps" and periventricular "bands" are scored as follows: 0, absent; 1, up to 5 mm; and 2, greater than 5 mm. We also scored WMHs in the external capsule region, which is not normally included in the scale of Scheltens et al. We did not include this subscore in the total WMHs score. The presence of subcortical lacunar lesions, considered specific for CADASIL, was recorded[92].

### Neuropsychological evaluation

All individuals followed a standardized neuropsychological test battery, lasting 3 hours. Details regarding administration, scoring, and clinical value of the administered neuropsychological tests have been extensively described by Spreen and Strauss[123]. Global cognitive functioning was assessed using the Cambridge Cognitive Examination, which incorporates the Mini-Mental State Examination[94]. The Cambridge Cognitive Examination provides a total score for global cognitive functioning and subscores for specific cognitive functions (memory, orientation, language, praxis, and gnosis). In addition, memory was evaluated using the Wechsler Memory Scale. Tests of executive functioning included the Trail-Making Test B, the Stroop colour and word test, the digit symbol subtest of the Wechsler Adult Intelligence Scale–Revised, and verbal and category fluency. For data analysis, the raw scores of the tests were used, except for the Wechsler Memory Scale memory quotient and the digit symbol subtest score, which were conventionally transformed into scaled scores[123].

### Statistical analysis

Statistical analysis was performed using the SPSS software package, version 10 (SPSS Inc, Chicago, Ill). Differences in mean test results between MCs and non-MCs (NMCs) were analyzed with the Student t-test.

## Results

### Subjects and clinical data

Of the 13 individuals at 50% carrier risk, 6 were *NOTCH3* MCs. These 6 individuals came from 5 unrelated families. The mutations were as follows: Arg141Cys (n=2), Arg153Cys (n=1), Arg182Cys (n=2), and Arg1076Cys (n=1). The mean ± SD age of the 6 MCs (2 men and 4 women) was 24.67 ± 4.32 years (range, 21-31 years), and that of the 7 NMCs (6 men and 1 woman) was 27.14 ± 3.80 years (range 22-33 years). Age (P=0.30) and sex (P=0.06) did not differ significantly between MCs and NMCs. None of the participants had visited a physician with symptoms leading to a diagnosis of CADASIL before the study, and none recalled any obvious episodes of focal neurological deficit with sudden onset. However, 2 individuals described aspecific episodes of sudden focal neurological deficits. In one individual (patient number [PN] 6), this involved speech disturbances lasting less than 1 minute, since roughly the age of 25 years; the other individual (PN 3) had experienced several weeks of blurred vision in late adolescence. Although both of these individuals had migraine with aura, these episodes did not resemble their usual auras, nor were they associated with headache. Both were MCs. A third MC (PN 4) had a confirmed stroke, consisting of sudden dysphasia and unilateral hand and tongue paresthesia, shortly after the study, at the age of 26 years. A total of 3 MCs (1 man and 2 women) had migraine, and 2 had migraine with aura. In one individual (PN 6), attacks started in the late 20s and consisted of typical visual aura followed by headache. The other individual (PN 3) had visual, sensory, and aphasic aura followed by unilateral headache, photophobia, phonophobia, and vomiting, with attacks clustering in the first 3 years of adolescence. The third individual (PN 1) had had several migraine attacks without aura, also clustering in early adolescence. At the time of the study, no focal neurological deficits were clinically observed in any of the participants. The Rankin scale score was 0 (no disability at all) for all MCs and NMCs. Cardiovascular risk factors were present as follows: diabetes mellitus, hypertension, and alcohol abuse in 0 MCs and NMCs; smoking in 4 of 7 NMCs and in 0 MCs (P=0.02); and hypercholesterolemia in 1 of 7 NMCs and in 0 MCs (P=0.38). The body mass index was not increased in either MCs or NMCs. Two MCs and 1 NMC had a history of minor depression in their early 20s, for which psychological help was sought. One NMC and 0 MCs had a global HADS score higher than 13. The mean ± SD global HADS score for MCs was 5.1 ± 3.8; and for NMCs, 7.4 ± 6.3 (P=0.46).

*Table 1 WMHs scores in MCs and NMCs younger than 35 years*

| | MCs (n=6) | | | | | | NMCs (n=7) | | | | | | | P |
|---|---|---|---|---|---|---|---|---|---|---|---|---|---|---|
| Variable | 1 | 2 | 3 | 4 | 5 | 6 | 1 | 2 | 3 | 4 | 5 | 6 | 7 | |
| Age, y | ≤23 | ≤23 | ≤23 | ≤26 | ≤29 | ≤32 | ≤23 | ≤23 | ≤29 | ≤29 | ≤29 | ≤32 | <35 | .3 |
| **Periventricular WMHs (0-2)** | | | | | | | | | | | | | | |
| Caps | | | | | | | | | | | | | | |
| Frontal | 0 | 1 | 1 | 2 | 2 | 2 | 0 | 0 | 0 | 0 | 0 | 0 | 0 | .001 |
| Occipital | 0 | 0 | 0 | 0 | 1 | 1 | 0 | 0 | 0 | 0 | 0 | 0 | 0 | .10 |
| Bands: lateral ventricles | 0 | 1 | 1 | 1 | 1 | 2 | 0 | 0 | 0 | 1 | 1 | 1 | 1 | .20 |
| Sum score (0-6) | 0 | 2 | 2 | 3 | 4 | 5 | 0 | 0 | 0 | 1 | 1 | 1 | 1 | .01 |
| **Subcortical WMHs (0-6)** | | | | | | | | | | | | | | |
| Frontal | 1 | 3 | 0 | 4 | 3 | 6 | 0 | 0 | 0 | 0 | 0 | 3 | 0 | .02 |
| Parietal | 0 | 0 | 0 | 3 | 3 | 6 | 0 | 0 | 0 | 0 | 0 | 0 | 0 | .05 |
| Occipital | 0 | 0 | 0 | 6 | 0 | 0 | 0 | 0 | 0 | 0 | 0 | 0 | 0 | .30 |
| Temporal | 3 | 5 | 5 | 3 | 3 | 6 | 0 | 0 | 0 | 0 | 0 | 0 | 0 | <.001 |
| Sum score (0-24) | 4 | 8 | 5 | 16 | 9 | 18 | 0 | 0 | 0 | 0 | 0 | 3 | 0 | .001 |
| **Basal ganglia WMHs (0-6)** | | | | | | | | | | | | | | |
| Caudate nucleus | 0 | 0 | 0 | 0 | 0 | 0 | 0 | 0 | 0 | 0 | 0 | 0 | 0 | NA |
| Putamen | 0 | 0 | 0 | 0 | 0 | 0 | 0 | 0 | 0 | 0 | 0 | 0 | 0 | NA |
| Globus pallidus | 0 | 0 | 0 | 0 | 0 | 0 | 0 | 0 | 0 | 0 | 0 | 0 | 0 | NA |
| Thalamus | 0 | 0 | 0 | 0 | 0 | 1 | 0 | 0 | 0 | 0 | 0 | 0 | 0 | .30 |
| Sum score (0-36) | 0 | 0 | 0 | 0 | 0 | 1 | 0 | 0 | 0 | 0 | 0 | 0 | 0 | NA |
| Internal capsule | 0 | 0 | 0 | 0 | 0 | 0 | 0 | 0 | 0 | 0 | 0 | 0 | 0 | .30 |
| External capsule region† | 0 | 0 | 0 | 1 | 0 | 1 | 0 | 0 | 0 | 0 | 0 | 0 | 0 | .10 |
| **Infratentorial WMHs (0-6)** | | | | | | | | | | | | | | |
| Cerebellum | 0 | 0 | 0 | 0 | 0 | 0 | 0 | 0 | 0 | 0 | 0 | 0 | 0 | NA |
| Mesencephalon | 0 | 0 | 0 | 0 | 0 | 0 | 0 | 0 | 0 | 0 | 0 | 0 | 0 | NA |
| Pons | 0 | 0 | 0 | 0 | 0 | 5 | 0 | 0 | 0 | 0 | 0 | 0 | 0 | .30 |
| Medulla | 0 | 0 | 0 | 0 | 0 | 0 | 0 | 0 | 0 | 0 | 0 | 0 | 0 | NA |
| Sum score (0-24) | 0 | 0 | 0 | 0 | 0 | 5 | 0 | 0 | 0 | 0 | 0 | 0 | 0 | .30 |
| **Total WMHs Score** | 4 | 10 | 7 | 19 | 13 | 29 | 0 | 0 | 0 | 1 | 1 | 4 | 1 | .004 |

MCs = mutation carriers, NMCs = . non-mutation carriers, WMHs = white matter hyperintensities. To ensure patient confidentiality, sex was not specified for each patients individually.† The subscore for this region was not included in the total WMHs score because WMHs in this\ region are not normally included in the scale of Scheltens et al.

## MR imaging

Table 1 shows an overview of WMHs scores according to Scheltens et al.[59] The mean ± SD total WMHs score in MCs was 13.67 ± 9.10 (range, 4-29), vs. 1.00 ± 1.40 (range, 0-4) in NMCs (P=0.004). None of the MCs or NMCs had (subcortical) infarctions on MR imaging. One MC had subcortical lacunar lesions, abutting temporal lobe WMHs.

*Table 2 Neuropsychological test results*

| Cognitive Domain | Measure | MCs (n = 6) | NMCs (n = 7) |
|---|---|---|---|
| Global cognitive functioning | CAMCOG | 99 (1) | 94 (3) |
| | MMSE | 30 (1) | 29 (1) |
| Memory | CAMCOG memory | 23 (1) | 22 (1) |
| | WMS memory quotient | 116 (8) | 108 (11) |
| | WMS verbal memory | 11 (3) | 9 (2) |
| | WMS picture memory | 12 (1) | 12 (1) |
| Language | CANCOG language | 29 (1) | 27 (2) |
| Praxis | CAMCOG praxis | 12 (1) | 11(1) |
| Gnosis | CAMCOG gnosis | 10 (0) | 10 (0) |
| Executive functioning | word fluency (animals) | 56 (8) | 42 (14) |
| | category fluency (animals) | 24 (2) | 22 (4) |
| | TMT b (seconds) | 49 (10) | 76 (27) |
| | TMS B (errors) | 0.1 (0.4) | (0.4) |
| | Stroop colour/word (seconds) | 71 (4) | 87 (16) |
| | Stroop colour/word (errors) | 0 (0) | 1 (1) |
| | Stroop interference (s) | 23 (6) | 30 (12) |
| | digit symbol (seconds) | 63 (13) | 57 (10) |

*Data are presented as mean (SD). CAMCOG = Cambridge Cognitive examination; MMSE = mini mental state examination; WMS = Wechsler Memory scale; TMT = Trail Making Test. T-test did not reveal any significant (P<0.01) differences between mutation carriers (MCs) and non-mutation carriers (NMCs)*

A distinct pattern of WMHs emerged in MCs, consisting of deep WMHs of the temporal lobes (6 of 6 individuals), frontal lobes (5 of 6 individuals), and frontal periventricular caps (5 of 6 individuals). Figure 1 shows MR scan results. The WMHs of the temporal lobe were specifically located in the anterior pole. Next to being present in all MCs, temporal lobe WMHs were also the most extensive, with a mean ± SD WMHs score of 4.20 ± 1.30 (range, 3-6), followed by a score of 2.80 ± 2.14 (range, 0-6) for the frontal lobe. Basal ganglia and infratentorial WMHs were seen only in the MC older than 30 years (table 1). Two MCs had

WMHs in the external capsule region. Periventricular bands were seen in 5 of 6 MCs, but these were also relatively frequent in NMCs (4 of 7 individuals). One NMC had a frontal subcortical WMHs that could be attributed to head trauma experienced 1 year previous to the present MR investigation.
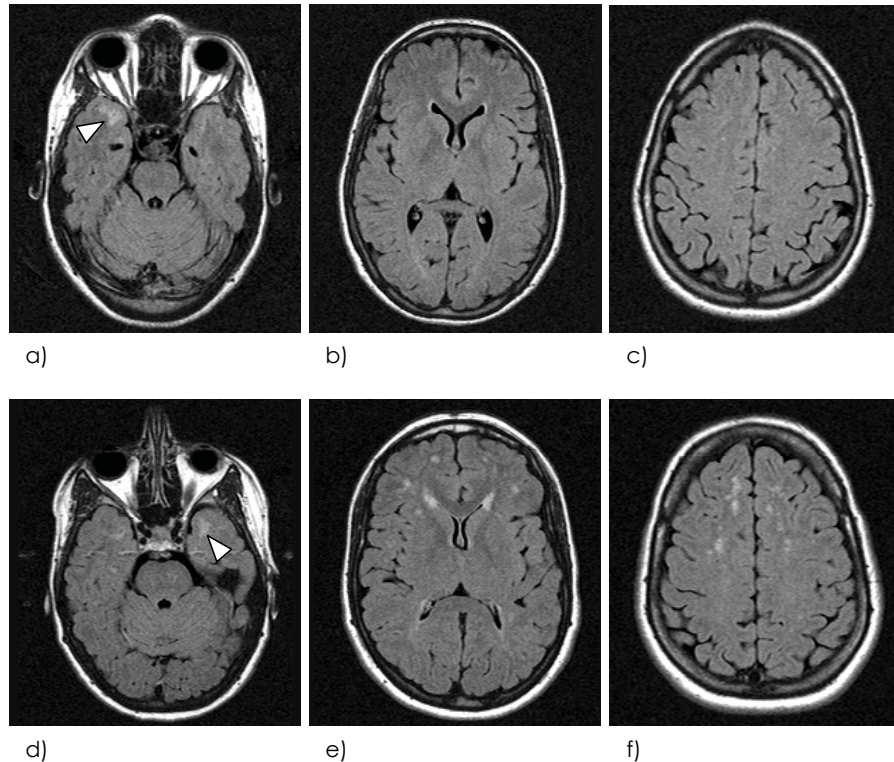


*Figure 1 FLAIR MR images of 2 mutation carries(a-c, d-f respectively). Axial slices are shown through the level of the temporal lobes, the basal ganglia, and the centrum semiovale in individuals ages 21 and 31 years. In both individuals, hyperintensities are seen in the anterior temporal lobe (arrowheads in a and d), and both have frontal caps. Imaging of the 31-year old individual illustrates the typical pattern of frontal lobe hyperintensities that can be seen in CADASIL mutation carriers younger than 35 years*

### Neuropsychological evaluation

The neuropsychological test results are represented in table 2. The MCs and NMCs did not differ in mean years of education after primary school (8 and 7 years, respectively) or in level of education. There was no significant difference in global or specific neuropsychological functioning between MCs and NMCs.

## Discussion

The aim of this study was to learn more about the status of young adult *NOTCH3* MCs. Clinical, neuropsychological, and radiological data were compared between *NOTCH3* MCs and NMCs younger than 35 years, in a setting blinded to MC status. Inherent to the study of a subgroup with a comparatively rare disease, this study was hampered by a relatively small study population. However, to our knowledge, it is the first to simultaneously and comprehensively study all relevant disease features in this age group. Furthermore, the lack in numbers is partially compensated by the multipedigree background of the participants and the presence of a highly representative control group of family members without a *NOTCH3* mutation. Follow-up of this patient cohort will be performed, and should provide further knowledge of the natural history of disease in young *NOTCH3* MCs.

The main result is that there was no quantifiable physical or cognitive impairment in young adult *NOTCH3* MCs. Disease expression was confined to migraine (with aura) and, less frequently, stroke. The MR scans showed a characteristic pattern of early WMHs. Migraine (with aura) was more common in MCs than in NMCs (3 of 6 vs. 0 of 7 individuals) presenting in the second and third decades of life. This confirms that migraine (with aura) can be an early disease manifestation of CADASIL[8,10,95]. Stroke presented in 1 MC at the age of 26 years (shortly after the study), and 2 MCs described atypical episodes of immediate-onset focal neurological deficits, of possible ischemic origin. In 2 multifamily studies of the CADASIL phenotypic spectrum, ischemic episodes are reported to occur at the mean ± SD ages of 49.3 ± 10.7 years5 and 46.1 ± 9.0 years (range, 30-66 years)[10]. However, from this study population, and from our clinical experience, we find that transient ischemic attacks and stroke can already present in the third decade of life, although most do not lead to permanent dysfunction. There were no psychiatric disorders, as defined by the medical history and the HADS score. The age at onset of psychiatric disorders in individuals with CADASIL has not been defined, but from our results, we conclude that these are not present before the age of 35 years. An extensive neuropsychological assessment did not reveal any differences in cognitive function between MCs and NMCs. Taillia et al studied neuropsychological function in 8 individuals without dementia, aged 35 to 66 years, who had neurologically symptomatic CADASIL, and found subtle cognitive impairment in all, specifically in tasks involving the frontal lobes[96]. We did not find any dysfunction concerning these executive tasks, or any other tasks, in those younger than 35 years. The age of 35 years, therefore, may be the lower age limit at which neuropsychological dysfunction can begin to become manifest. Possible subtle cognitive changes in this age group need to be assessed in a larger follow-up study.

The MR imaging abnormalities in young adult *NOTCH3* MCs, although relatively subtle in the early 20s, were consistently present much earlier than the maintained age of 30 to 35 years[8,86]. Furthermore, the MR lesion pattern proved to be distinct, with landmark features being anterior temporal lobe WMHs, frontal lobe WMHs, and frontal caps. Temporal lobe lesions were present in all MCs, with a WMHs score between 3 and 6, corresponding to the presence of at least 1 lesion of 4 mm in diameter. The scale of Scheltens et al does not reflect the sublocation of WMHs within the cerebral lobes, but we observed that the temporal lobe lesions were specifically located anteriorly[59]. In the general population with CADASIL, temporal lobe WMHs are often, but not always, present (sensitivity, 95%; and specificity, 80%)[43]. Frontal caps and frontal deep WMHs were seen in 5 of 6 MCs, although the latter were not specific for MCs, because one NMC also had frontal WMHs. Another nonspecific MR imaging feature was lateral periventricular bands, which were observed in MCs and NMCs. Subcortical lacunar lesions, although apparently infrequent in individuals younger than 35 years (1 of 6 MCs), are a specific sign for CADASIL[92]. Overall, our MR findings correspond with those of recent studies describing periventricular, temporal pole, frontal lobe, and external capsule region WMHs as radiological markers in (older) patients with CADASIL[39,41,43]. White matter hyperintensities in older patients, however, are much more extensive, with the heaviest lesion load in the frontal lobes,24 constituting a visually altogether different MR result from the one we observed in young MCs[41]. Furthermore, contrary to what has been previously suggested, we did not find external capsule region WMHs to be a distinguishing feature early in the radiological disease process[43]. We have no clear-cut answer as to why CADASIL-related WMHs initiate in the temporal and frontal lobes. Apparently, certain vessels may be more susceptible to CADASIL-related vasculopathy than others, possibly for reasons of calibre or length[43]. At any rate, acquaintance with the WMHs lesion pattern and load in those younger than 35 years should be an important means of recognizing CADASIL in this age group, especially in the differential diagnosis of multiple sclerosis, which can mimic the signs and symptoms of CADASIL[49,97]. Once the diagnosis of CADASIL is considered based on clinical and neuroimaging data, *NOTCH3* mutation analysis or pathological examination of a skin biopsy specimen is required to confirm the diagnosis[66,98].

Familiarity with the clinical and neuroimaging features of CADASIL in young adults should promote early diagnosis and prevent misdiagnosis and needless (invasive) diagnostic or therapeutic procedures.

# Radiological distinction between patients with CADASIL and MS

S
I
X

# Radiological distinction between patients with CADASIL and MS

R. van den Boom
S.A.J. Lesnik Oberstein
E.C.G.J. Schafrat
F. Behloul
H. Olofson
M.D. Ferrari
E.L.E.M. Bollen
J. Haan
M.A. van Buchem

## Abstract

Purpose was to study whether there is a difference in magnetic resonance (MR) lesion pattern between young patients with cerebral autosomal dominant arteriopathy with subcortical infarcts and leukoencephalopathy (CADASIL) and multiple sclerosis (MS).

The presence of lacunar infarcts, microbleeds, subcortical lacunar lesions, and white matter hyperintensities (WMHs) in the anterior temporal lobe and the external and internal capsule was assessed on MR images. Images were obtained in 24 CADASIL patients and 19 MS patients under the age of 50 years, comprising T1-weighted, dual fast spin-echo, fluid attenuated inversion recovery (FLAIR), and T2*-gradient-echo images in the axial plane. Differences were assessed with the Fisher's exact test.

CADASIL patients showed significantly more subcortical lacunar lesions, lacunar infarcts, and hyperintensities in the anterior temporal lobe and the external capsule compared with MS. The presence of WMHs in the internal capsule and microbleeds did not differ significantly between the patient groups.

Based on the presence and pattern of abnormalities observed on MR images of CADASIL patients, young CADASIL patients can be discriminated from young patients with MS.

## Introduction

Cerebral autosomal dominant arteriopathy with subcortical infarcts and leucoencephalopathy (CADASIL) is a late-onset hereditary syndrome caused by mutations in the *NOTCH3* gene[19]. The pathological substrate is a microangiopathy characterized by distinctive granular osmiophilic material in the vascular media, leading to degeneration of vascular smooth muscle cells[7]. The disease is clinically characterized by initially attacks of migraine with aura (<age 30) and later on (>age 40) transient ischemic attacks, strokes, progressive subcortical dementia, and mood disturbances[8]. The radiological hallmarks of CADASIL are the presence on magnetic resonance (MR) imaging of white matter hyperintensities (WMHs) with a specific distribution, and lacunar infarcts, subcortical lacunar lesions, and microbleeds[39-41,43,76,77,92]. Recently we described that these lesions develop in a predictable way during the course of the disease[78]. As early as in the third decade of life subcortical lacunar lesions and patchy WMHs usually located in the anterior temporal lobe can be found whereas in the sixth decade a full-blown picture with confluent WMHs, subcortical lacunar lesions, lacunar infarcts, and microbleeds is observed in most patients.

Whereas the radiological picture of advanced stages of CADASIL is well documented, and can usually be discriminated from Binswanger's disease, the radiological appearance at earlier stages of CADASIL may mainly comprise only of WMHs, similar to those found in multiple sclerosis (MS)[67]. As MS may also have a similar clinical presentation as CADASIL many CADASIL patients are misdiagnosed as MS[49,50]. Here we compared the cerebral MR pictures of relatively young CADASIL patients with those of age-matched MS patients in order to identify radiological features that may help to discriminate CADASIL already at the early stages from MS.

## Materials and methods

### Subjects

We included 24 patients (<50 years) with proven *NOTCH3* mutations from 15 unrelated Dutch CADASIL families, participating in our ongoing prospective study on clinical, radiological and genetic aspects of CADASIL[22]. These patients were compared with 19 age-matched patients with laboratory-supported definite MS who were recruited from the authors' institution[99]. Only subjects who were able to understand the informed consent were included and informed consent was obtained from all subjects. The medical ethics committee of our institution approved the study protocol.

## MR imaging

All MR examinations were performed on a 1.5T MR system (Philips Medical systems, Best, The Netherlands). All participants were subjected to the same standardized MR protocol, comprising: conventional T1-weighted spin echo images (slice thickness 6 mm with a 0.6 mm interslice gap [6.0/0.6 mm], repetition time [TR]/echo time [TE] 600/20 ms, matrix 256x205, and a 220x165 mm field of view [FOV]), dual T2-weighted fast spin echo (FSE) images (3.0/0.0 mm, TR/TE 3000/27/120 ms, matrix 256x205, FOV 220x220 mm), and fast fluid-attenuated inversion recovery (FLAIR) images (3.0/0.0 mm, TR/TE 8000/100 ms, inversion time 2000 ms, matrix 256x192, FOV 220x176 mm). In addition, T2*-weighted gradient echo planar (EPI) sequence (6.0/0.6 mm, TR/TE 2598/48 ms, matrix 256x192, FOV 220x198 mm, EPI factor 25) were performed to detect haemosiderin deposits. All images were performed in the axial plane parallel to the inferior border of the genu and splenium of the corpus callosum.

## Visual rating

Two radiologists (MAvB, RvdB) blinded to the diagnosis of CADASIL and MS assessed for each patient the presence of the radiological hallmarks of CADASIL: lacunar infarcts, microbleeds, subcortical lacunar lesions, and WMHs in the anterior temporal lobe, the external and internal capsule.

Lacunar infarcts were defined as parenchymal defects not extending to the cortical grey matter with a signal intensity following that of cerebral spinal fluid (CSF) on all pulse sequences, irrespective of size (figure 1). In an effort to differentiate lacunar infarcts from dilated perivascular spaces, areas that were isointense to CSF on all pulse sequence and located in the lower one-third of the corpus striatum, were excluded[80,100]. Subinsular perivascular spaces were differentiated from lacunar infarcts based on the description of Song et al: enlarged perivascular spaces have a featherlike configuration, are isointense to CSF on T2- and T1-weighted images, but do not have high signal on FLAIR images[73]. In an effort to differentiate perivascular spaces along the perforating arteries from lacunar infarcts a modification of the descriptive criteria for perivascular spaces as used by Bokura et al was applied: all lesions with a transverse diameter smaller or equal to 2 mm or with a tubular appearance following the course of perforating arteries were most likely to represent perivascular spaces and were excluded as well[81].

Microbleeds were defined as focal areas of signal loss on T2-weighted FSE images that increased in size on the T2*-weighted gradient echo pulse sequence ("blooming effect") (figure 1)[76]. In this way, microbleeds were differentiated from areas of signal loss based on vascular flow voids. Areas of symmetric hypointensity of the globus pallidus likely to represent calcification or nonhemorrhagic iron deposits were excluded.

Subcortical lacunar lesions were defined as linearly arranged groups of rounded, circumscribed lesions just below the cortex, at the grey-white matter junction with a signal intensity that was identical to that of CSF on all pulse sequences (figure1)[92].

WMHs were defined as white matter areas with increased signal intensity on dual and FLAIR weighted images without mass effect. The border between anterior and posterior temporal lobe was defined as the posterior margin of the amygdale (figure1)[43].

### Group comparison with automated statistical image analysis tool

WMH volume (in ml) measurements were performed using locally developed automated segmentation software (Sniper®, Department of Radiology, Division of Image Processing, Leiden University Medical Centre, Leiden, The Netherlands). Volume of WMHs was corrected for total brain volume by dividing the individual volume of WMHs by intracranial volume and expressed in percent. WMHs detection approach consisted of three main steps:

1. Brain stripping: An average proton density image (from the Montreal Neurological Institute (MNI)) is first co-registered to the proton density image of a subject using a multi-resolution 12-parameter affine registration. The standard deviation of ratio images was used as cost function. The resulting transformation matrix is used to resize an intracranial prior probability map in order to mask automatically non-brain voxels (skin, bone and eyeballs). A prior probability map of white matter (from MNI) is aligned using the same transformation matrix to guide the detection of the WMHs. For a more accurate intracranial delineation, fuzzy clustering, mathematical morphology and region growing, are applied and constraint to remain within the resliced intracranial mask. This step takes on average less than 1 minute per scan.

2. CSF detection: The FLAIR image is first co-registered to the T2-weighted image. A ratio image (FLAIR/T2) is then computed after rescaling the FLAIR voxel-intensity range to that of the T2-weighted image. The CSF is extracted in this ratio image using fuzzy clustering (c=2). The voxels belonging to the cluster with the darkest signal intensities within the intracranial mask are classified as CSF.

3. Lesion detection: The voxels of the T2-weighted image and those of the FLAIR image are clustered in 3 clusters. A voxel is labelled as WMH if it fulfils three conditions: (i) Its T2 intensity belongs to the brightest cluster and it does not intersect with the CSF mask detected in step 2; (ii) its FLAIR intensity belongs to the brightest cluster; (iii) it has a relatively high probability (>0.4) to belong to the white matter (using the aligned white matter map). Finally figure 2 shows at the level of the anterior temporal lobe and the external and internal capsule for every voxel whether WMHs were present at these

locations, in bleu for CADASIL, in red for MS. The brighter the colour the more frequently WMHs were found in that location. As background we used a normalized T1-weighted image.

### Statistical analysis

Descriptive statistics were calculated for differences in age and sex between CADASIL and MS patients. Differences in presence of subcortical lacunar lesions, lacunar infarcts, microbleeds and hyperintensities in the anterior temporal lobe, the external and internal capsule between CADASIL and MS patients were assessed with the Fisher's exact test. Differences in WMH volume was assessed with a Student t-test for unpaired data. To compensate for multiple comparisons, we considered a P-value of $P<0.005$ as significant. The agreement between the two readers was determined with Cohen's K. The statistical package SPSS-10 (SPSS, Inc) was used for data analysis.

Table 1 Characteristics of the CADASIL and MS patients

| Study group | Subjects (n) | Age (y) | | Sex (n) | |
| --- | --- | --- | --- | --- | --- |
| | | Mean ± SD | Range | Men | Women |
| CADASIL | 24 | 40 ± 10 | 21-50 | 10 | 14 |
| MS | 19 | 42 ± 9 | 26-53 | 4 | 15 |

Table 2 Presence of MR lesions in CADASIL and MS patients

| | CADASIL (n=24) | MS (n=19) | P value |
| --- | --- | --- | --- |
| Subcortical lacunar infarcts (n) | 9 | 0 | 0.002* |
| Lacunar infarcts (n) | 15 | 0 | <0.001* |
| Microbleeds (n) | 4 | 0 | 0.12* |
| Anterior temporal lobe (n) | 23 | 1 | <0.001* |
| External capsule (n) | 14 | 0 | <0.001* |
| Internal capsule (n) | 15 | 1 | 0.04* |
| Volume of WMHs (mean %) | 4.5% | 0.7% | <0.001** |

*Fischer exact test
** Student t-test

## Results

### Subjects

Table 1 gives an overview of the characteristics of the CADASIL and MS patients. There were no significant differences in age (Student-t test, P=0.57) and sex (Fisher's exact, P=0.20) between CADASIL and MS patients.

### Visual rating

The interobserver agreement was high for all MR imaging abnormalities (Kappa=0.88-1). The presence of subcortical lacunar lesions, lacunar infarcts, microbleeds and hyperintensities in the anterior temporal lobe, the external and internal capsule in CADASIL and MS patients are given in table 2. The following radiological features were significantly higher in patients with CADASIL compared with those with MS (Fisher's exact test, P<0.005): subcortical lacunar lesions, lacunar infarcts, and hyperintensities in the anterior temporal lobe and the external capsule (table 2). Although microbleeds were absent in MS patients, only four CADASIL patients had microbleeds and therefore no statistically difference was found between the two diseases. There was one MS patient with hyperintensities in the internal capsule. In CADASIL, WMHs in the internal capsule were seen in 15 patients. This radiological hallmark also did not reach significance.
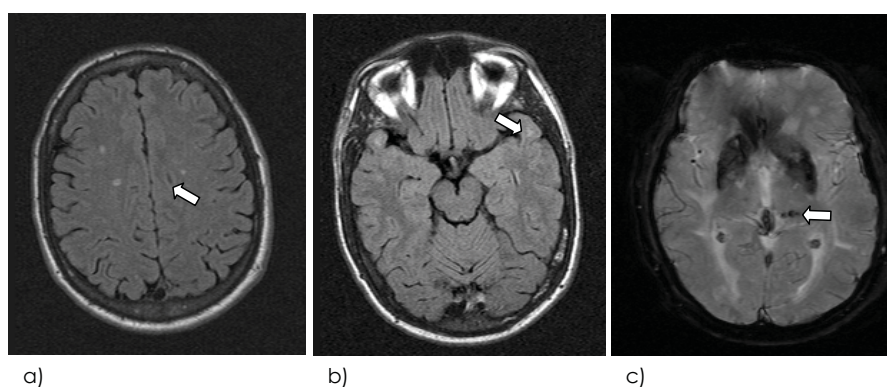


a)　　　　　　　　　　b)　　　　　　　　　　c)

*Figure 1 Axial FLAIR (a-b) and T2\*-weighted (c) MR images of CADASIL patients. Complete MR spectrum of CADASIL: lacunar infarcts (arrow in a), subcortical lacunar lesions (arrow in b) and microbleeds (arrow in c).*

### Group comparison with automated statistical image analysis tool

As shown in figure 2, there is a difference in WMHs distribution between CADASIL and MS patients. Also, the volume of WMHs, corrected for intracranial volume was significantly higher in CADASIL (mean 4.5%, SD 3.7) as compared with MS patients (mean 0.7%, SD 1.1, Student t-test, P<0.001, table 2).
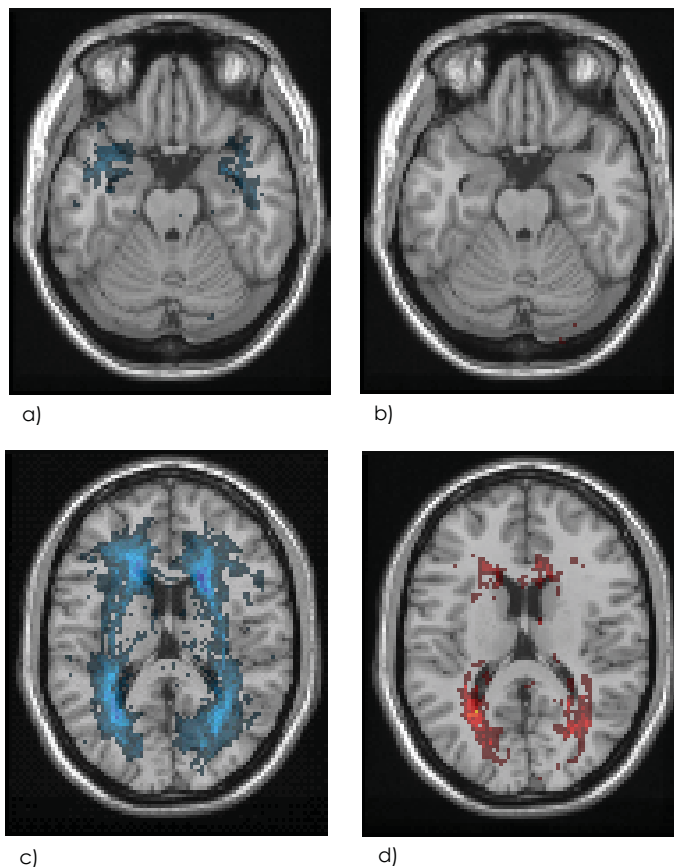
*Figure 2 Frequency maps of the distribution of WMHs generated with automated statistical image analysis tool. Areas where WMHs occurred are displayed in colour; the brighter the colour, the higher the frequency of WMHs in these locations. The distribution of the WMHs in the CADASIL group is shown left (a and c) and in the MS group right (b and d) at the level of the anterior temporal lobe (a and b) and the external and internal capsule (c and d). Almost no WMHs were seen in the anterior temporal lobe, and internal and external capsule in MS patients whereas WMHs were more often present in these locations in the CADASIL population.*

## Discussion

We compared brain MR images of young patients with CADASIL with those of patients with MS and found significant differences with respect to the volume and distribution of WMHs and the presence of concomitant lesions. MR images of young CADASIL patients revealed a significantly higher load of WMHs and a characteristically higher prevalence of WMHs in the anterior temporal lobe (23/24 in CADASIL versus 1/19 in MS) and the external and internal capsule (14-15/24 in CADASIL versus 0-1/19 in MS). The results show that involvement

of the anterior temporal lobe is not only a useful radiological hallmark to differentiate CADASIL from Binswanger's disease in elderly patients but also to differentiate CADASIL from MS in younger patients[67].

In addition to a characteristic pattern of WMHs, the spectrum of MR abnormalities in CADASIL patients also comprises lacunar infarcts, subcortical lacunar lesions, and microbleeds which were not found in any of our MS patients.

A potential limitation of our study may be that we did not exclude CADASIL in our MS cases by routine screening for *NOTCH3* mutations because of the elaborate and costly nature of the procedure. However, by using the most restricted POSER criteria, namely the laboratory-supported definite MS, we reduced the chance of misclassifying MS patients[99]. In any case, if we would have erroneously misclassified a CADASIL patient as a MS patient, this would have decreased the differences we found between the two patient groups.

In this study, our goal was to assess whether the presence or absence of the radiological hallmarks of CADASIL helped differentiating young CADASIL and MS patients. In other studies MR criteria suggestive of MS have been defined. These MR criteria for MS help further strengthening the diagnostic confidence of differentiating CADASIL from MS. MS frequently involves the spinal cord, while spinal cord lesions are virtually absent in CADASIL[43,44]. WMHs in the subcortical U fibers suggest MS, whereas these fibers are spared in CADASIL[40,101]. The periventricular lesions in MS are frequently ovoid and orientated perpendicular to the lateral ventricles which has not been observed in CADASIL[102]. Gadolinium enhancement of the WMHs frequently occurs in MS, and has not been described in CADASIL patients[41,103].

CADASIL can be differentiated radiologically from MS already at the young age, primarily on the basis of WMHs in the anterior temporal lobe and the external and internal capsule.

CADASIL: structural MR imaging changes and apolipoprotein E genotype

S
E
V
E
N

# CADASIL: structural MR imaging changes and apolipoprotein E genotype

R. van den Boom
S.A.J. Lesnik Oberstein
A.A. van den Berg-Huysmans
M.D. Ferrari
M.A. van Buchem
J. Haan

## Abstract

Apolipoprotein E (apoE) genotype plays an important role in the development, maintenance, and response to injury of the central nervous system. It has been suggested that apoE ε4 genotype is a risk factor for several neurological disorders. We investigated the correlation between the apoE genotype and radiological data in patients with cerebral autosomal dominant arteriopathy with subcortical infarcts and leukoencephalopathy (CADASIL).

T1-weighted, dual fast spin-echo, T2*-weighted gradient echo, and FLAIR magnetic resonance (MR) scans were obtained from 36 CADASIL patients (21-59 years). The number of lacunar infarcts and microbleeds, and the presence of subcortical lacunar lesions were determined. The amount of white matter hyperintensities was assessed using semi-automated segmentation software. The relation between the radiological endophenotype of CADASIL and the apoE genotype was assessed using a Student t-test for unpaired data and Fisher's exact test.

White matter hyperintensities, lacunar infarcts, microbleeds, and subcortical lacunar lesions were not found to be associated with the presence of an ε4 allele.

The variability of structural MR lesions in CADASIL is independent of apoE genotype and other processes must underlie the variable natural history of the disease.

*Introduction*

Cerebral autosomal dominant arteriopathy with subcortical infarcts and leukoencephalopathy (CADASIL) is a hereditary small-artery vasculopathy caused by mutations in the *NOTCH3* gene on chromosome 19[19]. The disease is clinically characterized by transient ischemic attacks, strokes, progressive subcortical dementia, migraine with aura, and mood disturbances. In general, death follows at an age of 55 to 65 years after a mean disease duration of 20 years[10]. Magnetic resonance (MR) imaging findings in CADASIL are present in symptomatic as well as asymptomatic mutation carriers, and consist of diffuse white matter hyperintensities (predominantly in the subcortical areas) and lacunar infarcts (in the centrum semiovale, thalamus, basal ganglia and pons). Recent MR studies have established microbleeds and subcortical lacunar lesions as additional radiological features of CADASIL[78].

The phenotypic and radiological expression of CADASIL is variable, both between and within families. The mean age of onset is in the late thirties to early forties, with a wide range. Some individuals develop microbleeds and subcortical infarcts, while others do not. On MR imaging, the extent of white matter hyperintensities and lacunar infarction is variable. This suggests modulation by additional genetic and, or environmental factors. We postulated that the apolipoprotein E (apoE) gene is a candidate genetic modifier in CADASIL.

ApoE is a glycoprotein that transports cholesterol and other lipids[104]. The apoE gene is located on chromosome 19 and has ε2, ε3, and ε4 alleles. It has been suggested that apoE dependent uptake of lipoproteins may play an important role in the development, maintenance, and response to injury of the central nervous system[105]. In recent studies, the apoE ε4 genotype has been consistently associated with severe neurodegeneration and seems to constitute a risk factor for several neurological disorders. The ε4 allele has turned out to be a major risk factor for Alzheimer's disease, and lobar haemorrhages caused by amyloid angiopathy[106]. Adverse recovery after head trauma or other injury of the brain has also been linked to the ε4 allele[105].

The aim of this study was to assess whether the radiological endophenotype of CADASIL is correlated to the apoE genotype. We hypothesised that ε4 allele carriers have more white matter hyperintensities, lacunar infarcts, microbleeds, and subcortical lacunar lesions than those with the ε2 and ε3 genotype.

## Materials and methods

### Subjects

Members of 15 unrelated CADASIL families were asked to participate in a study on the clinical, radiological, and genetic aspects of CADASIL. In each family, the index patient had a proven *NOTCH3* mutation. Patients were referred from various medical centres to our institution, which serves as a CADASIL referral centre. Patients were referred with the suspicion of CADASIL based on clinical signs and symptoms, a family history consistent with autosomal dominant inheritance, or suggestive MR changes. The diagnosis CADASIL was confirmed by direct sequencing analysis of the *NOTCH3* gene, according to previously described techniques[22].

A total of 36 DNA proven CADASIL mutation carriers were studied (19 women and 17 men, aged 21-59 years, mean 45 years). Symptomatic as well as asymptomatic mutation carriers were included. ApoE genotype in all mutation carriers was determined as described by Haan et al[107].

### MR imaging

MR imaging was performed in all mutation carriers. All MR examinations were performed on a 1.5T MR system (Philips Medical systems, Best, The Netherlands). T1-weighted spin echo images (slice thickness 6 mm with a 0.6 mm interslice gap [6/0.6 mm], repetition time [TR]/echo time [TE] 600/20 ms, matrix 256x205, and a field of view [FOV] 220x165 mm), dual T2-weighted fast spin echo (FSE) images (3.0/0.0 mm, TR/TE 3000/27/120 ms, matrix 256x205, FOV 220x220 mm), T2*-weighted gradient echo planar (EPI) sequence (6/0.6 mm, TR/TE 2598/48 ms, matrix 256x192, FOV 220x198 mm, EPI factor 25), and fast fluid-attenuated inversion recovery (FLAIR) images (3.0/0.0 mm, TR/TE 8000/100 ms, inversion time 2000 ms, matrix 256x192, FOV 220x176 mm) were obtained in the axial plane parallel to the inferior border of the genu and splenium of the corpus callosum.

White matter hyperintensities were defined as white matter areas with increased signal intensity as compared to the surrounding white matter on T2-, proton density weighted and FLAIR images (figure 1). The amount of white matter hyperintensities was assessed using semi-automated segmentation software (Department of Radiology, Division of Image Processing, Leiden University Medical Centre, Leiden, The Netherlands). Volume of white matter hyperintensities was corrected for total brain volume by dividing the individual volume of white matter hyperintensities by intracranial volume and expressed in %.

Lacunar infarcts were defined as parenchymal defects not extending to the cortical grey matter with a signal intensity following that of CSF on all pulse sequences, irrespective of size (figure 1). In an effort to differentiate lacunar infarcts from dilated perivascular spaces, areas that were isointense to CSF on all pulse sequence and located in the lower one-third of the corpus striatum, were excluded[80,100]. Subinsular perivascular spaces were differentiated from lacunar infarcts based on the description of Song et al: enlarged perivascular spaces have a featherlike configuration, are isointense to CSF on T2- and T1-weighted images, but do not have high signal on FLAIR images[73]. In an effort to differentiate perivascular spaces along the perforating arteries from lacunar infarcts a modification of the descriptive criteria for perivascular spaces as used by Bokura et al was applied: all lesions with a transverse diameter smaller or equal to 2 mm or with a tubular appearance following the course of perforating arteries were most likely to represent perivascular spaces and were excluded as well[81].

Microbleeds were defined as focal areas of signal loss on T2-weighted FSE images that increased in size on the T2*-weighted gradient echo pulse sequence ("blooming effect")[76]. In this way, microbleeds were differentiated from areas of signal loss based on vascular flow voids. Areas of symmetric hypointensity of the globus pallidus likely to represent calcification or nonhemorrhagic iron deposits were excluded (figure 1)[78].

Subcortical lacunar lesions were defined as linearly arranged groups of rounded, circumscribed lesions just below the cortex, at the grey-white matter junction with a signal intensity that was identical to that of CSF on all pulse sequences (figure 1)[92]. One experienced neuroradiologist (MAvB) assessed the number of lacunar infarcts and microbleeds, and the presence of subcortical lacunar lesions. He was blinded to the apoE status.

Only cognitively capable subjects were included into this study to ensure acquisition of informed consent. Informed consent was obtained from all subjects. The medical ethics committee of our institution approved the study protocol.

### Statistical analysis

As subdivision by genotype would reduce the group size and thereby decrease the statistical power too much, we obtained descriptive statistics for the mean volume of white matter hyperintensities, number of lacunar infarcts, number of microbleeds and presence of subcortical lacunar lesions. Differences in age, white matter hyperintensities, lacunar infarcts, and microbleeds between ε4 allele carriers and non-ε4 allele carriers were then investigated with a Student

t-test for unpaired data. Differences in subcortical lacunar lesions were tested using the Fisher's exact test. A P-value of P<0.05 was considered significant. The statistical package SPSS-10 (SPSS, Inc) was used for data analysis.

## Results

Of the 36 mutation carriers studied, 29 had neurological symptoms, ranging from one transient ischemic attack to multiple strokes and cognitive deficits. Eight were ε4 allele carriers and 28 had no ε4 allele. The complete distribution of apoE genotype was as follows: ε2/ε3 n=1(3%); ε3/ε3 n=26 (72%); ε3/ε4 n=8 (22%); ε2/ε2 n=1(3%); ε4/ε4 n=0.

Results of the MR imaging analysis are shown in table 1. No significant difference was found between the ε4 allele carriers and the non-ε4 allele carriers in age (P=0.46) volume of white matter hyperintensities (P=0.84), number of infarcts (P=0.27), number of microbleeds (P=0.58), or subcortical lacunar lesions (P=0.66).

*Table 1 MR imaging findings in apoE genotype subgroups. There is no significant difference in MR imaging findings between ε4 allele carriers and non-ε4 allele carriers*

|  | All (n=36) | ε4 allele carriers (n=8) | Non-ε4 allele arriers (n=28) | 95% confidence interval of the difference |
|---|---|---|---|---|
| Age in years* | 44.9 (11) | 47.5 (7.9) | 44.2 (11.7) | -4.2–10.9 |
| Percentage white matter hyperintensities* | 8.2 (5.9) | 8.6 (6.4) | 8.1 (5.9) | -5.1–6.0 |
| Number lacunar infarcts* | 8.8 (12.6) | 13.1 (14.7) | 7.5 (11.9) | -7.1–18.3 |
| Number of microbleeds* | 2.4 (6.5) | 1.3 (2.6) | 2.7 (7.3) | -4.8–1.9 |
| Number of persons with subcortical lacunar infarcts** | 18 (50%) | 4 (50%) | 14 (50%) |  |

*Data are given as \*mean (SD) and \*\*frequency (percent)*

## Discussion

There are several studies that address the issue of the considerable variability in the rate of progression and survival between individual CADASIL patients. Evidence suggests that male patients have a shorter survival than female patients[10,108]. One study has systematically compared the influence of different *NOTCH3* mutations on the disease phenotype and found no obvious effect of single mutations on the volume of lesions seen on brain MR imaging[109]. Other studies focused on the influence of vascular comorbidity including hypertension, smoking, diabetes mellitus and hypercholesterolemia

on phenotype and the development of white matter hyperinstensities and microbleeds[76,110]. No strong genotype-phenotype relationships in CADASIL was found.
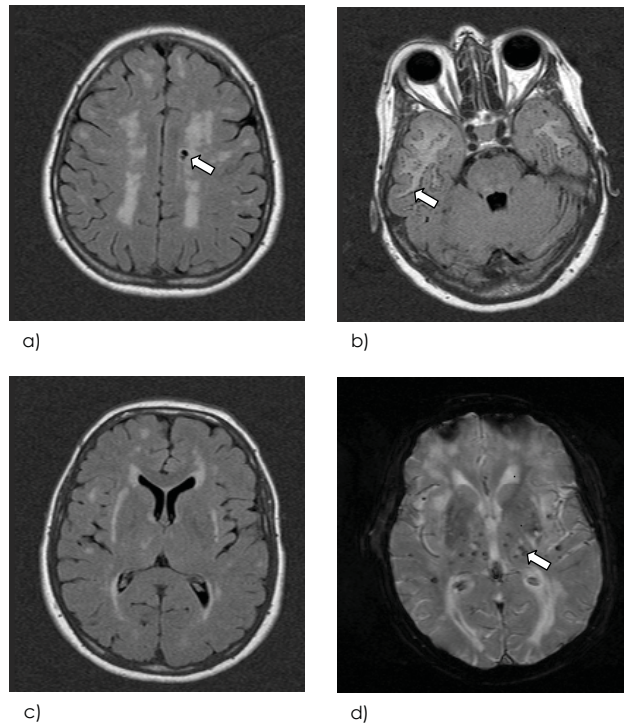


*Figure 1 Axial FLAIR (a-c) and T2\*-weighted gradient (d) MR images of CADASIL patients. Complete MR spectrum of CADASIL: confluent hyperintensities (a-c), lacunar infarcts (arrow in a), subcortical lacunar lesions (arrow in b) and microbleeds (arrow in d).*

In sporadic amyloid angiopathy as well as in Alzheimer's disease, the apoE genotype is a strong predictor of the clinical expression of disease and the development of cerebral structural (including vascular) lesions. There are indications that in Alzheimer's disease concomitant vascular lesions, such as infarcts, white matter hyperintensities, and haemorrhagic infarcts are associated with the ε4 allele[106]. In our CADASIL study population, the ε4 allele frequency was almost the same (22%) as in the general Dutch population (30%), offering the possibility to compare ε4 carriers with non-carriers[111]. In our study the apoE genotype was not significantly associated with structural changes seen on MR imaging, suggesting that in CADASIL, structural lesions caused by vascular changes are independent of apoE ε4 genotype. It is possible that the vascular effect of apoE genotype observed in other diseases, is dependent on amyloid angiopathy.

Our results extend those of an earlier study of Singhal et al, that found no correlation of the apoE genotype with white matter hyperintensities on MR imaging[110]. In addition to that observation we also observed a lack of correlation between apoE genotype and occurrence of the other radiological hallmarks of CADASIL: lacunar infarcts, microbleeds, and subcortical lacunar infarcts. In contrast to that study, we used a more extensive MR protocol as objective measure of disease severity. We believe that clinical parameters, contrary to structural MR lesions, are a less valid measure of the burden of the disease because of superimposed external factors. Furthermore, not all brain lesions produce clinical symptoms.

A potential limitation of our study may be that only patients who were able to understand the informed consent were included and therefore the most severely affected patients might have been excluded. However, at this end stage of the disease the phenotypic as well as the radiological expression of CADASIL does not differ as much as at a younger age and therefore we believe that our results are not influenced by excluding these patients.

In conclusion, our population included 36 CADASIL mutation carriers. By using a very rigorous objective measure for the disease burden, namely the MR imaging-endophenotype, we may conclude that the variability of structural MR lesions in CADASIL patients are independent of apoE ε4 genotype and that other processes such as environmental and other genetic factors must underlie the variable natural history of the disease.

# Cerebral haemodynamics and white matter hyperintensities in CADASIL

EIGHT

# Cerebral haemodynamics and white matter hyperintensities in CADASIL

R. van den Boom
S.A.J. Lesnik Oberstein
A. Spilt
F. Behloul
M.D. Ferrari
J. Haan
R.G. Westendorp
M.A. van Buchem

## Abstract

Cerebral autosomal dominant arteriopathy with subcortical infarcts and leukoencephalopathy (CADASIL) is a hereditary small-vessel disease caused by mutations in the *NOTCH3* gene on chromosome 19. On magnetic resonance (MR) imaging, subcortical white matter hyperintensities and lacunar infarcts are visualised. It is unknown whether a decrease in cerebral blood flow or cerebrovascular reactivity is primarily responsible for the development of white matter hyperintensities and lacunar infarcts.

We used phase contrast MR imaging in 40 *NOTCH3* mutation carriers (mean age 45 ±10 years) and 22 non-mutated family members (mean age 39 ±12 years), to assess baseline total cerebral blood flow (TCBF) and cerebrovascular reactivity after acetazolamide.

Mean baseline TCBF was significantly decreased *in NOTCH3* mutation carriers. In young subjects, baseline TCBF was significantly lower than in non-mutation carriers (mean difference 124 ml/min). Furthermore, baseline TCBF did not differ significantly between mutation carriers with minimal and mutation carriers with moderate or severe white matter hyperintensities. No significant difference in mean cerebrovascular reactivity was found between mutation carriers and non-mutation carriers.

This study suggests that a decrease in baseline TCBF in *NOTCH3* mutation carriers precedes the development of white matter hyperintensities.

## Introduction

Cerebral autosomal dominant arteriopathy with subcortical infarcts and leukoencephalopathy (CADASIL) is a hereditary small-artery disease, clinically characterised by transient ischemic attacks, strokes, progressive subcortical dementia, migraine with aura, and mood disturbances[8,10,11]. Mutations in the *NOTCH3* gene are associated with CADASIL[19]. On pathological examination, characteristic depositions of granular osmiophilic material within the media of the small and medium sized leptomeningeal and long perforating arteries of the brain are found. This vasculopathy results in destruction of vascular smooth muscle cells and fibrous thickening of the arterial wall[7,26]. Magnetic resonance (MR) imaging reveals symmetrical white matter hyperintensities (WMHs), often associated with small lacunar infarcts in the white matter and basal ganglia[39-41].

Cerebrovascular reactivity reflects the compensatory dilatory capacity of cerebral arterioles to a stimulus such as carbon dioxide or acetazolamide. In elderly individuals impaired cerebrovascular reactivity is associated with WMHs and lacunar infarcts[27-29]. In patients with CADASIL, alterations in cerebral blood flow and cerebrovascular reactivity have also been shown, with a significant reduction in baseline cerebral blood flow and cerebrovascular reactivity in areas of WMHs[30-33].

The aim of the present study was to further explore the correlation of flow disturbance and WMHs. We hypothesised that flow disturbance is the primary event that gives rise to the development of WMHs. To address this issue, we assessed baseline total cerebral blood flow (TCBF) and cerebrovascular reactivity using phase contrast MR imaging in CADASIL patients with minimal WMHs, in CADASIL patients with moderate or severe WMHs, and in non-mutated family members.

## Materials and methods

### Subjects

Sixty-three members of 15 CADASIL families participating in an ongoing study of CADASIL, agreed to undergo MR imaging. *NOTCH3* mutation screening was performed for all subjects by direct sequencing analysis[22]. Family members who proved not to have a *NOTCH3* mutation served as a control group. Participants were considered symptomatic when they had a history of neurologic deficits or cognitive decline. In addition to the standard MR imaging protocol, 38 participants gave permission for the administration of acetazolamide. The institutional medical ethical committee approved the study.

*MR imaging*

All imaging was performed on a MR system operating at a field-strength of 1.5 Tesla (Philips Medical Systems, Best, The Netherlands). Conventional T1-weighted spin echo images (slice thickness 6 mm with a 0.6 mm interslice gap, TR/TE 600/20 ms, matrix 256 x 205, and a field of view (FOV) 220 x 165 mm), dual T2-weighted fast spin echo (FSE) images (slice thickness 3 mm without interslice gap, TR/TE 3000/27/120 ms, matrix 256 x 205, FOV 220 x 220 mm), and fast fluid-attenuated inversion recovery (FLAIR) images (3.0/0.0 mm, TR/TE 8000/100 ms, inversion time 2000 ms, matrix 256 x 192, FOV 220 x 176 mm) were obtained. All images were performed in the axial plane parallel to the inferior border of the genu and splenium of the corpus callosum. A gradient echo phase contrast technique (TR/TE 16/9 ms; flip angle 7.5°; 5 mm slice thickness; FOV 250 x 188 mm; matrix 256 x 154) with a velocity encoding of 100 cm/s was used for non-triggered flow measurements[112]. The scan plane was chosen perpendicular to the basilar artery and both internal carotid arteries. Cerebral blood flow was measured ten minutes before the administration of 14 mg/kg acetazolamide intravenously and repeated at 5, 10, 15, and 20 minutes after the administration of acetazolamide. The same position of the scan plane was used for repeated flow measurements. Blood pressure, peripheral saturation, and heart rate were continuously monitored.

For cerebral blood flow assessment, images were analysed using the software package FLOW®[93,113]. A region of interest was manually drawn around the basilar artery and the left and right internal carotid artery in the phase image by one observer (RvdB). The flow volume was calculated by integrating the flow velocity values within the contour multiplied by the area. Flow in the basilar artery and the left and right internal carotid artery were added and considered to represent TCBF in ml/min[114]. The baseline TCBF and maximum TCBF were respectively defined TCBF before and the maximum TCBF obtained after the administration of acetazolamide. Cerebrovascular reactivity was defined as: cerebrovascular reactivity = (maximum TCBF - baseline TCBF) / baseline TCBF x 100%.

*WMHs and lacunar infarcts rating*

WMHs were defined as white matter areas with increased signal intensity on intermediate, T2-, and FLAIR weighted images. WMHs volume (in ml) measurements were performed on FSE dual images by one observer, using a locally developed semi-automated segmentation software that combines knowledge-based fuzzy clustering and region growing techniques. The software computes an additional T2/proton density angle image in order to distinguish the lesions from cerebrospinal fluid. Volume of WMHs was corrected for total brain volume by dividing the individual volume of WMHs by

intracranial volume and expressed in percentage. The whole post processing procedure yielded an intraclass correlation coefficient of >0.99 (95% CI: 0.96-1.0) in an analysis of data sets from 10 patients examined twice by the same observer who performed the automated segmentation.

In addition, the number of lacunar infarcts, defined as parenchymal defects not extending to the cortical grey matter with a signal intensity following that of cerebrospinal fluid on all pulse sequences, irrespective of size, were counted on hardcopies by an experienced neuroradiologist. In the basal ganglia, areas that were isointense to cerebrospinal fluid on all pulse sequence and located in the lower one-third of the corpus striatum were excluded in an effort to differentiate lacunar infarcts from normal dilated perivascular spaces[80,100].

### Statistical analysis

Differences between NOTCH3 mutation carriers and non-mutated individuals in volume of WMHs, number of lacunar infarcts and flow parameters, were performed with ANOVA. Increase of TCBF after acetazolamide was analysed with paired t-test and the effect of age on volume of WMHs and baseline TCBF with linear regression analysis. In a second phase of the analysis the mutation carriers were separated into groups with minimal volume of WMHs and with moderate or severe volume of WMHs, to assess the nature of the correlation between WMHs and flow changes. ANOVA was performed with age and sex as covariates. A P-value of $P<0.05$ was considered significant. The statistical package SPSS-10 (SPSS, Inc) was used for data analysis.

*Table 1 Baseline characteristics of the CADASIL population*

|  | NOTCH3 non-mutation carriers (n=22) | NOTCH3 mutation carriers (n=40) |
|---|---|---|
| Mean age, yr (SD) | 39 (±12) | 45 (±10) |
| Male, n (%) | 10 (45) | 19 (48) |
| Hypertension, n (%) | 5 (23) | 3 (8) |
| Symptomatic/ asymtomatic, n | 0/22 | 33/7 |

## Results

### Subjects

Of 63 CADASIL family members, 41 subjects had a mutation in the NOTCH3 gene and 22 did not. One individual had an incomplete MR imaging examination due to claustrophobia and was therefore excluded from the analysis. The mean age of the remaining 40 NOTCH3 mutation carriers was

45 years ±10 years. Thirty-three patients of this group were symptomatic, with symptoms ranging from one transient ischemic attacks to multiple strokes and cognitive decline. Seven mutation carriers were asymptomatic. The 22 non-mutation carriers had a mean age of 39 years ±12 years, and were all asymptomatic (table 1). Twenty-three mutation carriers (six with minimal and 17 with moderate and severe WMHs) and 15 non-mutated carriers consented to administration of acetazolamide.

*Table 2 Differences between NOTCH3 non-mutation and NOTCH3 mutation carriers in WMHs volume, number of lacunar infarcts, and flow parameters.*

|  | *NOTCH3* non-mutation carriers (n=22) | *NOTCH3* mutation carriers (n=40) | P-value |
|---|---|---|---|
| Mean WMH volume, % (range) | 0.01 (0-0.08) | 5.2 (0-15) | < 0.001 |
| Mean no. of lacunar infarcts (range) | 0.5 (0-10) | 15 (0-60) | < 0.001 |
| Mean bTCBF, ml/min (±SD) | 721 (±156) | 566 (±133) | < 0.001 |
| Mean CVR, % (±SD)* | 69 (±21) | 62 (±18) | 0.26 |

*P values by analysis of variance. For mean CVR, n=38 (seem methods). WMH=white matter hyperintensities; bTCBF baseline total cerebral blood flow; CVR=cerebrovascular reactivty*
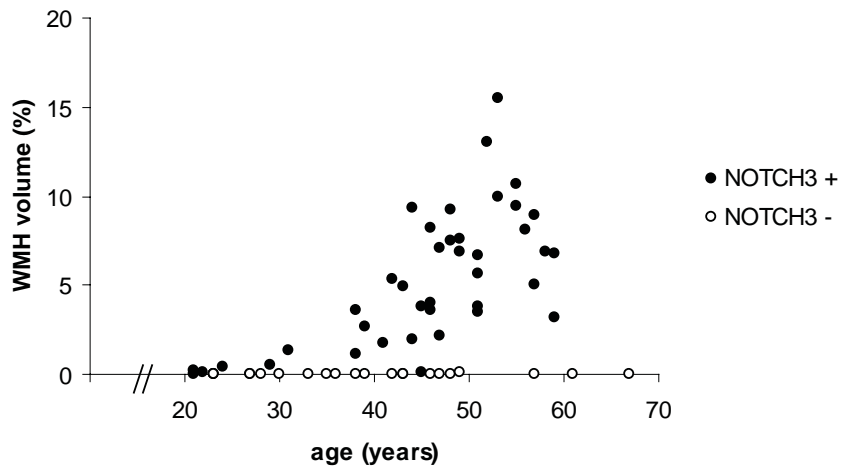


*Figure 1. Graph shows white matter hyperintensities (WMH) volume according to age in NOTCH3 non-mutation and mutation carriers. WMH increase with age in NOTCH3 mutation carriers but not in NOTCH3 non-mutation carriers.*

*Comparison between NOTCH3 mutation carriers and non-mutation carriers.*

The total volume of WMHs, number of lacunar infarcts, and flow parameters are given in table 2. The mutation carriers had a significantly higher volume of WMHs and a higher number of lacunar infarcts, whereas baseline TCBF was significantly lower. In both groups, the average TCBF increased significantly after the administration of acetazolamide (P<0.001). Because the increase in TCBF on administration of acetazolamide was proportional to baseline TCBF, no significant difference in cerebrovascular reactivity was found.

The changes in volume of WMHs according to age are graphically represented in figure 1. This figure shows that there is an increase in volume of WMHs in mutation carriers with age; volume of WMHs in non-mutated carriers did not increase.

In figure 2, changes in baseline TCBF versus age are demonstrated. As shown by the parallel regression lines through the *NOTCH3* mutation carriers and the *NOTCH3* non-mutation carriers the TCBF was lower at any age in the *NOTCH3* mutation carriers (mean difference 124 ml/min, P=0.001).

*Table 3. Flow parameters in NOTCH3 non-mutation carriers and the NOTCH3 mutation carriers with minimal WMH and moderate and severe WMH*

|  | *NOTCH3* non-mutation carriers | *NOTCH3* mutation carriers | | |
|  |  | minimal WMH | moderate/ severe WMH | P-value |
| --- | --- | --- | --- | --- |
| n | 22 | 8 | 32 |  |
| Mean age, yr (±SD) | 39 (±12) | 29 (±9) | 49 (±6) | < 0.001 |
| Mean WMH volume % (range) | 0.01 (0-0.08) | 0.5 (0.02-1.3) | 6.5 (1.7-15) | < 0.001 |
| Mean bTCBF, ml/min (±SD) |  |  |  |  |
| Uncorrected | 721 (±136) | 682 (±136) | 537 (±136) | < 0.001 |
| Corrected for age | 705 (±136) | 624 (±150) | 562 (±147) | 0.003 |
| Corrected for age and sex | 704 (±136) | 620 (±158) | 563 (±147) | 0.004 |

*P values by analysis of variance. WMH=white matter hyperintensities; bTCBF=baseline total cerebral blood flow*

**Comparison between NOTCH3 mutation carriers with minimal and moderate/ severe WMHs.**

Figure 1 shows that there were eight *NOTCH3* mutation carriers with minimal and 32 *NOTCH3* mutation carriers with moderate or severe WMHs. The cut off value of volume of WMHs was 1.5%. To study the correlation between low TCBF and WMHs in patients with a *NOTCH3* mutation, we used this cut off value to separate the *NOTCH3* mutation carriers in those with minimal WMHs and those with moderate or severe WMHs (table 3). The highest baseline TCBF was present in the *NOTCH3* non-mutation carriers, followed by the *NOTCH3*

mutation carriers with minimal and *NOTCH3* mutation carriers with moderate or severe WMHs (ANOVA, P<0.001). After adjustment for age and adjustment for age and sex, the difference in corrected baseline TCBF values remained significant. Post hoc analysis showed that the difference in baseline TCBF between *NOTCH3* mutation carriers with and without moderate or severe WMHs was not significant.
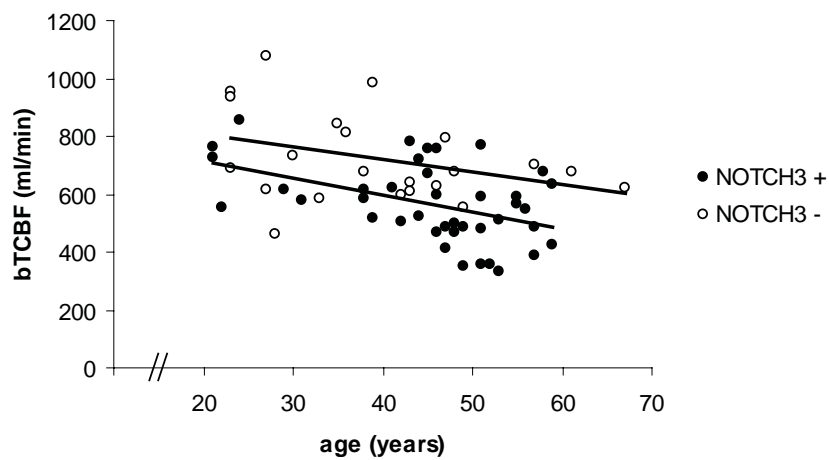


*Figure 2. Baseline total cerebral blood flow (bTCBF) in NOTCH3 mutation and non-mutation carriers. bTCBF is significantly lower in NOTCH3 mutation carriers compared with NOTCH3 non-mutation carriers (mean difference 124 ml/min).*

## Discussion

In CADASIL patients two types of lesions affecting small cerebral arteries are observed that might affect cerebral haemodynamics. First, the arteriolar lumen is narrowed as a consequence of fibrous thickening of the arterial wall. This phenomenon presumably reduces baseline blood flow. Second, vascular smooth muscle cells are destroyed, which might impair the vascular dilatory response to hypoxia[30,32]. In this study, we found a decrease in baseline TCBF in *NOTCH3* mutation carriers as compared with *NOTCH3* non-mutation carriers, whereas the capacity of the arterial wall to dilate, measured by acetazolamide response, appeared normal in *NOTCH3* mutation carriers. These observations suggest that narrowing of the arterial lumen has a more profound effect on cerebral haemodynamics in CADASIL patients than dysfunction of vascular smooth muscle cells.

An alternative explanation for the observed reduced baseline TCBF in *NOTCH3* mutation carriers could also be raised. NOTCH3 encodes for a transmembrane protein with a receptor and cell signal transduction function. Besides to NOTCH3, there are three other known mammalian NOTCH proteins[115]. Evidence from several of studies has indicated a role for Notch signalling during vascular development[116]. For example, an activated form of NOTCH4 in the embryonic vasculature causes abnormal vessel structure and patterning[117]. Possibly, mutations in NOTCH3 may also lead to an abnormal development of the cerebral vasculature in CADASIL. The observation that flow abnormalities were present in all age groups in this study could thus be explained by such an innate structural abnormality of cerebral blood vessels, and not necessarily acquired structural abnormalities.

Using MR bolus tracking and acetazolamide in CADASIL patients, Chabriat et al found a reduction in both baseline perfusion and cerebrovascular reactivity within WMHs[32]. Similarly, Mellies et al observed a reduction in grey matter perfusion that correlated with the amount of WMHs, using SPECT[31]. These observations, however, have not made it clear whether structural brain changes are secondary to impaired flow, or whether impaired flow is a consequence of brain damage.

Several observations in our study provide insight into the nature of the correlation between WMHs and lacunar infarcts on the one hand, and cerebral flow disturbance on the other. In this study, we assessed TCBF based on phase contrast MR imaging. This method provides robust quantitative data on the total amount of blood flowing to the brain[114,118]. Using phase contrast MR imaging we found a significantly diminished baseline TCBF at any age, even in young *NOTCH3* mutation carriers with minimal structural lesions (figure 2). It is unlikely that the cerebral blood flow to the brain is significantly reduced by a flow reduction in these small lesions, which only represent a very small percentage of the brain volume. A more realistic explanation is that the observed TCBF reduction in these patients is the result of more widespread flow impairment, which not just affects the areas of WMHs and lacunar infarcts. Furthermore, in all CADASIL patients with minimal WMHs and minimal lacunar infarcts, irrespective of age, baseline TCBF was observed to be abnormal. Both observations suggest that a reduction in baseline flow precedes, and is responsible for, the occurrence of WMHs and lacunar infarcts in CADASIL.

In this study we did not find evidence for a decreased cerebrovascular reactivity in CADASIL patients. This finding differs from observations in other studies. Several explanations for this seeming contradiction can be put forward. First, the CADASIL patients who participated in our study were younger then those in the other studies. A reduced cerebrovascular reactivity might be more pronounced in an older patient population. Second, in our study a different

technique for flow quantification was used as compared with previous studies. In these other studies, single-photon emission computed tomography, positron emission tomography, MR bolus tracking, and transcranial Doppler ultrasound were used to estimate changes in cerebral blood flow[30,31,32,119]. With the exception of transcranial Doppler, these techniques detect flow changes in brain parenchyma, not changes in the supplying vessels of the brain. In a recent article, poor correlations were found between estimates of cerebrovascular reactivity based on MR bolus tracking and those based on phase contrast MR imaging, which was attributed to the two methods reflecting different aspects of the cerebrovascular reactivity[120]. However, both transcranial Doppler and phase contrast MR imaging enable the measurement of blood flow velocity in extraparenchymal vessels. Still, others showed poor correlation between flow data resulting from these two methods, which was attributed to a lack of reproducibility of transcranial Doppler measurements because of operator dependency[121]. In this study we decided to use phase contrast MR imaging as this technique has the advantage of being operator independent and involving straightforward flow volume quantification as demonstrated by Bakker and Spilt et al[112,120,122]. In addition, phase contrast MR imaging has the advantage of providing during one examination both flow data and morphological data which is not possible with other techniques.

In conclusion, our findings suggest that flow impairment gives rise to the development of WMHs and lacunar infarcts in CADASIL patients. Furthermore, in CADASIL patients with minor white matter hyperintensities the TCBF is reduced in rest, whereas the cerebral vascular dilatory capacity is preserved. This novel observation is relevant, because it may imply that by increasing the cerebral blood flow through a challenge of the remaining vasodilatory capacity, vasodilatory agents might limit the development of WMHs and lacunar infarcts in CADASIL patients. Further studies are needed to determine the efficacy of pharmacological improvement of cerebral blood flow in CADASIL patients.

# Summary and conclusions

*Summary and conclusions*

Magnetic resonance (MR) imaging plays an important role in the diagnostic work-up of CADASIL patients. This thesis describes the typical appearance of MR abnormalities in CADASIL patients, the natural history of these abnormalities, and the differences of these lesions as compared to the lesions that occur in multiple sclerosis (MS). Also included are the results of a study on the influence of apolipoprotein E (apoE) genotype and a study of cerebral blood flow on the development of MR abnormalities.

In chapter 1 a short introduction is given on the aetiology and clinical appearance of CADASIL, the initial radiological descriptions of cerebral lesions, and the role of imaging in the diagnostic work-up of these patients. Furthermore the goal and outline of this thesis are portrayed.

In chapter 2 we assessed whether microbleeds are present in CADASIL and, if so, whether they are associated with other patient characteristics. Several studies have shown that microbleeds are associated with the presence of intracerebral haemorrhage. Although there are some descriptions on the occurrence of intracerebral haemorrhage in patients with CADASIL, the prevalence of haemorrhages in CADASIL patients was unknown at the start of this study. By using a T2* gradient-echo technique, detection of haemosiderin deposits reflecting remnants of intracerebral microbleeds is possible. In this study we found that 31% of symptomatic CADASIL patients had microbleeds on MR imaging, predominantly in the thalamus (figure 1). This suggests that CADASIL patients might be at risk for developing intracerebral haemorrhage.

In chapter 3 we describe a new radiological finding in CADASIL patients, the so called subcortical lacunar lesions (SLLs). SLLs are linearly arranged groups of rounded, circumscribed lesions just below the cortex, at the grey white matter junction with a signal intensity that is identical to that of CSF on all pulse sequences. These lesions are best seen on thin sections (3mm) fluid-attenuated inversion-recovery (FLAIR) images (figure 2a,b). SLLs were found in 59% of CADASIL patients, and when present, SLLs invariably occurred in the anterior temporal lobe, always in combination with white matter hyperintensities (WMHs). Because none of the control subjects showed SLLs, we believe that SLLs are highly characteristic for CADASIL and detection of SLLs might help in establishing de diagnosis of CADASIL. Histological examination revealed that the lesions are caused by a distention of the perivascular space of perforating arteries (figure 2c).

In chapter 4 we describe the natural history of the various brain lesions that can be observed in CADASIL patients. These lesions include not only WMHs and lacunar infarcts but also the recently reported microbleeds and SLLs. The results of this study showed that these lesions develop in a predictable way

during the course of the disease. Hyperintensities were present in all CADASIL patients, increasing with age and with a predilection for the temporal and frontal lobe (figure 3). In young CADASIL patients (20-30 years), hyperintensities in the anterior temporal lobe, in one patient in combination with SLLs, are the only abnormalities seen on MR imaging. The development of lacunar infarcts starts in the fourth decade. Microbleeds occurred during the fifth and sixth decade. In patients older than 50 years all four abnormalities were frequently observed. Knowledge of these age dependent MR patterns should help to make the diagnosis of CADASIL.
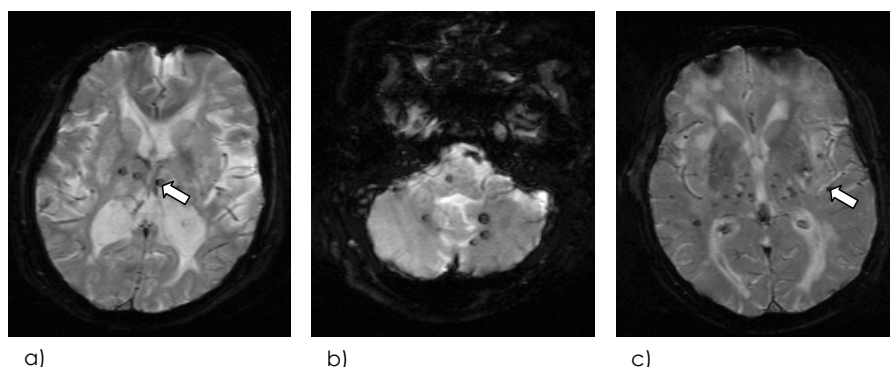


a)                              b)                              c)

*Figure 1 Axial T2\*-weighted gradient echo planar images show numerous microbleeds, located in the thalamus, cerebellum as well as deep and subcortical white matter (arrows).*

In chapter 5 we describe the results of a study in which we compared the neuropsychological, clinical, and neuroradiological features of CADASIL patients and controls between 21 and 35 years of age. The main results were that there was no quantifiable physical or cognitive impairment in young CADASIL patients. Disease expression was only confined to migraine and, less frequently, TIA and (minor) stroke. Radiologically, a characteristic MR lesion pattern was present in all CADASIL patients. WMHs, sometimes subtle, were present in the frontal lobes and periventricular frontal caps, but most importantly, first appeared in the anterior temporal lobe (figure 3).

In chapter 6 we compared the radiological appearance of CADASIL to that of multiple sclerosis (MS), a disease with clinical and radiological similarities to CADASIL. CADASIL patients showed significantly more SLLs and hyperintensities in the anterior temporal lobe and the external capsule compared with MS. Although in general practice the prevalence of MS is higher than of CADASIL, the hyperintensities in the anterior temporal lobe especially in combination

with one of the other CADASIL MR hallmarks should lead to the diagnosis of CADASIL. MR imaging permits discriminating between CADASIL and MS, even at a young age, so that misdiagnosis can be avoided.
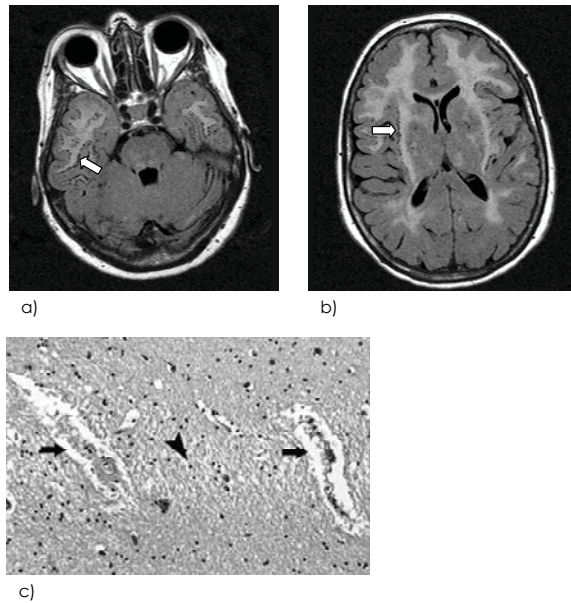


a)

b)



c)

*Figure 2 Axial FLAIR MR images show SLLs affecting the anterior part of the temporal lobe (a) and the subinsular region (b). Photomicrograph (c) shows detail of two vessels. The lower part of the vessel on the left shows characteristic thickening of the arterial wall; both vessels have a distended perivascular space (arrows) and spongiosis of the adjacent parenchyma (arrowhead) (Haematoxylin-eosin stain; original magnification, x100.).*

In chapter 7 the influence of apoE genotype on the development of structural brain lesions of CADASIL is studied. The apoE genotype, a well known genetic risk factor for Alzheimer's disease and sporadic cerebral amyloid angiopathy, does not influence the amount of structural cerebral changes as seen on MR imaging in CADASIL patients. Therefore other genetic or non-genetic factors probably underlie the variable natural history of the disease.

Chapter 8 deals with the question whether a decrease in cerebral blood flow or cerebrovascular reactivity is primarily responsible for the development of WMHs and lacunar infarcts. To address this issue, phase contrast MR imaging was used to assess baseline total cerebral blood flow and cerebrovascular reactivity after acetazolamide. The response on acetazolamide was not decreased relative to the baseline total cerebral blood flow. However, the mean baseline total cerebral blood flow was significantly decreased in

patients with CADASIL. These findings suggest that vascular stenosis plays a larger role in the development WMHs and lacunar infarcts in CADASIL patients, than diminished vascular reactivity.
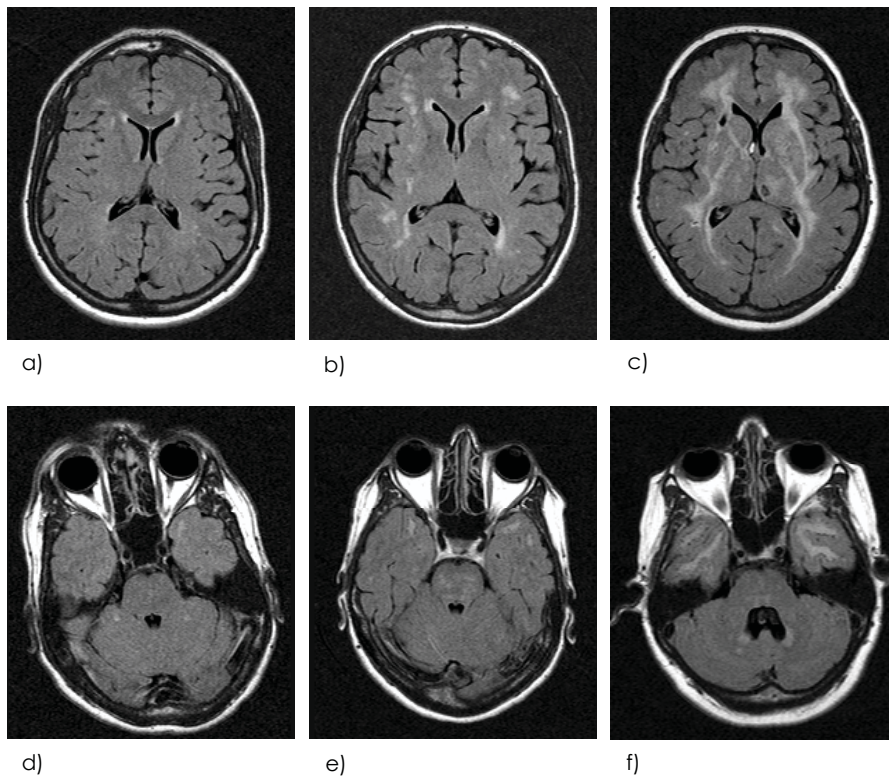


*Figure 3 FLAIR MR images of three mutation carriers aged 26, 46 and 53 years. Axial slices through the level of the temporal lobes and basal ganglia showing the development of WMHs in the temporal lobe and external and internal capsule.*

# Samenvatting en conclusies

## Samenvatting en conclusies

Sinds de zeventiger jaren van de vorige eeuw zijn families beschreven met dominant overervende herseninfarcten, dementie en witte stofafwijkingen zichtbaar op CT- en MRI-onderzoek. De aandoening werd met verschillende namen aangeduid waaronder onder andere "hereditaire multi-infarct dementie en chronische familiaire vasculaire encephalopathie". In 1993 werd het acroniem CADASIL (cerebrale autosomaal dominante arteriopathie met subcorticale infarcten en leukoencephalopathie) geïntroduceerd en in 1996 werd een gemuteerd gen, het *NOTCH3* gen op chromosoom 19, ontdekt bij CADASIL-patiënten.

De voornaamste kenmerken van deze dominant overervende aandoening zijn recidiverende transient ischemic attacks (TIA's; aanvallen van kortdurende neurologische uitval), herseninfarcten en een progressieve vasculaire dementie. Tevens zijn migraine met aura, stemmingstoornissen en in mindere mate epilepsie beschreven. Patiënten met CADASIL overlijden over het algemeen op een leeftijd van 55 tot 65 jaar, na een ziekteduur van 10 à 20 jaar.

CADASIL berust op een non-atherosclerotische, non-amyloidotische angiopathie met typische granulaire deposities in de media van de kleine cerebrale arteriën. Ook zijn deze vaatwandveranderingen aangetoond elders in het lichaam, bijvoorbeeld in de huidarteriolen. Echter hier geven deze veranderingen niet zoveel schade als in de hersenen.

MRI-onderzoek van de hersenen bij CADASIL-patiënten toont witte stofafwijkingen en lacunaire infarcten. De meeste witte stofafwijkingen bevinden zich periventriculair en frontotemporaal. Opvallend is dat de witte stofafwijkingen ook gevonden kunnen worden bij familieleden van CADASIL-patiënten die nog geen klinische verschijnselen van de ziekte hebben. MRI speelt een belangrijke rol in de diagnostische work-up van CADASIL-patiënten.

Het proefschrift bestaat uit zeven studies die zich achtereenvolgens richten op de volgende vragen:

1) Hebben CADASIL-patiënten een verhoogd risico op hersenbloedingen?
2) Is er een relatie tussen de hoeveelheid microbloedingen en de ernst van de ziekte?
3) Wat is de prevalentie en distributie van zogenaamde subcorticale lacunaire laesies?
4) Welke MRI-afwijkingen worden aangetroffen bij CADASIL-patiënten en wat is de prevalentie van deze afwijkingen bij verschillende leeftijdcategorieën?

5) Wat zijn de klinische, neuropsychologische en radiologische bevindingen bij CADASIL-patiënten jonger dan 35 jaar?

6) Is het mogelijk om CADASIL en multiple sclerosis radiologisch van elkaar te onderscheiden?

7) Wat is de invloed van het apolipoproteine E (apoE) genotype op het ontwikkelen van radiologische afwijkingen bij CADASIL?

8) Is primair een afname in cerebrale bloedstroom of een afname in de cerebrovasculaire reactiviteit verantwoordelijk voor de ontwikkeling van witte stofafwijkingen en lacunaire infarcten?

In hoofdstuk 1 wordt een korte beschrijving gegeven van het ziektebeeld CADASIL. Vervolgens worden doel en opzet van dit proefschrift beschreven.

In hoofdstuk 2 wordt onderzocht of cerebrale microbloedingen voorkomen bij CADASIL patiënten en of ze geassocieerd zijn met andere patiëntenkarakteristieken. Met behulp van een speciale MRI-techniek om haemosiderine te detecteren, de zogenaamde T2* gradient-echo sequentie, is in deze studie aangetoond dat 31% van de CADASIL-patiënten microbloedingen heeft, met name in de thalamus. Cerebrale microbloedingen worden in andere studies geassocieerd met een verhoogd risico op hersenbloedingen, derhalve dient men ook bij CADASIL-patiënten bedacht te zijn op dit mogelijk verhoogd risico op hersenbloedingen. Er is geen duidelijke relatie gevonden tussen de hoeveelheid microbloedingen en de hevigheid van de ziekte.

Hoofdstuk 3 beschrijft een nieuwe radiologische bevinding bij CADASIL-patiënten, de zogenaamde subcorticale lacunaire laesie. Subcorticale lacunaire laesies zijn kleine ronde laesies, lineair gerangschikt op de grens van de grijze en witte stof, met dezelfde signaalintensiteit als liquor cerebrospinalis. Deze laesies zijn het beste te zien op een fluid-attenuated inversion recovery sequentie (FLAIR) met dunne coupes. In 59% van de CADASIL-patiënten worden subcorticale lacunaire laesies gevonden. Subcorticale lacunaire laesies bevinden zich altijd in de anterieure temporaal kwab en altijd aangrenzend aan afwijkende witte stof. Histologisch blijken subcorticale lacunaire laesies te berusten op verwijde perivasculaire ruimtes. Deze afwijking wordt niet gezien op MRI-onderzoeken van controlegroepen en daarom kan de aanwezigheid van subcorticale lacunaire laesies een specifieke diagnostische aanwijzing zijn voor CADASIL.

In hoofdstuk 4 worden het patroon en het natuurlijke beloop van alle MRI-afwijkingen die bij CADASIL zijn beschreven, namelijk witte stofafwijkingen, lacunaire infarcten, microbloedingen en subcorticale lacunaire laesies, onderzocht. Deze MRI-afwijkingen ontwikkelen zich volgens een vast

patroon. Bij jonge CADASIL-patiënten (tussen de 20 en 30 jaar) staan witte stofafwijkingen in de anterieure temporaalkwab en subcorticale lacunaire laesies op de voorgrond. Na de leeftijd van 30 jaar komen lacunaire infarcten voor bij de meerderheid van de CADASIL-patiënten en boven de 40 jaar zijn microbloedingen te zien. Bij patiënten ouder dan 50 jaar komen in de meerderheid van de gevallen deze afwijkingen gelijktijdig voor. De uitgebreidheid van de witte stofafwijkingen neemt toe met de leeftijd. Kennis van deze leeftijdgerelateerde MRI-afwijkingen is met name belangrijk voor de diagnostiek van CADASIL.

In hoofdstuk 5 zijn de resultaten beschreven van een studie waarin neuropsychologische, klinische en neuroradiologische veranderingen bij CADASIL-patiënten tussen de leeftijd van 21 en 35 jaar worden vergeleken met dezelfde parameters bij niet-gemuteerde leeftijdgenoten. Het belangrijkste resultaat is dat er bij jonge CADASIL-patiënten geen meetbare lichamelijke of cognitieve stoornissen aanwezig zijn. Wel komt bij mutatiedragers meer migraine met aura voor en bij een klein aantal mutatiedragers zijn er aanwijzingen voor TIA's en (minor) stroke. Alle CADASIL-patiënten hebben, soms subtiel, witte stofafwijkingen bij het MRI-onderzoek. Opvallend is dat de eerste witte stofafwijkingen ontstaan in de anterieure temporaal kwab.

In hoofdstuk 6 wordt onderzocht of er verschillen bestaan in de MRI-afwijkingen die bij jonge CADASIL- en jonge multiple sclerosis-patiënten worden aangetroffen. Zowel in klinische als radiologisch opzicht heeft CADASIL overeenkomsten met multiple sclerosis en wordt bij veel CADASIL-patiënten in eerste instantie de diagnose multiple sclerosis gesteld. CADASIL-patiënten hebben significant meer witte stofafwijkingen in de anterieure temporaal kwab en subcorticale lacunaire laesies. Ondanks het feit dat multiple sclerosis veel vaker voorkomt dan CADASIL moet toch aan de diagnose CADASIL gedacht worden bij de aanwezigheid van deze afwijkingen. Met behulp van MRI is het mogelijk om al op een jonge leeftijd onderscheid te maken tussen CADASIL en multiple sclerosis en kennis van deze verschillen kan het stellen van de verkeerde diagnose verminderen.

In hoofdstuk 7 wordt de invloed van het apoE genotype op de ontwikkeling van structurele afwijkingen in de hersenen van CADASIL-patiënten onderzocht. ApoE is een bekende genetische risicofactor voor het ontwikkel van de ziekte van Alzheimer en sporadische amyloid angiopathie. Er is een grote variatie in het natuurlijk beloop van CADASIL, echter in CADASIL heeft apoE geen invloed op de ontwikkeling van afwijkingen in de hersenen. Daarom moeten er andere factoren zijn die verantwoordelijk zijn voor het verschil in beloop van de ziekte.

In hoofdstuk 8 wordt bestudeerd of primair een afname in cerebrale bloedstroom of aantasting van de cerebrovasculaire reactiviteit verantwoordelijk is voor de ontwikkeling van witte stofafwijkingen en lacunaire infarcten. We laten zien dat in CADASIL-patiënten de cerebrovasculaire reactiviteit niet is afgenomen maar dat er wel een significante daling is van de cerebrale bloedstroom. Aangezien een daling van cerebrale bloedstroom veroorzaakt kan worden door wijdverspreide vernauwing van cerebrale bloedvaten lijkt het aannemelijk dat bij CADASIL-patiënten vernauwing van cerebrale bloedvaten een belangrijker rol speelt bij de ontwikkeling van witte stofafwijkingen en lacunaire infarcten dan aantasting van de cerebrovasculaire reactiviteit.

# References

ELEVEN

1   Sourander P, Walinder J. Hereditary multi-infarct dementia. Lancet 1977; 1(8019):1015.

2   Sourander P, Walinder J. Hereditary multi-infarct dementia. Morphological and clinical studies of a new disease. Acta Neuropathol (Berl) 1977; 39(3):247-254.

3   Sonninen V, Savontaus ML. Hereditary multi-infarct dementia. Eur Neurol 1987; 27(4):209-215.

4   Stevens DL, Hewlett RH, Brownell B. Chronic familial vascular encephalopathy. Lancet 1977; 1(8026):1364-1365.

5   Mas JL, Dilouya A, de Recondo J. A familial disorder with subcortical ischemic strokes, dementia, and leukoencephalopathy. Neurology 1992; 42(5):1015-1019.

6   Tournier-Lasserve E, Iba-Zizen MT, Romero N, Bousser MG. Autosomal dominant syndrome with strokelike episodes and leukoencephalopathy. Stroke 1991; 22(10):1297-1302.

7   Baudrimont M, Dubas F, Joutel A, Tournier-Lasserve E, Bousser MG. Autosomal dominant leukoencephalopathy and subcortical ischemic stroke. A clinicopathological study. Stroke 1993; 24(1):122-125.

8   Chabriat H, Vahedi K, Iba-Zizen MT, Joutel A, Nibbio A, Nagy TG et al. Clinical spectrum of CADASIL: a study of 7 families. Cerebral autosomal dominant arteriopathy with subcortical infarcts and leukoencephalopathy. Lancet 1995; 346(8980):934-939.

9   Ducros A, Nagy T, Alamowitch S, Nibbio A, Joutel A, Vahedi K et al. Cerebral autosomal dominant arteriopathy with subcortical infarcts and leukoencephalopathy, genetic homogeneity, and mapping of the locus within a 2-cM interval. Am J Hum Genet 1996; 58(1):171-181.

10  Dichgans M, Mayer M, Uttner I, Bruning R, Muller-Hocker J, Rungger G et al. The phenotypic spectrum of CADASIL: clinical findings in 102 cases. Ann Neurol 1998; 44(5):731-739.

11  Desmond DW, Moroney JT, Lynch T, Chan S, Chin SS, Mohr JP. The natural history of CADASIL: a pooled analysis of previously published cases. Stroke 1999; 30(6):1230-1233.

12  Wielaard R, Bornebroek M, Ophoff RA, Winter-Warnars HA, Scheltens P, Frants RR et al. A four-generation Dutch family with cerebral autosomal dominant arteriopathy with subcortical infarcts and leukoencephalopathy (CADASIL), linked to chromosome 19p13. Clin Neurol Neurosurg 1995; 97(4):307-313.

13  Ferrari MD. Migraine. Lancet 1998; 351(9108):1043-1051.

14  Rasmussen BK, Olesen J. Symptomatic and nonsymptomatic headaches in a general population. Neurology 1992; 42(6):1225-1231.

15  Chabriat H, Tournier-Lasserve E, Vahedi K, Leys D, Joutel A, Nibbio A et al. Autosomal dominant migraine with MRI white-matter abnormalities mapping to the CADASIL locus. Neurology 1995; 45(6):1086-1091.

16  Feuerhake F, Volk B, Ostertag CB, Jungling FD, Kassubek J, Orszagh M et al. Reversible coma with raised intracranial pressure: an unusual clinical manifestation of CADASIL. Acta Neuropathol (Berl) 2002; 103(2):188-192.

17  Schon F, Martin RJ, Prevett M, Clough C, Enevoldson TP, Markus HS. "CADASIL coma": an underdiagnosed acute encephalopathy. J Neurol Neurosurg Psychiatry 2003; 74(2):249-252.

18  Tournier-Lasserve E, Joutel A, Melki J, Weissenbach J, Lathrop GM, Chabriat H et al. Cerebral autosomal dominant arteriopathy with subcortical infarcts and leukoencephalopathy maps to chromosome 19q12. Nat Genet 1993; 3(3):256-259.

19  Joutel A, Corpechot C, Ducros A, Vahedi K, Chabriat H, Mouton P et al. Notch3 mutations in CADASIL, a hereditary adult-onset condition causing stroke and dementia. Nature 1996; 383(6602):707-710.

20  Peters N, Opherk C, Bergmann T, Castro M, Herzog J, Dichgans M. Spectrum of mutations in biopsy-proven CADASIL: implications for diagnostic strategies. Arch Neurol 2005; 62(7):1091-1094.

21  Fryxell KJ, Soderlund M, Jordan TV. An animal model for the molecular genetics of CADASIL. Stroke 2001; 32(1):6-11.

22  Oberstein SA, Ferrari MD, Bakker E, Van Gestel J, Kneppers AL, Frants RR et al. Diagnostic Notch3 sequence analysis in CADASIL: three new mutations in Dutch patients. Dutch CADASIL Research Group. Neurology 1999; 52(9):1913-1915.

23  Tibben A, Frets PG, Van de Kamp JJ, Niermeijer MF, Vegter-Van der Vlis M, Roos RA et al. Presymptomatic DNA-testing for Huntington disease: pretest attitudes and expectations of applicants and their partners in the Dutch program. Am J Med Genet 1993; 48(1):10-16.

24  Tibben A, Duivenvoorden HJ, Niermeijer MF, Vegter-Van der Vlis M, Roos RA, Verhage F. Psychological effects of presymptomatic DNA testing for Huntington's disease in the Dutch program. Psychosom Med 1994; 56(6):526-532.

25  Davous P, Fallet-Bianco C. [Familial subcortical dementia with arteriopathic leukoencephalopathy. A clinico-pathological case. Rev Neurol (Paris) 1991; 147(5):376-384.

26  Brulin P, Godfraind C, Leteurtre E, Ruchoux MM. Morphometric analysis of ultrastructural vascular changes in CADASIL: analysis of 50 skin biopsy specimens and pathogenic implications. Acta Neuropathol (Berl) 2002; 104(3):241-248.

27  Bakker SL, de Leeuw FE, de Groot JC, Hofman A, Koudstaal PJ, Breteler MM. Cerebral vasomotor reactivity and cerebral white matter lesions in the elderly. Neurology 1999; 52(3):578-83.

28  Molina C, Sabin JA, Montaner J, Rovira A, Abilleira S, Codina A. Impaired cerebrovascular reactivity as a risk marker for first-ever lacunar infarction: A case-control study. Stroke 1999; 30(11):2296-2301.

29  Cupini LM, Diomedi M, Placidi F, Silvestrini M, Giacomini P. Cerebrovascular reactivity and subcortical infarctions. Arch Neurol 2001; 58(4):577-581.

30  Pfefferkorn T, Stuckrad-Barre S, Herzog J, Gasser T, Hamann GF, Dichgans M. Reduced cerebrovascular $CO_2$ reactivity in CADASIL : A transcranial doppler sonography study [In Process Citation]. Stroke 2001; 32(1):17-21.

31  Mellies JK, Baumer T, Muller JA, Tournier-Lasserve E, Chabriat H, Knobloch O et al. SPECT study of a German CADASIL family: a phenotype with migraine and progressive dementia only. Neurology 1998; 50(6):1715-1721.

32  Chabriat H, Pappata S, Ostergaard L, Clark CA, Pachot-Clouard M, Vahedi K et al. Cerebral hemodynamics in CADASIL before and after acetazolamide challenge assessed with MRI bolus tracking. Stroke 2000; 31(8):1904-1912.

33    Bruening R, Dichgans M, Berchtenbreiter C, Yousry T, Seelos KC, Wu RH et al. Cerebral autosomal dominant arteriopathy with subcortical infarcts and leukoencephalopathy: decrease in regional cerebral blood volume in hyperintense subcortical lesions inversely correlates with disability and cognitive performance. AJNR Am J Neuroradiol 2001; 22(7):1268-1274.

34    Ruchoux MM, Guerouaou D, Vandenhaute B, Pruvo JP, Vermersch P, Leys D. Systemic vascular smooth muscle cell impairment in cerebral autosomal dominant arteriopathy with subcortical infarcts and leukoencephalopathy. Acta Neuropathol (Berl) 1995; 89(6):500-512.

35    Ruchoux MM, Chabriat H, Bousser MG, Baudrimont M, Tournier-Lasserve E. Presence of ultrastructural arterial lesions in muscle and skin vessels of patients with CADASIL. Stroke 1994; 25(11):2291-2292.

36    Goebel HH, Meyermann R, Rosin R, Schlote W. Characteristic morphologic manifestation of CADASIL, cerebral autosomal-dominant arteriopathy with subcortical infarcts and leukoencephalopathy, in skeletal muscle and skin. Muscle Nerve 1997; 20(5):625-627.

37    Rubio A, Rifkin D, Powers JM, Patel U, Stewart J, Faust P et al. Phenotypic variability of CADASIL and novel morphologic findings. Acta Neuropathol (Berl) 1997; 94(3):247-254.

38    Schultz A, Santoianni R, Hewan-Lowe K. Vasculopathic changes of CADASIL can be focal in skin biopsies. Ultrastruct Pathol 1999; 23(4):241-247.

39    Chabriat H, Levy C, Taillia H, Iba-Zizen MT, Vahedi K, Joutel A et al. Patterns of MRI lesions in CADASIL. Neurology 1998; 51(2):452-7.

40    Skehan SJ, Hutchinson M, MacErlaine DP. Cerebral autosomal dominant arteriopathy with subcortical infarcts and leukoencephalopathy: MR findings. AJNR Am J Neuroradiol 1995; 16(10):2115-2119.

41    Yousry TA, Seelos K, Mayer M, Bruning R, Uttner I, Dichgans M et al. Characteristic MR lesion pattern and correlation of T1 and T2 lesion volume with neurologic and neuropsychological findings in cerebral autosomal dominant arteriopathy with subcortical infarcts and leukoencephalopathy (CADASIL). AJNR Am J Neuroradiol 1999; 20(1):91-100.

42    Coulthard A, Blank SC, Bushby K, Kalaria RN, Burn DJ. Distribution of cranial MRI abnormalities in patients with symptomatic and subclinical CADASIL. Br J Radiol 2000; 73(867):256-265.

43    O'Sullivan M, Jarosz JM, Martin RJ, Deasy N, Powell JF, Markus HS. MRI hyperintensities of the temporal lobe and external capsule in patients with CADASIL. Neurology 2001; 56(5):628-634.

44    Chabriat H, Mrissa R, Levy C, Vahedi K, Taillia H, Iba-Zizen MT et al. Brain stem MRI signal abnormalities in CADASIL. Stroke 1999; 30(2):457-459.

45    Tournier-Lasserve E, Joutel A, Melki J, Weissenbach J, Lathrop GM, Chabriat H et al. Cerebral autosomal dominant arteriopathy with subcortical infarcts and leukoencephalopathy maps to chromosome 19q12. Nat Genet 1993; 3(3):256-259.

46    Chabriat H, Pappata S, Poupon C, Clark CA, Vahedi K, Poupon F et al. Clinical severity in CADASIL related to ultrastructural damage in white matter: in vivo study with diffusion tensor MRI. Stroke 1999; 30(12):2637-2643.

47    Iannucci G, Dichgans M, Rovaris M, Bruning R, Gasser T, Giacomotti L et al. Correlations between clinical findings and magnetization transfer imaging metrics of tissue damage in individuals with cerebral autosomal dominant arteriopathy with subcortical infarcts and leukoencephalopathy. Stroke 2001; 32(3):643-648.

48    Auer DP, Schirmer T, Heidenreich JO, Herzog J, Putz B, Dichgans M. Altered white and gray matter metabolism in CADASIL: a proton MR spectroscopy and 1H-MRSI study. Neurology 2001; 56(5):635-642.

49    Vahedi K, Tournier-Lasserve E, Vahedi K, Chabriat H, Bousser MG. An additional monogenic disorder that masquerades as multiple sclerosis. Am J Med Genet 1996; 65(4):357-358.

50    O'Riordan S, Nor AM, Hutchinson M. CADASIL imitating multiple sclerosis: the importance of MRI markers. Mult Scler 2002; 8(5):430-432.

51    Ruchoux MM, Maurage CAa. CADASIL: Cerebral autosomal dominant arteriopathy with subcortical infarcts and leukoencephalopathy. J Neuropathol Exp Neurol 1997; 56(9):947-964.

52    Brott T, Thalinger K, Hertzberg V. Hypertension as a risk factor for spontaneous intracerebral hemorrhage. Stroke 1986; 17(6):1078-1083.

53    Kase CS. Intracerebral hemorrhage: non-hypertensive causes. Stroke 1986; 17(4):590-595.

54  Tanaka A, Ueno Y, Nakayama Y, Takano K, Takebayashi S. Small chronic hemorrhages and ischemic lesions in association with spontaneous intracerebral hematomas. Stroke 1999; 30(8):1637-1642.

55  Kwa VI, Franke CL, Verbeeten B, Jr., Stam J. Silent intracerebral microhemorrhages in patients with ischemic stroke. Amsterdam Vascular Medicine Group. Ann Neurol 1998; 44(3):372-377.

56  Fazekas F, Kleinert R, Roob G, Kleinert G, Kapeller P, Schmidt R et al. Histopathologic analysis of foci of signal loss on gradient-echo T2*-weighted MR images in patients with spontaneous intracerebral hemorrhage: evidence of microangiopathy-related microbleeds. AJNR Am J Neuroradiol 1999; 20(4):637-642.

57  Roob G, Lechner A, Schmidt R, Flooh E, Hartung HP, Fazekas F. Frequency and location of microbleeds in patients with primary intracerebral hemorrhage [In Process Citation]. Stroke 2000; 31(11):2665-2669.

58  Roob G, Schmidt R, Kapeller P, Lechner A, Hartung HP, Fazekas F. MRI evidence of past cerebral microbleeds in a healthy elderly population. Neurology 1999; 52(5):991-994.

59  Scheltens P, Barkhof F, Leys D, Pruvo JP, Nauta JJ, Vermersch P et al. A semiquantative rating scale for the assessment of signal hyperintensities on magnetic resonance imaging. J Neurol Sci 1993; 114(1):7-12.

60  Thrift AG, McNeil JJ, Forbes A, Donnan GA. Risk factors for cerebral hemorrhage in the era of well-controlled hypertension. Melbourne Risk Factor Study (MERFS) Group. Stroke 1996; 27(11):2020-2025.

61  Greenberg SM, Finklestein SP, Schaefer PWa. Petechial hemorrhages accompanying lobar hemorrhage: detection by gradient-echo MRI. Neurology 1996; 46(6):1751-1754.

62  Offenbacher H, Fazekas F, Schmidt R, Koch M, Fazekas G, Kapeller P. MR of cerebral abnormalities concomitant with primary intracerebral hematomas. AJNR Am J Neuroradiol 1996; 17(3):573-578.

63  Joutel A, Chabriat H, Vahedi K, et al. Notch3 splice site mutation causing autosomal dominant migraine with MRI white matter abnormalities. Neurology 1998;50:A441. Abstract

64 Ceroni M, Poloni TE, Tonietti S, Fabozzi D, Uggetti C, Frediani F et al. Migraine with aura and white matter abnormalities: Notch3 mutation. Neurology 2000; 54(9):1869-1871.

65 A randomized trial of anticoagulants versus aspirin after cerebral ischemia of presumed arterial origin. The Stroke Prevention in Reversible Ischemia Trial (SPIRIT) Study Group. Ann Neurol 1997; 42(6):857-865.

66 Joutel A, Vahedi K, Corpechot C, Troesch A, Chabriat H, Vayssiere C et al. Strong clustering and stereotyped nature of Notch3 mutations in CADASIL patients. Lancet 1997; 350(9090):1511-1515.

67 Auer DP, Putz B, Gossl C, Elbel GK, Gasser T, Dichgans M. Differential Lesion Patterns in CADASIL and Sporadic Subcortical Arteriosclerotic Encephalopathy: MR Imaging Study with Statistical Parametric Group Comparison. Radiology 2001; 218(2):443-451.

68 Van Broeckhoven C, Haan J, Bakker E, Hardy JA, Van Hul W, Wehnert A et al. Amyloid beta protein precursor gene and hereditary cerebral hemorrhage with amyloidosis (Dutch). Science 1990; 248(4959):1120-1122.

69 Haan J, Roos RA, Algra PR, Lanser JB, Bots GT, Vegter-Van der Vlis Ma. Hereditary cerebral haemorrhage with amyloidosis--Dutch type. Magnetic resonance imaging findings in 7 cases. Brain 1990; 113(Pt 5):1251-67.

70 Bornebroek M, Haan J, Maat-Schieman ML, Van Duinen SG, Roos RAa. Hereditary cerebral hemorrhage with amyloidosis-Dutch type (HCHWA-D): I--A review of clinical, radiologic and genetic aspects. Brain Pathol 1996; 6(2):111-4.

71 Shepherd J, Blauw GJ, Murphy MB, Cobbe SM, Bollen EL, Buckley BM et al. The design of a prospective study of Pravastatin in the Elderly at Risk (PROSPER). PROSPER Study Group. PROspective Study of Pravastatin in the Elderly at Risk. Am J Cardiol 1999; 84(10):1192-1197.

72 Lexa FJ, Trojanawski JQ, B raffman BH, et al. The aging brain and neurodegenerative disease. In: Atlas SW, ed. Magnetic resonance imaging of the brain and spine, 2nd ed. Philadelphia, Pa:Lippincott-Raven,1996;803-870

73    Song CJ, Kim JH, Kier EL, Bronen RA. MR imaging and histologic features of subinsular bright spots on T2- weighted MR images: Virchow-Robin spaces of the extreme capsule and insular cortex. Radiology 2000; 214(3):671-677.

74    Sasaki M, Sone M, Ehara S, Tamakawa Y. Hippocampal sulcus remnant: potential cause of change in signal intensity in the hippocampus. Radiology 1993; 188(3):743-746.

75    Chabriat H, Vahedi K, Iba-Zizen MT, Joutel A, Nibbio A, Nagy TG et al. Clinical spectrum of CADASIL: a study of 7 families. Cerebral autosomal dominant arteriopathy with subcortical infarcts and leukoencephalopathy. Lancet 1995; 346(8980):934-939.

76    Lesnik Oberstein SA, Van den Boom R, Van Buchem MA, Van Houwelingen HC, Bakker E, Vollebregt E et al. Cerebral microbleeds in CADASIL. Neurology 2001; 57(6):1066-1070.

77    Dichgans M, Holtmannspotter M, Herzog J, Peters N, Bergmann M, Yousry TA. Cerebral microbleeds in CADASIL: a gradient-echo magnetic resonance imaging and autopsy study. Stroke 2002; 33(1):67-71.

78    Van den Boom R, Lesnik Oberstein SA, Ferrari MD, Haan J, Van Buchem MA. Cerebral autosomal dominant arteriopathy with subcortical infarcts and leukoencephalopathy: MR imaging findings at different ages--3rd-6th decades. Radiology 2003; 229(3):683-690.

79    Jungreis CA, Kanal E, Hirsch WL, Martinez AJ, Moossy J. Normal perivascular spaces mimicking lacunar infarction: MR imaging. Radiology 1988; 169(1):101-104.

80    Heier LA, Bauer CJ, Schwartz L, Zimmerman RD, Morgello S, Deck MD. Large Virchow-Robin spaces: MR-clinical correlation. AJNR Am J Neuroradiol 1989; 10(5):929-936.

81    Bokura H, Kobayashi S, Yamaguchi S. Distinguishing silent lacunar infarction from enlarged Virchow-Robin spaces: a magnetic resonance imaging and pathological study. J Neurol 1998; 245(2):116-122.

82    Pantoni L, Garcia JH. Pathogenesis of leukoaraiosis: a review. Stroke 1997; 28(3):652-659.

83    Kwa VI, Stam J, Blok LM, Verbeeten B, Jr. T2-weighted hyperintense MRI lesions in the pons in patients with atherosclerosis. Amsterdam Vascular Medicine Group. Stroke 1997; 28(7):1357-1360.

84    Lammie GA. Pathology of small vessel stroke [In Process Citation]. Br Med Bull 2000; 56(2):296-306.

85    Davous P. CADASIL: a review with proposed diagnostic criteria. Eur J Neurol 1998; 5(3):219-233.

86    Sabbadini G, Francia A, Calandriello L, Di Biasi C, Trasimeni G, Gualdi GF et al. Cerebral autosomal dominant arteriopathy with subcortical infarcts and leucoencephalopathy (CADASIL). Clinical, neuroimaging, pathological and genetic study of a large Italian family. Brain 1995; 118(Pt 1):207-215.

87    Trojano L, Ragno M, Manca A, Caruso G. A kindred affected by cerebral autosomal dominant arteriopathy with subcortical infarcts and leukoencephalopathy (CADASIL). A 2-year neuropsychological follow-up. J Neurol 1998; 245(4):217-222.

88    Koeppen AH. The history of iron in the brain. J Neurol Sci 1995; 134 Suppl:1-9.

89    Rankin J. Cerebral vascular accidents in patients over the age of 60. II. Prognosis. Scott Med J 1957; 2(5):200-215.

90    Zigmond AS, Snaith RP. The hospital anxiety and depression scale. Acta Psychiatr Scand 1983; 67(6):361-370.

91    Spinhoven P, Ormel J, Sloekers PP, Kempen GI, Speckens AE, Van Hemert AM. A validation study of the Hospital Anxiety and Depression Scale (HADS) in different groups of Dutch subjects. Psychol Med 1997; 27(2):363-370.

92    Van den Boom R, Lesnik Oberstein SA, Van Duinen SG, Bornebroek M, Ferrari MD, Haan J et al. Subcortical Lacunar Lesions: An MR Imaging Finding in Patients with Cerebral Autosomal Dominant Arteriopathy with Subcortical Infarcts and Leukoencephalopathy. Radiology 2002; 224(3):791-796.

93    Van Mil AH, Spilt A, Van Buchem MA, Bollen EL, Teppema L, Westendorp RG et al. Nitric oxide mediates hypoxia-induced cerebral vasodilation in humans. J Appl Physiol 2002; 92(3):962-966.

94    Roth M, Tym E, Mountjoy CQ, Huppert FA, Hendrie H, Verma S et al.
      CAMDEX. A standardised instrument for the diagnosis of mental disorder
      in the elderly with special reference to the early detection of dementia.
      Br J Psychiatry 1986; 149:698-709.

95    Verin M, Rolland Y, Landgraf F, Chabriat H, Bompais B, Michel A et al. New
      phenotype of the cerebral autosomal dominant arteriopathy mapped
      to chromosome 19: migraine as the prominent clinical feature. J Neurol
      Neurosurg Psychiatry 1995; 59(6):579-585.

96    Taillia H, Chabriat H, Kurtz A, Verin M, Levy C, Vahedi K et al. Cognitive
      alterations in non-demented CADASIL patients. Cerebrovasc Dis 1998;
      8(2):97-101.

97    Fazekas F, Barkhof F, Filippi M, Grossman RI, Li DK, McDonald WI et al. The
      contribution of magnetic resonance imaging to the diagnosis of multiple
      sclerosis. Neurology 1999; 53(3):448-456.

98    Ebke M, Dichgans M, Bergmann M, Voelter HU, Rieger P, Gasser T et al.
      CADASIL: skin biopsy allows diagnosis in early stages. Acta Neurol Scand
      1997; 95(6):351-357.

99    Poser CM, Paty DW, Scheinberg L, McDonald WI, Davis FA, Ebers GC et
      al. New diagnostic criteria for multiple sclerosis: guidelines for research
      protocols. Ann Neurol 1983; 13(3):227-231.

100   Jungreis CA, Kanal E, Hirsch WL, Martinez AJ, Moossy J. Normal perivascular
      spaces mimicking lacunar infarction: MR imaging. Radiology 1988;
      169(1):101-104.

101   Miki Y, Grossman RI, Udupa JK, Wei L, Kolson DL, Mannon LJ et al. Isolated
      U-fiber involvement in MS: preliminary observations. Neurology 1998;
      50(5):1301-1306.

102   Horowitz AL, Kaplan RD, Grewe G, White RT, Salberg LM. The ovoid lesion:
      a new MR observation in patients with multiple sclerosis. AJNR Am J
      Neuroradiol 1989; 10(2):303-305.

103   Tas MW, Barkhol F, Van Walderveen MA, Polman CH, Hommes OR, Valk J.
      The effect of gadolinium on the sensitivity and specificity of MR in the initial
      diagnosis of multiple sclerosis. AJNR Am J Neuroradiol 1995; 16(2):259-
      264.

104 Mahley RW. Apolipoprotein E: cholesterol transport protein with expanding role in cell biology. Science 1988; 240(4852):622-630.

105 Nathoo N, Chetty R, Van Dellen JR, Barnett GH. Genetic vulnerability following traumatic brain injury: the role of apolipoprotein E. Mol Pathol 2003; 56(3):132-136.

106 Premkumar DR, Cohen DL, Hedera P, Friedland RP, Kalaria RN. Apolipoprotein E-epsilon4 alleles in cerebral amyloid angiopathy and cerebrovascular pathology associated with Alzheimer's disease. Am J Pathol 1996; 148(6):2083-2095.

107 Haan J, Van Broeckhoven C, Van Duijn CM, Voorhoeve E, Van Harskamp F, Van Swieten JC et al. The apolipoprotein E epsilon 4 allele does not influence the clinical expression of the amyloid precursor protein gene codon 693 or 692 mutations. Ann Neurol 1994; 36(3):434-437.

108 Opherk C, Peters N, Herzog J, Luedtke R, Dichgans M. Long-term prognosis and causes of death in CADASIL: a retrospective study in 411 patients. Brain 2004; 127(Pt 11):2533-2539.

109 Dichgans M, Filippi M, Bruning R, Iannucci G, Berchtenbreiter C, Minicucci L et al. Quantitative MRI in CADASIL: correlation with disability and cognitive performance. Neurology 1999; 52(7):1361-7.

110 Singhal S, Bevan S, Barrick T, Rich P, Markus HS. The influence of genetic and cardiovascular risk factors on the CADASIL phenotype. Brain 2004.

111 Bornebroek M, Haan J, Van Duinen SG, Maat-Schieman ML, Van Buchem MA, Bakker E et al. Dutch hereditary cerebral amyloid angiopathy: structural lesions and apolipoprotein E genotype. Ann Neurol 1997; 41(5):695-8.

112 Bakker CJ, Hartkamp MJ, Mali WP. Measuring blood flow by nontriggered 2D phase-contrast MR angiography. Magn Reson Imaging 1996; 14(6):609-614.

113 Van der Geest RJ, Niezen RA, Van der Wall EE, de Roos A, Reiber JH. Automated measurement of volume flow in the ascending aorta using MR velocity maps: evaluation of inter- and intraobserver variability in healthy volunteers. J Comput Assist Tomogr 1998; 22(6):904-911.

114   Buijs PC, Krabbe-Hartkamp MJ, Bakker CJ, de Lange EE, Ramos LM, Breteler MM et al. Effect of age on cerebral blood flow: measurement with ungated two-dimensional phase-contrast MR angiography in 250 adults. Radiology 1998; 209(3):667-674.

115   Gridley T. Notch signaling in vertebrate development and disease. Mol Cell Neurosci 1997; 9(2):103-108.

116   Gridley T. Notch signaling during vascular development. Proc Natl Acad Sci U S A 2001; 98(10):5377-5378.

117   Uyttendaele H, Ho J, Rossant J, Kitajewski J. Vascular patterning defects associated with expression of activated Notch4 in embryonic endothelium. Proc Natl Acad Sci U S A 2001; 98(10):5643-5648.

118   Spilt A, Box FM, Van der Geest RJ, Reiber JH, Kunz P, Kamper AM et al. Reproducibility of total cerebral blood flow measurements using phase contrast magnetic resonance imaging. J Magn Reson Imaging 2002; 16(1):1-5.

119   Chabriat H, Bousser MG, Pappata S. Cerebral autosomal dominant arteriopathy with subcortical infarcts and leukoencephalopathy: a positron emission tomography study in two affected family members [letter]. Stroke 1995; 26(9):1729-1730.

120   Spilt A, Van den Boom R, Kamper AM, Blauw GJ, Bollen EL, Van Buchem MA. MR assessment of cerebral vascular response: a comparison of two methods. J Magn Reson Imaging 2002; 16(5):610-616.

121   Seitz J, Strotzer M, Schlaier J, Nitz WR, Volk M, Feuerbach S. Comparison between magnetic resonance phase contrast imaging and transcranial Doppler ultrasound with regard to blood flow velocity in intracranial arteries: work in progress. J Neuroimaging 2001; 11(2):121-128.

122   Bakker CJ, Kouwenhoven M, Hartkamp MJ, Hoogeveen RM, Mali WP. Accuracy and precision of time-averaged flow as measured by nontriggered 2D phase-contrast MR angiography, a phantom evaluation. Magn Reson Imaging 1995; 13(7):959-965.

123   Spreen O, Strauss E. A compendium of neuropsychological test: administration, norms, and commentary. 2nd ed. New York, NY: Oxford University Press Inc; 1998

Curriculum Vitae

# Curriculum Vitae

De auteur van dit proefschrift werd geboren op 21 maart 1973 op Curaçao. In 1991 werd het VWO diploma behaald aan het Stella Maris college te Meerssen. Een jaar later werd begonnen met de studie geneeskunde aan de Rijksuniversiteit te Leiden. Het doctoraal examen werd behaald in 1996 en het artsexamen in 1999. Als afstudeeronderzoek verrichtte zij een half jaar onderzoek naar de reproduceerbaarheid van magnetization transfer imaging op de afdeling Radiologie van het Leids Universitair Medisch Centrum. Vanaf juli 1999 tot maart 2003 was zij werkzaam op de afdeling Radiologie van het Leids Universitair Medisch Centrum, waar zij het onderzoek verrichtte dat geleid heeft tot dit proefschrift. Sinds 1 maart 2003 volgt zij de opleiding tot radioloog (opleider Prof. Dr. J.L. Bloem) in hetzelfde ziekenhuis.